MASTER EN BIOCHIMIE ET BIOLOGIE MOLÉCULAIRE ET CELLULAIRE À FINALITÉ APPROFONDIE

Identification of the O-chain ligase in Brucella abortus

VERHAEGHE, Audrey

Award date:
2022

Awarding institution:
Universite de Namur

UNIVERSITÉ DE NAMUR

Faculté des Sciences

IDENTIFICATION OF THE O-CHAIN LIGASE IN *BRUCELLA ABORTUS*

Mémoire présenté pour l'obtention

du grade académique de master 120 en biochimie et biologie moléculaire et cellulaire

Audrey VERHAEGHE

Janvier 2022

Université de Namur
FACULTE DES SCIENCES
Secrétariat du Département de Biologie
Rue de Bruxelles 61 - 5000 NAMUR
Téléphone: + 32(0)81.72.44.18 - Téléfax: + 32(0)81.72.44.20
E-mail: joelle.jonet@unamur.be - http://www.unamur.be

Identification de la ligase de la chaîne O dans *Brucella abortus*

VERHAEGHE Audrey

Résumé

Les bactéries Gram-négatives présentent à leur surface comme composant principal du lipopolysaccharide (LPS), formé de lipide A, d'un noyau de sucres et un long polysaccharide, nommé chaîne O. *Brucella* spp. est un genre comportant des pathogènes intracellulaires facultaire et présentant deux types de LPS, un rugueux et un lisse, le premier manquant la chaîne O. Alors que la ligase de la chaîne O, nécessaire à l'ajout de ce polysaccharide au reste du LPS, a été identifiée dans de nombreuses espèces bactériennes, cette protéine reste non-identifiée dans *Brucella* spp. Dans ce travail, nous avons visé à caractériser deux candidats putatifs. Bien que le premier candidat BAB2_0106, un homologue de *Escherichia coli* WaaL, n'a pas apporté de résultats indiquant cette protéine d'être la ligase de la chaîne O dans *Brucella* spp., le second candidat BAB1_0639 (*wadA*) s'est révélé intéressant. Premièrement, nous avons pu déterminer l'essentialité de *wadA* dans *B. abortus*, alors que ce gène se révèle non-essentiel dans *B. melitensis*, une espèce génétiquement proche. En outre, la possibilité de déléter ce gène exclusivement en absence de chaîne O suggère une toxicité potentiellement due à une accumulation de chaîne O sur son transporteur lipidique, le bactoprénol, auquel se lient également les précurseurs de peptidoglycans. Ainsi, la saturation de ce transporteur pourrait mener à une pénurie de synthèse de peptidoglycan. WadA a préalablement été identifiée en tant que glycosyltransférase ajoutant le dernier sucre du noyau LPS. De plus, nous avons pu identifier une deuxième activité putative à WadA avec un domaine agissant en tant que la ligase de la chaîne O. Cette activité de ligase de la chaîne O a été suggéré comme correcte suite aux résultats obtenus par Western Blot et par microscopie à immunofluorescence ayant démontrés une absence de chaîne O en délétant ce domaine exclusivement. De plus, nous avons démontré l'intérêt d'acides aminés chargées positivement dans ce domaine de ligase de chaîne O pour son activité catalytique. En outre, nous avons mis en évidence qu'un noyau LPS complet est requis à la stabilité de membrane et à la croissance bactérienne. Nous avons émis l'hypothèse que l'absence du dernier sucre pourrait perturber l'interaction avec des protéines de la membrane externe, comme par exemple avec des porines nécessaires à l'apport nutritionnel. Globalement, nos données confèrent de nouvelles connaissances sur la voie de synthèse du LPS, en identifiant WadA en tant que ligase de la chaîne O dans *Brcuella* spp., ainsi qu'en décrivant pour la première fois une enzyme bifonctionnelle dans cette voie de synthèse.

Mémoire de master 120 en biochimie et biologie moléculaire et cellulaire

Janvier 2022

Promoteur: X. De Bolle

Université de Namur
FACULTE DES SCIENCES
Secrétariat du Département de Biologie
Rue de Bruxelles 61 - 5000 NAMUR
Téléphone: + 32(0)81.72.44.18 - Téléfax: + 32(0)81.72.44.20
E-mail: joelle.jonet@unamur.be - http://www.unamur.be

Identification of the O-chain ligase in *Brucella abortus*

VERHAEGHE Audrey

Summary

Gram-negative bacteria are known to present on their surface a major component called lipopolysaccharide (LPS), formed of a lipid A, a sugar core and a long polysaccharide, called O-chain. *Brucella* spp*.,* which are facultative intracellular pathogens, show two types of LPS, rough and smooth, the first one lacking this O-chain polysaccharide. While the O-chain ligase necessary to add this O-chain has been identified in many bacterial species, this protein has not yet been described in *Brucella* spp. In this work, we aimed to characterize two putative candidates. While our first candidate BAB2_0106, a homolog of *Escherichia coli* WaaL, did not show any results suggesting this protein to be the O-chain ligase in *Brucella* spp., our second candidate BAB1_0639 (*wadA*) revealed to be interesting. First of all, *wadA* is essential in *B. abortus*, while it is not in its close relative *B. melitensis.* Furthermore, the ability to delete this gene in absence of O-chain suggests a potential toxicity due to O-chain accumulation on its lipid carrier bactoprenol, as peptidoglycan precursors bind to this component as well. Thereby, saturation of the carrier could lead to a shortage of peptidoglycan synthesis. Previous reports identified WadA as the glycosyltransferase necessary to add the last core sugar during the synthesis of the LPS core. Additionally, we identified a second putative activity for WadA with a domain acting as the O-chain ligase. The O-chain ligase activity was suggested accurate through results found by Western Blot and immunofluorescence microscopy that indicate absence of the polysaccharide when deleting this O-chain ligase domain. Additionally, we demonstrate the significance of positively charged amino acids in the O-chain ligase domain for its activity. Moreover, we showed that the full LPS core is required for membrane integrity and for bacterial growth. We hypothesized that the lack of the last core sugar could impair interaction with outer membrane proteins, such as porins that are necessary for nutrient intake. Overall, our data gives new insights on the LPS synthesis, identifying WadA as the main O-chain ligase in *Brucella* spp., but also describing for the first time a bifunctional enzyme in this pathway.

Thesis for the master 120 in biochemistry and molecular and cellular biology

January 2022

Promotor: X. De Bolle

ACKNOWLEDGEMENTS

Tout d'abord, j'aimerais remercier mon promoteur Xavier De Bolle de m'avoir donné cette opportunité de réaliser mon mémoire dans son équipe. Merci pour votre soutien et de votre enthousiasme tout au long de ces derniers mois, des longues discussions autour des résultats et du temps passé à la relecture de ce travail. Merci du partage de vos connaissances et de toutes vos anecdotes, merci de m'avoir à chaque fois accueillie dans votre bureau avec un sourire.

Je tiens également à remercier l'URBM et tous ses membres pour leur accueil dans l'unité, la bonne ambiance (parfois autour d'une bonne bière) et leur gentillesse. Je remercie en particulier la « Xa » team, Adélie, Agnès, Angy, Elodie, Eme, Pierre, pour son accueil, ses conseils et sa volonté d'aider. Merci à Pierre pour ton aide avec CRISPRi et tes bonnes (et parfois mauvaises) blagues. Merci à Adélie de m'avoir dépanné plusieurs fois en SDS et DOC et de ton partage des résultats Tn-seq.

Un énorme merci à toi Caro, sans qui ce mémoire n'aurait pas pu être possible. Merci pour ton encadrement et toutes les discussions que nous avons pu avoir. Merci pour ta confiance, ta disponibilité, et ta patience ces derniers mois. Merci de m'avoir toujours poussé à aller plus loin. Merci pour toutes ces heures passées à la relecture et rerelecture de ce travail. Merci de m'avoir aidé à trouver un fil rouge dans toutes mes idées. Merci pour m'avoir donné goût à la recherche et au travail en labo. J'espère que tu garderas un bon souvenir de ta dernière mémorante. Et bonne chance pour ta dernière année !

Évidemment je ne peux pas oublier les mémos. Merci Cérine, Julia, Laura, Marine, Petra et Thomas ! Merci d'avoir fait d'un couloir un endroit pas si désagréable, un lieu où papoter de tout et n'importe quoi, à raconter les derniers ragots, à échanger des idées et partager des solutions pour nos manips ratées. J'ai l'impression que tous les jours il y avait un petit « T'en veux un ? » en proposant des biscuits ou bonbons (même avec cette bonne odeur). On était toujours bien nourris ! Merci à Laura pour tous tes « Attention, la porte ! ». Merci Tchoupi pour tous tes Memes et mauvaises blagues / commentaires déplacés (?). Merci Marine de toujours apporter de la bonne humeur ; sans oublier tous les surnoms. Merci pour les repas avec notre dégustation de tous les humus ou autres du Proxy. Merci pour toutes ces discussions, ces soirées, ces pas de danse. Big up à Jagaban et aux Marseillais. Merci à tous pour vos conseils, l'entre-aide et votre soutien durant les moments difficiles. Merci de m'avoir montré à quel point on peut se rapprocher des gens en quelques mois. Merci pour tous les fous-rires. Natürlich auch ein Danke schön an dich Nina, mit der Hoffnung sich bald wiederzusehen. Vielleicht sogar in Marburg!

Je souhaite aussi remercier ma famille pour leur soutien tout au long des années. Merci Papa de n'avoir jamais douté de moi et de m'avoir permis d'arriver où j'en suis aujourd'hui. Merci Mamy d'avoir toujours été fière de moi, même si tu ne comprenais pas toujours tout. Merci Alice d'avoir toujours été là pour me changer les idées et faire face à mes petits sauts d'humeur sous le stress. Merci Sandra fier all deng Hëllef an deene leschte Joeren an eis stonnelaang Diskussiounen. Ech hu dës puer Pausen gebraucht.

Enfin, merci aux membres de mon jury, M. Thierry Arnould, M. Elie Marchand, Mme. Audrey Progneaux et M. Francesco Renzi, pour votre temps et votre attention consacrés à ce travail. Je vous souhaite une bonne lecture !

“The illiterate of the 21st century will not be those who cannot read and write, but those who cannot learn, unlearn, and relearn.”

Alvin Toffler

TABLE OF CONTENTS

ABBREVIATIONS

ABC transporter	ATP-binding cassette transporter
Amp	Ampicillin
B.	Brucella
BctP(P)	Bactoprenol
BCV	Brucella-containing vacuole
Bp	Base pair
CβG	Cyclic-β-1,2-glucan
CFU	Colony-forming unit
Cm	Chloramphenicol
DOC	Sodium deoxycholate
ER	Endoplasmic reticulum
Glc	Glucose
GlcN	Glucosamine
Gmd	GDP mannose dehydratase
GT	Glycosyltransferase
ER	Endoplasmic reticulum
IF	Immunofluorescence microscopy
IM	Inner membrane
IPTG	Isopropyl β-D-1-thiogalactopyranoside
Kan	Kanamycin
KDO	3-deoxy-D-manno-octulosonic acid
LB	Lennox lysogeny broth
LPS	Lipopolysaccharide
Lpt	Lipopolysaccharide transport machinery
OAg	O-antigen ligase (domain)
OD	Optical density
OM	Outer membrane
Omp	Outer membrane protein
ON	Over-night
Man	Mannose
Nal	Nalidixic acid sodium salt
NAG	N-acetylglucosamine
NAM	N-actetylmuramic acid
NGlcN	Diaminoglucose
PBS	Phosphate Buffer Sodium
PCR	Polymerase Chain Reaction
Per	N-formylperosamine
PG	Peptidoglycan
PI	Post-infection
Quin	Quinovosamine
R-LPS	Rough lipopolysaccharide
RNA	Ribonucleic Acid
RPM	Rotation per minutes
RT	Room Temperature
SDS	Sodium dodecyl sulfate
S-LPS	Smooth lipopolysaccharide
TSB	Tryptic soy broth
WB	Western blot
WT	Wild type
YT	Yeast extract Tryptone

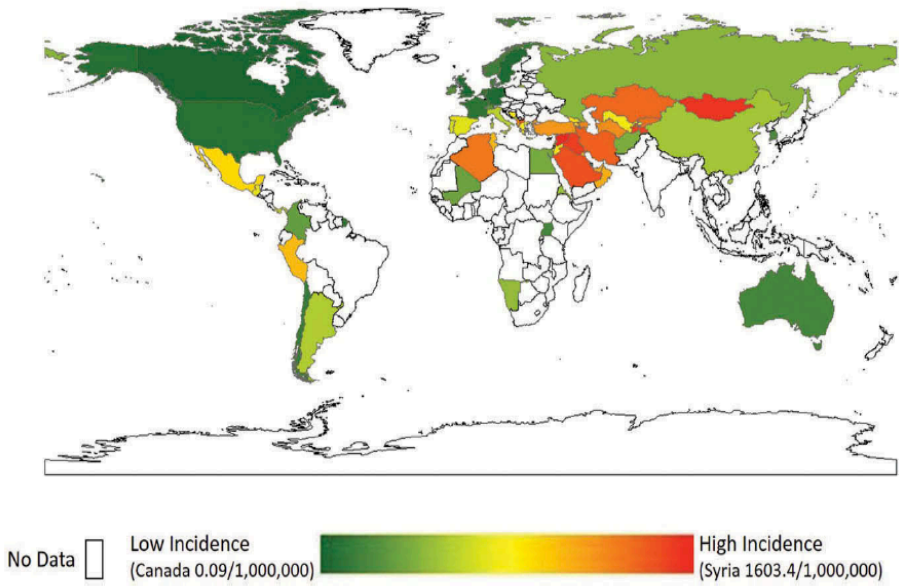

Figure 1: Heat map of human brucellosis incidence (per 1,000,000 individuals) (Hull & Schumaker, 2018)

INTRODUCTION

1. Brucellosis

1.1. History

The earliest traces of *Brucella spp.* date from 2.8 million years ago and were discovered in a late Pliocene hominin skeleton (D'Anastasio *et al.,* 2009). Moreover, other data indicating the past association of *Brucella* spp. to humans were identified through DNA found in a 700-year old skeleton from Italy (Kay *et al*., 2014). However, the first report of *Brucella* as a pathogen was made in 1887 by Sir David Bruce. He was able to identify the pathogen in the liver of a deceased soldier on Malta (Bruce D., 1887). Indeed, it appeared that many British soldiers standing in the island of Malta manifested a new type of undulant fever, which sometimes led to death (Bruce D., 1889). As this microorganism was identified as being a small coccobacillus, it was named "*Micrococcus melitensis*" due to its size and with a reference to Malta (*melita* in latin) as its place of discovery (Bruce D., 1887). A decade later, Bernard Bang isolated a second species and named it *Bacillus abortus* (Bang B., 1897). In honors of Sir David Bruce, the nomenclature was standardized and the genus was named *Brucella*. The two species were renamed *Brucella melitensis* and *Brucella abortus* (Meyer & Shaw, 1920). While the main denomination for the zoonosis is called brucellosis, the disease can be found under a variety of names, including: undulant fever, Malta fever, Mediterranean fever, contagious abortion and Bang's disease (Moreno E., 2014). Although the bacteria had been isolated in patients, the ways of transmission remained unknown over the next decades until Themistocles Zammit determined that the infection of British soldier's was due to consumption of contaminated goat's milk (Zammit T., 1905). This discovery led to many eradication campaigns over the years in an effort to eradicate brucellosis (Hull & Schumaker, 2018).

1.2. Epidemiology

Despite campaigns to exterminate the pathogen, brucellosis remains the world's most widespread anthropo-zoonosis. It appears that around 500,000 cases of human brucellosis are reported annually. However, estimations predict a true incidence of minimum 5,000,000 cases annually (Berger S., 2016). While there has been some progress in the last decades to control the disease, several regions remain impacted by animal infection and thus transmission to human beings. These regions are mostly represented by the Mediterranean countries, north and east Africa, the Middle East, south and central Asia and Central and South America (Corbel, 2006). Concerning the European Union, many countries have been granted the status "brucellosis-free"[1]. However, countries such as Spain and Greece remain endemic areas with some of the highest incidence in Europe (Dean *et al.,* 2012; Pappas *et al*., 2006). Worldwide, Syria has been reported as being the country with the highest incidence with 1,603.4 cases per 1,000,000 individuals, followed by Mongolia, Iraq, Tajikistan, Saudi Arabia and Iran (Dean *et al.,* 2012; Pappas *et al*., 2006). *Figure 1* represents a heat map of the incidence of human brucellosis (Hull & Schumaker, 2018).

[1] Regions presenting a low incidence of annual human cases ; the reported cases are believed to be travel-acquired or from immigrants from endemic countries (Pappas *et al.,* 2006)

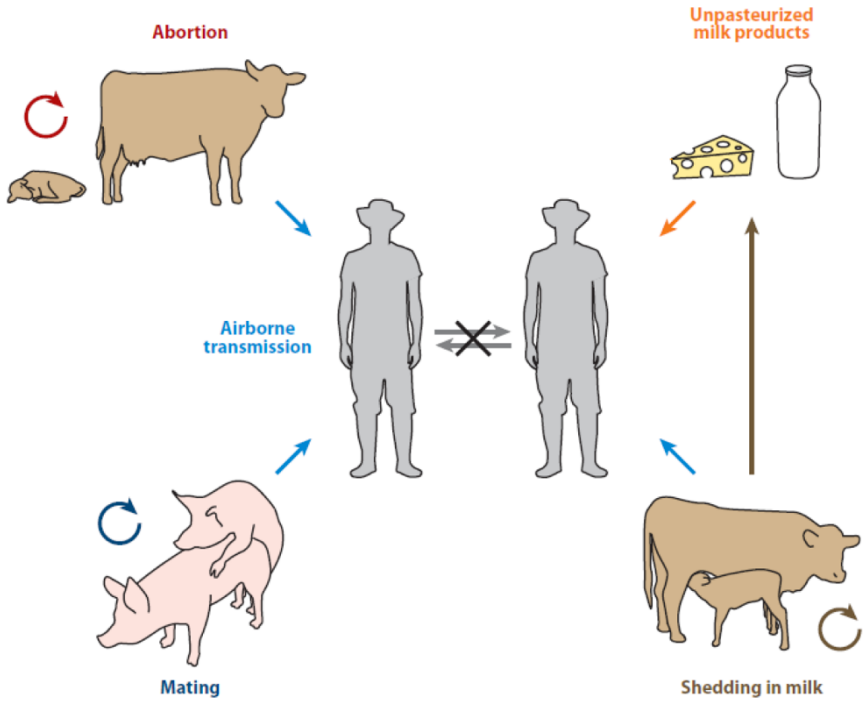

Figure 2: Ways of transmission of brucellosis between human and animal hosts. (Atluri *et al*., 2011) Transmission can occur between animals through direct contact with aborted fetuses, through genital secretions during mating or through milk suckling. Transmission from animals to human beings can occur through aerosolization or consumption of unpasteurized contaminated dairy products. Transmission between human beings is rare.

The species mostly responsible for human and animal brucellosis in the developing countries are *Brucella abortus, Brucella melitensis* and *Brucella suis.* Efforts to evaluate the number of animal brucellosis cases have been done but remain insufficient due to lack of resources and due to sufferings of reporting bias. However, the numbers allow us to have a rough idea of the incidence, with the most animal cases being due to *B. abortus,* followed by *B. melitensis* and finally *B. suis* (Hull & Schumaker, 2018).

1.3. The disease

As mentioned earlier on, the bacteria of the *Brucella* genus are responsible for an anthropozoonosis called brucellosis. In animals, including domesticated and wild-life, this disease is characterized by infertility in males and spontaneous abortion in females (Cardoso *et al.,* 2006). The transmission between animals can be done vertically from the mother to the fetus, or horizontally through close contact with mating secretions or licking of aborted fetuses (*Figure 2*) (Atluri *et al.,* 2011).

Moreover, for some bacterial species, human beings can become infected via direct contact with tissues or blood of infected animals or by ingesting contaminated dairy products (Cardoso *et al.,* 2006) (*Figure 2*). It appears that 10 to 100 bacteria are enough to generate the human disease (Pappas *et al*., 2006), allowing categorization of the bacteria of this bacterial genus as highly infectious (Haag *et al.,* 2010). This high infectivity can be explained through its infection by aerosolization or subcutaneous route (Hull & Schumaker, 2018). Reports of transmission between human beings remain rare (Meltzer *et al.,* 2010; Wyatt HV, 2010). In the case of human brucellosis, several symptoms can manifest themselves, such as fever, nausea, fatigue (Haag *et al.,* 2010), arthritis and neurological symptoms that can, if untreated, lead to chronic infection (Cardoso *et al.,* 2006) or even to lethality in 1-5% of the cases (Salvador *et al.,* 2018). The people at risk are mainly farmers, veterinarians and slaughterhouse workers due to their close contact to animals (Corbel, 2006), but also scientists working with the bacteria. Indeed, brucellosis was recognized as the world's most common laboratory-acquired infection (Weinstein & Singh, 2009). Considering its potential to cause a severe threat to public health, bacteria from the *Brucella* genus have been classified as biosafety group 3 microorganisms (Moreno *et al.,* 2002).

1.4. Diagnosis and treatment of human brucellosis

Human brucellosis frequently goes unreported due to its wide range of symptoms and to its similarities to flu-like symptoms and even ranks as one of the seven most neglected diseases (Corbel, 2006). This lack of pathognomonic signs for the disease explains why brucellosis is as difficult to diagnose. It is thereby necessary to conduct bacteriological and serological tests to diagnose the human disease. Such tests are often done depending on the clinical history and the presence of the patient at a risk area. Rapid screening can be done by performing a Rose Bengal plate test, but further tests are needed to confirm the results (Corbel, 2006). Bacteriological tests include the execution of bacterial cultures on Farrell medium (Godfroid *et al.*, 2010). Serological tests, such as the ELISA, can be performed by using antibodies (IgM and/or IgG) targeting the smooth lipopolysaccharide (S-LPS) of *Brucella.* However, there is a risk of cross-reaction with other Gram-negative bacteria such as *Yersinia enterocolitica* O:9. Thus, these tests are not highly reliable (Corbel, 2006). Another possible diagnostic test can be performed using the polymerase chain reaction (PCR), thereby allowing DNA detection. This last technique enables the only correct diagnosis, even allowing to distinguish between the different strains of *Brucella* (Godfroid *et al.*, 2010).

Table 1 : Different *Brucella* species and their host preference, as well as their zoonotic potential (Atluri *et al.*, 2011)

Species	Host preference	Zoonotic potential[a]
Brucella melitensis	Sheep, goat (*Ovis* spp. and *Capra* spp.)	High
Brucella abortus	Cattle (*Bos taurus* and *Bos indicus*)	Moderate
Brucella suis	Pig (*Sus scrofa*)	Moderate
Brucella canis	Dog (*Canis lupus familiaris*)	Mild
Brucella ceti	Dolphin, porpoise, whale (Cetacea)	Mild
Brucella pinnipedialis	Seal (Pinnipedia)	Mild
Brucella inopinata	Unknown	Mild
Brucella ovis	Sheep (*Ovis* spp.)	No reported infections
Brucella neotomae	Desert woodrat (*Neotoma lepida*)	No reported infections
Brucella microti	Common vole (*Microtus arvalis*)	No reported infections
Brucella sp. (baboon isolate)	Baboon (*Papio* spp.)	No reported infections

[a]Based on the number of human cases reported and depends on a combination of exposure to the pathogen and infectivity.

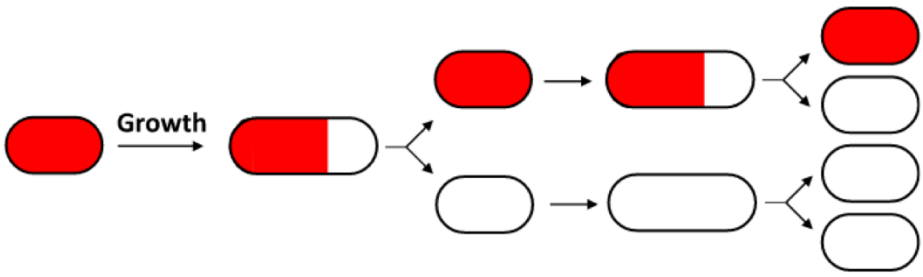

Figure 3 : Representation of unipolar growth in Rhizobiales. Previous cell envelope material is represented in red. Newly generated envelope material in white. (Van der Henst *et al.*, 2013)

Treatment with effective antibiotics is required to knock out human brucellosis. This administration should be applied as early as possible and by respecting an adequate length of time. Actual treatments are the administration of doxycycline alone or in combination with rifampicin that need to be taken over a period of six weeks (WHO, 2020). As the rate of relapse is of 10-20% when this treatment is given, it is recommended to additionally administrate amino-glycoside, such as Streptomycin or Gentamicin, during the first two or three weeks, as it was observed to further increase bacterial killing (Corbel, 2006).

1.5. Control of animal brucellosis

In an effort to control the spread of the disease, different methods have been set up such as vaccines, culling of infected animals and surveillance testing. Although no vaccine has been accepted for use on human beings, three main vaccines against animal brucellosis have been developed for use in endemic regions. These are represented by S19 and RB51 are used against *B. abortus* in bovines and Rev1 against *B. melitensis* in goats and sheep. These vaccines reduce the risk of abortion, thereby breaking the cycle of transmission between animals and enabling protection of the remaining animals (Hull & Schumaker, 2018). Moreover, in many developed countries, herds are monitored by serological tests. Sero-positive animals are sent to the slaughterhouse or culled by regulatory officials in an attempt to reduce spreading of the disease (Hull & Schumaker, 2018). In this manner, brucellosis is responsible for economic losses due to its impact on animal production and on Public Health (Salvador *et al*., 2018).

2. The *Brucella* genus: species and phylogeny

The genus *Brucella* is composed of facultative intracellular pathogenic bacteria (Whatmore *et al.,* 2021). The genus comprises 21 species, referred as "classical" and "non-classical" species (Moreno E., 2021). The different species show a length range from 0.5 to 1.5 μm and differ on metabolic and antigenic characteristics, as well as their 16S RNA sequences (Moreno & Moriyón, 2006). Most *Brucella* species present one large chromosome (ChrI) and one small chromosome (ChrII) with a size of 2.1 Mb and 1.2 Mb respectively (Cardoso *et al.,* 2006). Concerning characteristics that distinguish *Brucella* from other bacteria, the absence of flagella, pili, capsules and fimbriae can be named (Moreno & Moriyón, 2006). These Gram-negative bacteria primarily infect mammals, particularly livestock, showing host preferences for each species (*Table 1*). The main species, regarding this work, are *B. abortus* and *B. melitensis* infecting cattle and goats respectively.

The bacteria of this genus belong to the Rhizobiales order in the alpha-proteobacteria class (Batut *et al.,* 2004). This group of Gram-negative bacteria includes plant and animal pathogens, as well as free-living microorganisms of water and soil, both heterotrophic or photosynthetic (Moreno & Moriyón, 2006). Their closest relatives are species from the *Ochrobactrum* genus, with for example *Ochrobactrum intermedium* showing high genetical similarities. However, their lifestyles vary considerably, as *O. intermedium* represents an opportunistic bacterium which cycles from soil-rhizoplane to immunodepressed patients (Moreno & Moriyón, 2006).

Another characteristic of *Brucella spp.*, and shared by Rhizobiales, is their unipolar growth (Van der Henst *et al*., 2013), in contrast to the lateral elongation found in *Escherichia coli* (Randich & Brun, 2015). Indeed, before cell division, *Brucella* bacteria incorporate new material only at one pole, so that the bacterium presents a new pole, generated by division, and an old pole. Thereby, while the daughter cell presents a newly generated cell envelope, the mother cell keeps the old envelope material (*Figure 3*) (Van der Henst *et al*., 2013).

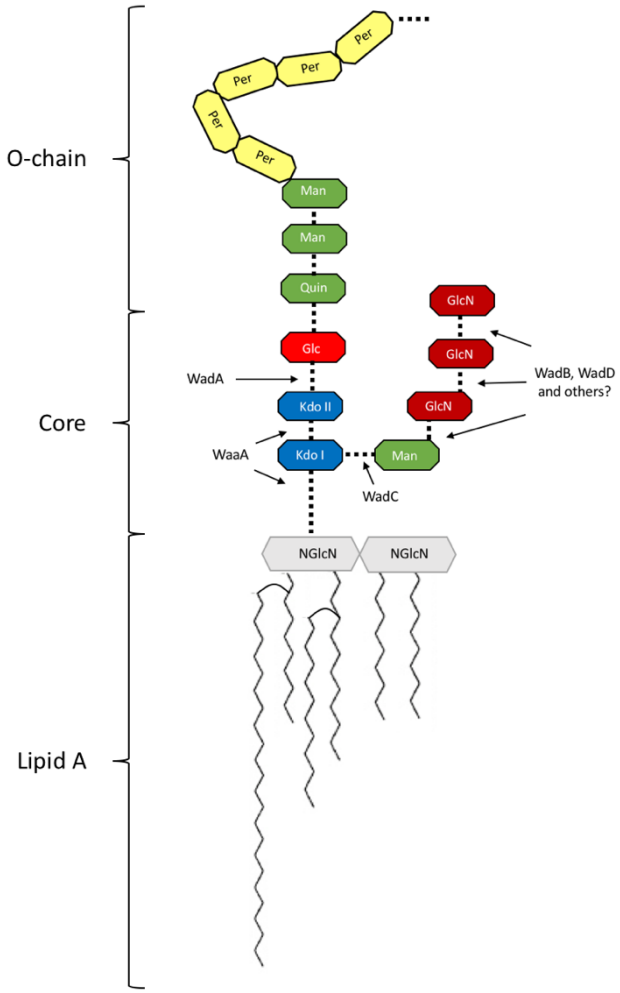

Figure 4 : Schematic representation of *B. abortus* LPS and the enzymes believed to be involved in the core synthesis. Site of action of identified GTs are represented by arrows. Man: mannose; NGlcN: diaminoglucose; GlcN: glucosamine; Kdo: 3-deoxy-D-manno-octulosonic acid; Per: N-formylperosamine; Quin : quinovosamine (inspired from Salvador *et al.*, 2018)

3. Cell envelope of *Brucella*

3.1. The outer membrane

3.1.1. Generalities

As *Brucella* are Gram-negative bacteria, their cell envelope is made of an inner membrane (IM), an outer membrane (OM) and a layer of peptidoglycans found in the periplasmic space between the two membranes (Cardoso *et al.,* 2006). Both the IM and the OM present a thickness of about 6.5 to 8.0 nm (Moreno & Moriyón, 2006). While the IM is mainly composed of phospholipids, the OM is an asymmetric bilayer mainly composed of phospholipids on the inner leaflet and lipopolysaccharides (LPS) on the outer leaflet (Haag *et al.,* 2010). Being the major component of the outer leaflet (75% of the bacterial surface) (Lerouge & Vanderleyden, 2002), the LPS is essential for both structural and functional integrity of the OM (Cardoso *et al.,* 2006). The remaining surface is among others covered with outer membrane proteins (Omp) (Vassen *et al*., 2019).

3.1.2. Structure of the *Brucella* LPS

Two types of LPS can be found at the bacterial surface, the smooth-LPS (S-LPS) and the rough-LPS (R-LPS). S-LPS molecules are composed of the lipid A, the core oligosaccharide, and an attached O-antigen polysaccharide (O-chain). R-LPS are characterized by the absence of the O-antigen polysaccharide (Moriyón & López-Goñi, 1998). When comparing the LPS of bacteria from the *Brucella* genus and other bacteria, it can be observed that the LPS shows a high heterogeneity. In fact, the LPS is highly conserved close to the membrane and gains on variations with distance to the membrane (Cardoso *et al.,* 2006).

The lipid A is the hydrophobic part of the LPS allowing its anchorage to the OM. It is the most conserved part of the LPS and is composed of a disaccharide backbone of diaminoglucose, amine and ester-linked long chain fatty acids (*Figure 4*). This sugar backbone binds to the core oligosaccharide forming the Lipid A-Core precursor (Cardoso *et al.,* 2006). Fatty acids of the lipid A can vary between bacteria in *Brucella* spp., but generally present C18 and C19 long chain acyls, as well as a very long C28 or C30 fatty acid, thereby longer than in other Gram-negative bacteria, and this length presumably extends the OM (Moreno & Moriyón, 2006).

Oppositely to the Gram-negative model *Escherichia coli* that presents a linear core, the core of *Brucella* is made out of branched oligosaccharides (*Figure 4*) (Conde-Álvarez *et al.,* 2012). Moreover, the core can be divided into two regions, the inner core and the outer core (Frirdich *et al.,* 2003). The inner core is formed out of mannose (Salvador *et al*., 2018) and 3-deoxy-D-manno-octulosonic acid (Kdo) with structural elements conserved between *Brucella* spp. and enterobacteria (Frirdich *et al.,* 2003). Whereas, the outer core presents a high degree of diversity even among the *Brucella* spp. and is constituted of glucose (Glc) and glucosamine (GlcN) (Salvador *et al*., 2018). The sugar backbone of the lipid A is covalently bound to the core oligosaccharide, thereby forming the Lipid A-Core precursor (Cardoso *et al.,* 2006).

The O-chain is an unbranched polysaccharide displaying a starter quinovosamine and two mannose residues, followed by an average chain length of 96 to100 glycosyl subunits of N-formylperosamine (Per) (Cardoso *et al.,* 2006; Bundle *et al.,* 1989). The presence of genes coding for Per polysaccharides and their ability to express this sugar on their cell surface is a characteristic that distinguishes *Brucella* from other bacteria (Moreno & Moriyón, 2006). The O-chain is not essential and is the component varying the most even between bacteria from the *Brucella* genus (Cardoso *et al.,* 2006). For examples, *B. abortus* presents a polysaccharide

structure with α-(1→2)-linked Per. While *B. melitensis* presents a polysaccharide structure of repeated blocks of four α-(1→2)-linked and one α-(1→3)-linked Per (Moreno & Moriyón, 2006).

It is to mention that the LPS of *E. coli* highly differs from the one found in *Brucella*. For instance, the lipid A is built of a disaccharide of glucosamine, while the core is composed of Kdo I and II, D-galactose, D-glucose and heptose subunits (D Ferguson *et al*., 2000). The O-chain strongly varies between different *E. coli* strains. However, in general, the sugar chain (0 to 50 sugar units) is composed of Galactose, N-acetylgalactosamine and N-acetylglucosamine, among others (Bagheri *et al*, 2011).

Most of *Brucella* strains present, in addition to the heterogeneity of the O-chain length, a heterogeneity of their bacterial surface with two types of LPS on their surface, R-LPS and S-LPS. This is true for *B. abortus* and *B. melitensis* and are so-called smooth-type *Brucella.* However, some exceptions exist with a few species presenting R-LPS exclusively, such as *B. ovis* and *B. canis*. Furthermore, it was observed that naturally smooth species can mutate into rough colonies under cultivation in laboratory condition (Braun W., 1946). As this smooth phenotype does not confer benefits *in vitro*, dissociation into rough colonies could be favored (Reeves P., 1995). Another example for dissociation in extracellular condition was suggested with findings of rough *B. microti* bacteria in environmental isolates (Al Dahouk *et al.,* 2012). Interestingly, *B. melitensis* rough variants have previously been isolated from goat milk, indicating that LPS dissociation in this smooth species does not alter *in vivo* survival in mammalian glands (Mancilla *et al*., 2012), but presumably imped virulence. Under host exposure, particularly macrophage exposure, selective pressure aids to maintain smooth phenotype (Mancilla M., 2016). While without selective pressure, mutations leading to loss of O-chain could be explained by the presence of mobile elements implicated in chromosomal deletion and could occur through recombination (Mancilla *et al*., 2010), an idea even more supported when considering that LPS loci are often located at recombination spots. Moreover, spontaneous mutations have also been observed, occurring for example in *wboA, wzm* or *manBA* and explaining the dissociation of strains into rough variants (Mancilla M., 2016).

3.1.3. Properties of *Brucella* LPS

The LPS core is a crucial structure for the survival of smooth and rough type *Brucella* spp. in infection (Soler-Lloréns *et al.,* 2014). The *Brucella* LPS is poorly endotoxic compared to enterobacteria (Haag *et al*., 2010), a characteristic shared by other alpha-proteobacteria. Indeed, intracellular proteobacteria such as *Bartonella, Rickettsia* or *Chlamydia* were found to present distinct properties related to their LPS structures (Lapaque *et al*., 2006). As the lipid A-core of *Brucella* distinguishes itself from the one of other Gram-negative bacteria, this could explain the difference in endotoxicity between species (Moreno & Moriyón, 2006). In fact, this low endotoxicity derives from the reduced susceptibility to stimulate host cells able to release immune mediators (Moreno & Moriyón, 2006) and can mainly be attributed to the lipid A-core (Haag *et al.,* 2010). Indeed, the lateral chain of the core has an important role for the virulence of the bacteria as this structure hampers the recognition of the LPS by the cells of the immune system. It is believed that the lateral chain is necessary to allow correct association of molecules, in order to impede binding of the anionic lipid A backbone and Kdo from the TLR4-MD2 receptor-coreceptor complex. In general, recognition by this complex triggers proinflammatory responses. Although this lateral branch allows immune system evasion, this component is non-essential, in contrast to the central core (Conde-Álvarez *et al.,* 2012).

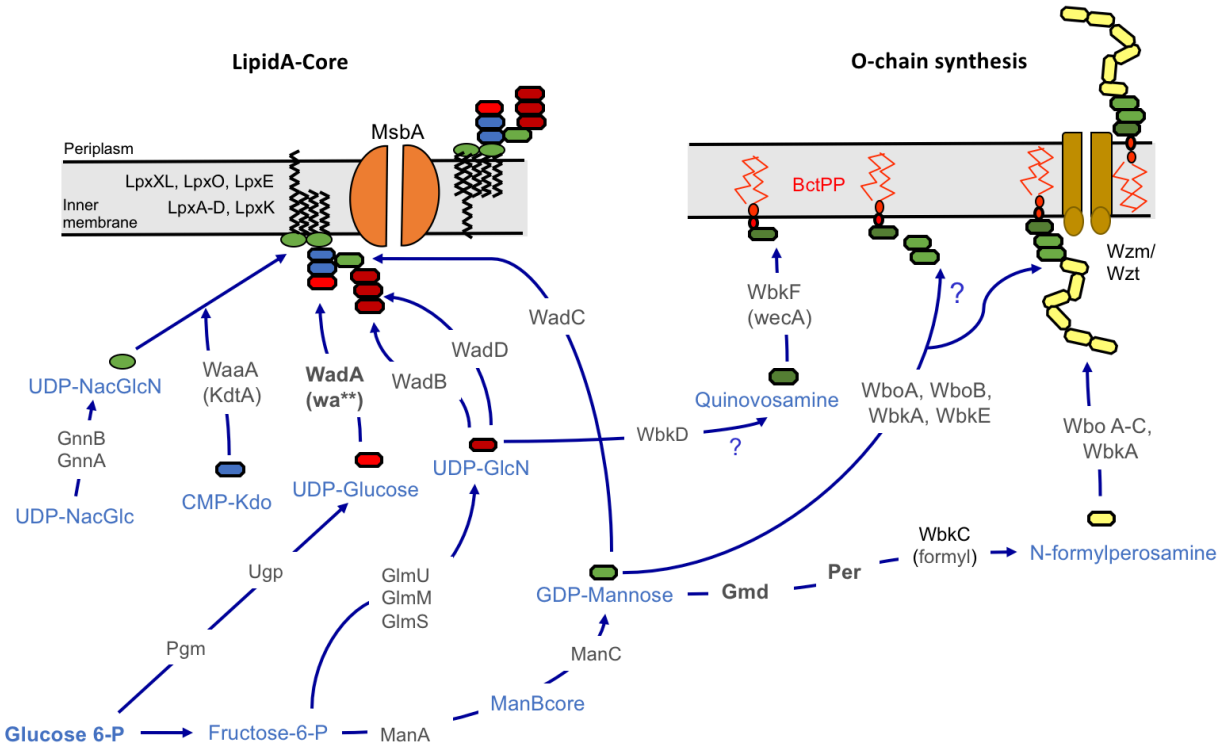

Figure 5 : Biosynthesis of the lipid A-core and the O-chain in *Brucella spp*. Glucose 6-phosphate is transformed into the different sugars (blue) composing the O-chain and the lipid A-core by means of several cytosolic proteins. The suggested proteins have been marked in grey and their suspected activity has been indicated by arrows. All have not been clearly characterized yet. Gmd is the first enzyme being involved only in the synthesis of the O-chain. Proteins from the Lpx group are thought to be involved in lipid A biosynthesis (Inspired by data kindly gifted by Conde-Alvarez R.).

Additionally, the LPS-type present on the bacteria seems to be closely related to the ability of *Brucella* to avoid interaction with complement components. In fact, the O-chain of *Brucella* presents a poor ability to activate the complement system, further contributing to the bacterial virulence and thus resistance to serum bactericidal activity of the innate immune system. These protective properties have been correlated to the presence of S-LPS, wherever rough mutants present a greater deposit of complement components on their bacterial surface, leading to macrophage activation due to opsonization and finally complement-mediated killing (Fernandez-Prada *et al.,* 2001). More precisely, the smooth strains show a greater resistance to complement then rough mutants (Stranahan & Arenas-Gamboa, 2021). Moreover, the S-LPS of *Brucella* appears to be 200 to 2,000 times less active for complementation properties than the LPS of *Salmonella* species (Moreno & Moriyón, 2006). This complement-mediated lysis could explain why many rough mutants present an avirulent phenotype in animal models (Ugalde *et al*., 2000), as well as low zoonotic potential (Atluri *et al.,* 2011).

Furthermore, the absence of the O-chain modifies the membrane topology since the O-chain typically masks the ionic groups present on the lipid A-core, as well as the charges present on other proteins of the membrane (Moreno & Moriyón, 2006). This change in topology could be an explanation to the reports that *Brucella* rough strains tend to form aggregates (Bello *et al.,* 2015). Moreover, it was observed that the O-chain confers resistance to polycations. Indeed, the polysaccharide limits access to the anionic lipid A-core in smooth strains. While rough mutants evidentially present a negatively charged surface at physiological pH due to the absence of the O-chain. Besides, the absence of the O-chain facilitates the exposure of Omps to the environment. Indeed, accessibility of antibodies targeting Omps is stronger in rough strains compared to smooth strains (Moreno & Moriyón, 2006).

The LPS is also suggested to be responsible for the membrane permeability to hydrophobic molecules. Indeed, the OM of *Brucella* present a stronger permeability to hydrophobic compounds than other Gram-negative bacteria such as *Salmonella.* It was proposed that this increased permeability, and resistance to polycations, could be explained by the low number of negative charges on the *Brucella* LPS compared to the common LPS of other Gram-negative bacteria, as well as the longer fatty acids anchoring the LPS which could provide further stability (Freer *et al.,* 1996).

3.1.4. LPS synthesis

The various proteins involved in the LPS synthesis of *E. coli* have been previously identified and characterized (Whitfield & Trent, 2014). The majority of the LPS synthesis pathway and the intervening transmembrane proteins can be transposed to *Brucella,* with some exceptions. In fact, some proteins were reported to be specific to *Brucella* and its close relatives from *Ochrobactrum.* Other proteins have not been identified yet and every candidate suggested has not been verified (Conde-Álvarez *et al*., 2018). All the genes involved in LPS biosynthesis are distributed on the two circular chromosomes that constitute the *Brucella* genome. However, most of them are clustered on the chromosome I (Haag *et al.,* 2010).

The LPS biosynthesis starts in the cytosol where the O-chain precursor and the lipid A-core precursor sugar units are formed, starting from glucose 6-phosphate under the control of multiple proteins (*Figure 5*).

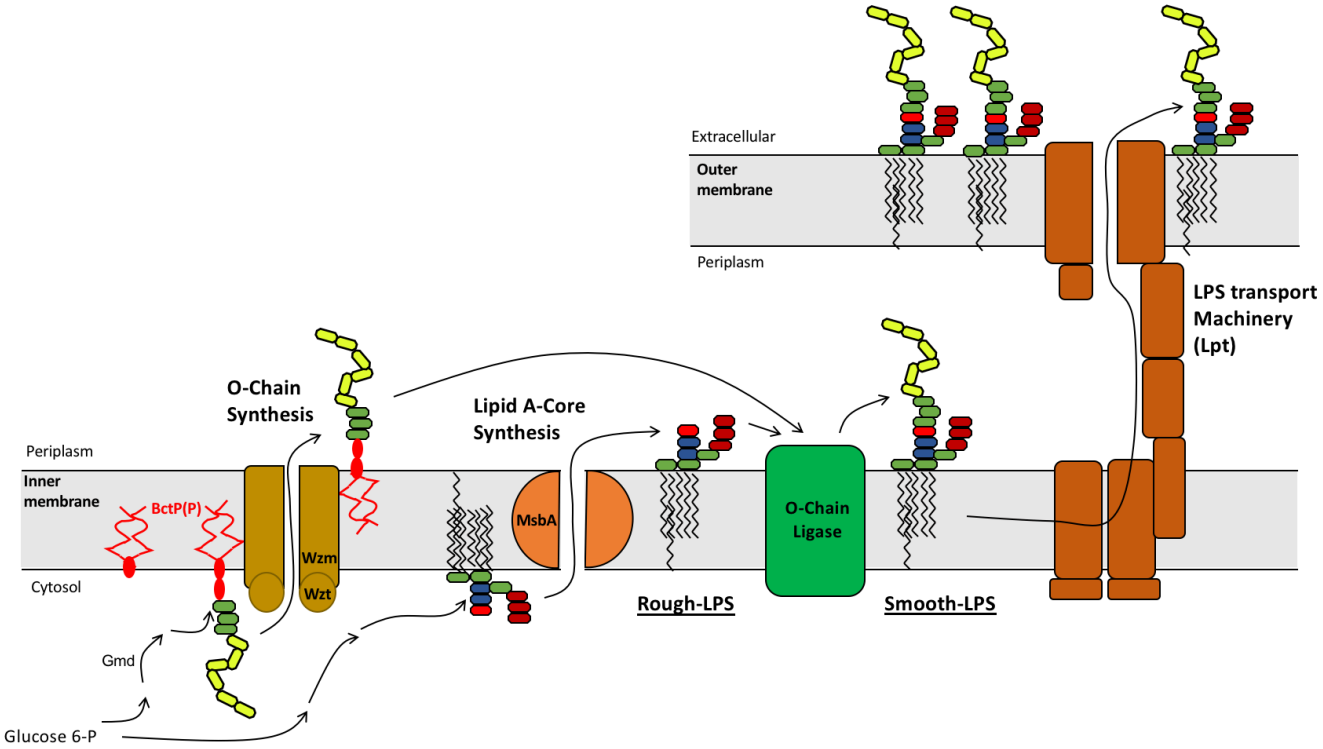

Figure 6 : Biosynthesis of R-LPS and S-LPS in *B. abortus*. (Inspired by Burgos *et al*., 2019 and unpublished data kindly gifted by Conde-Alverez R.) The pathway starts in the cytosol with Glucose 6-phosphate, which is transformed into the different sugars composing the O-chain and the lipid A-core by means of several cytosolic proteins. Gmd is the first enzyme being involved only in the synthesis of the O-chain. The resulting O-chain is covalently linked to the lipid carrier bactoprenol (BctPP), giving rise to the O-chain form that will be translocated to the oute leaflet of the inner membrane (IM) through an ABC transporter composed of Wzm and Wzt. On the other hand, several proteins are implicated in the formation of the lipid A-core, which binds to the IM through the fatty acids of the lipid A. The lipid A-core is translocated to the outer leaflet of the IM by an ABC transporter called MsbA. This lipid A-core component represents the R-LPS. By means of an O-chain ligase, unknown in *B. abortus*, the quinovosamine (Quin) of the Oantigen, previously linked to the BctPP, can be ligated to the glucose (Glc) of the lipid A-core and form the S-LPS. This SLPS is thereby formed of the three components: lipid A, core and O-chain. The synthesized LPS, smooth and rough, are translocated to the Outer membrane (OM) by the Lipopolysacharide transport machinery (Lpt). Man: mannose; NGlcN: diaminoglucose; GlcN: glucosamine; Kdo: 3-deoxy-D-manno-octulosonic acid; Per: N- formylperosamine

The assembled lipid A precursor is in the inner leaflet of the IM due to its hydrophobic fatty acids chain and presents its hydrophilic sugar backbone to the cytosol. The synthesis of these two parts involves Lpx proteins (Conde-Álvarez *et al*., 2018). Next to this, the synthesis of the core of *Brucella* depends on various cytosolic proteins. Indeed, one by one, the core sugars are added under the activity of these proteins on the lipid A sugar backbone in a specific order, thereby forming the lipid A-core (*Figure 5*) (Cardoso *et al.,* 2006). Indeed, in *Brucella* it was proposed that proteins involved in the lateral core synthesis were WadB, WadC and WadD (Fontana *et al*., 2016; Salvador *et al.,* 2018). The central core branch is under the control of WaaA adding the two Kdo units, and finally WadA (*wa***) adding the last core sugar, glucose (Glc) (*Figure 4 + 5*) (Cardoso *et al.,* 2006; Salvador *et al.,* 2018). Once assembled, the lipid A-core precursor is transported to the periplasmic side via an essential ABC transporter named MsbA (*Figure 6*) (Han *et al.,* 2012).

On the other hand, the synthesis of the O-chain starts from a glucose-6-phosphate into GDP-mannose in the cytoplasm. The GDP-mannose dehydratase (Gmd), specific to *Brucella*, is the first enzyme involved exclusively in the O-chain precursor synthesis (*Figure 5*). Therefore, in the absence of Gmd, no O-chain can be produced (Haag *et al*., 2010). It is suggested that *Brucella* spp. present a few mannosyltransferases and N-formyl-perosaminyltransferases involved in the O-chain synthesis in order to produce the long chain polysaccharide (*Figure 5*) (Cardoso *et al.,* 2006).

In *E. coli*, when it is synthesized, the O-chain is bound to a lipid carrier, the undecaprenyl pyrophosphate also called bactoprenol (BctP) (Jorgenson & Young, 2016). BctP is a 55-carbon isoprenoid and represents the dephosphorylated product of undecaprenyl pyrophosphate, which is produced by undecaprenyl pyrophosphatase synthetase (UppS). It was established that BctP plays a major role in the transport of the O-chain (*Figure 6*) (Pérez-Burgos *et al.,* 2019). However, the O-chain is not the only component using the BctP as a lipid carrier during its synthesis pathway. Indeed, during the synthesis of the periplasmic peptidoglycan layer, the peptidoglycan monomers (NAG-NAM-pentapeptide) also bind to BctP to be trafficked from the cytosol to the periplasm. The BctP thereby contributes to both LPS and peptidoglycan syntheses (Slade *et al.,* 2019; Pérez-Burgos *et al.,* 2019). Moreover, other components such as the synthesis of the enterobacteria common antigen, capsular polysaccharides, exopolysaccharides and other carbohydrates also require the action of BctP in *E. coli* (Jorgenson & Young, 2016). These components, including the O-chain, are indeed synthesized in the cytosol by binding individual sugar units to the BctP. It has been described in *E. coli* that mutations of the BctP recycling results in accumulation of BctPP-linked intermediates and thus to deleterious repercussions. BctPP sequestration could lead to an accumulation of toxic intermediates, or indirect effects due to a reduced availability in BctP (Jorgenson & Young, 2016). The binding to a lipid carrier enables the O-chain to be translocated through the IM to the periplasmic leaflet (Jorgenson & Young, 2016) through an ABC transporter formed of Wzm and Wzt proteins (*Figure 6*) (Pérez-Burgos *et al.,* 2019). As Wzm and Wzt are involved in the export of the O-chain, the deletion of at least one of these proteins leads to rough mutants and sometimes to an accumulation of the polysaccharide linked to the lipid carrier on the cytosolic leaflet of the IM (Moreno & Moriyón, 2006).

3.1.5. S-LPS and the O-chain ligase

By the action of the ABC transporters MsbA and Wzm/Wzt, the Lipid A-Core and the O-chain are respectively translocated to the outer leaflet of the IM. At this point, an O-chain ligase performs the ligation of the O-chain to the lipid A-core, on the terminal Glc, thereby forming a S-LPS molecule (*Figure 6*). Importantly, in absence of the last core sugar Glc, it is impossible to ligate the O-chain to the core. While many proteins involved in the LPS biosynthesis have been characterized, such as the ABC transporters MsbA, Wzm/Wzt and the Lpt system, the O-chain ligase enabling the ligation of the O-chain to the lipid A-core remains unknown in *B. abortus*.

Regarding *E. coli,* it has been described that WaaL acts as the O-antigen ligase during the LPS synthesis and furthermore the only protein presumed to be required for the O-chain ligation reaction (Raetz & Whitfield, 2002). This protein is a membrane protein formed of multiple transmembrane domains and two periplasmic loops (Han *et al.,* 2012). The O-chain ligase activity of WaaL consists of using the BctPP linked to the O-chain as donor and linking the first O-chain sugar (NAG) to the last LPS core sugar (Glc) (Pérez *et al*., 2008).

When looking at the WaaL structure, it was determined that the protein presents one large periplasmic loop and a second smaller periplasmic loop. Compelling data suggests several critical catalytic amino acids in these two periplasmic loops and thereby exposed to the periplasmic space, which could form a putative catalytic center necessary for the interaction of the donor and acceptor molecules (Ruan & Valvano, 2013). This interaction is crucial for the subsequent release of the O-chain from the BctPP (Han *et al.,* 2012). It is suggested that the three residues arginine (Arg)-215, histidine (His)-338 and aspartic acid (Asp)-389, three charged amino acids located in the periplasmic loops, are crucial for the ligation reaction of WaaL, as alanine replacement of these residues led to a nonfunctional WaaL protein. With alanine being a residue with a small hydrophobic side chain ($-CH_3$). However, replacement of Arg-215 by a positively charged amino acid, the lysine, did not alter the protein functionality, highlighting the importance of these charges in the periplasmic loop, and further suggesting that this Arg is not directly involved in catalysis. Every WaaL homolog presented a positive charge at the position corresponding to Arg-215 in the small periplasmic loop, and one corresponding to His-338 in the large periplasmic loop. It was proposed that these positively charged amino acids located at the periplasmic loops are required for the O-chain ligation, as these might enable to stabilize the BctP phosphate after cleavage of the O-chain (Ruan *et al*., 2012). Additionally, reports suggest that the ligation activity occurs in absence of ATP and magnesium ions. While the exact mechanism of action has not been described yet, the accessible data strongly suggest a common reaction mechanism with features shared with ion-independent inverting glycosyltransferases (Ruan *et al*., 2012).

WaaL homologs have also been described as the O-chain ligase in other Gram-negative species, such as *Myxococcus xanthus*, a Gram-negative deltaproteobacterium (Pérez-Burgos *et al.,* 2019), in *Vibrio cholerae,* in *Salmonella enterica* (Schild *et al.,* 2005), in *Helicobacter pylori* (Li *et al*., 2017) and in *Pseudomonas aeruginosa* (Islam *et al*., 2010) among others. These homologs, although they present some divergence in amino acid sequence, are suggested to present a similar topology, with several transmembrane domains and the presence of a large periplasmic loop (Raetz & Whitfield, 2002).

Once synthesized, both S-LPS and R- LPS are translocated to the OM using the LPS translocation pathway, also called the Lpt system. In *E. coli*, this complex is formed out of 7 essential proteins that span the whole envelope (Han *et al.,* 2012). Concerning *Brucella* spp., a conserved homolog of this Lpt protein complex has been identified (Sternon *et al*., 2018).

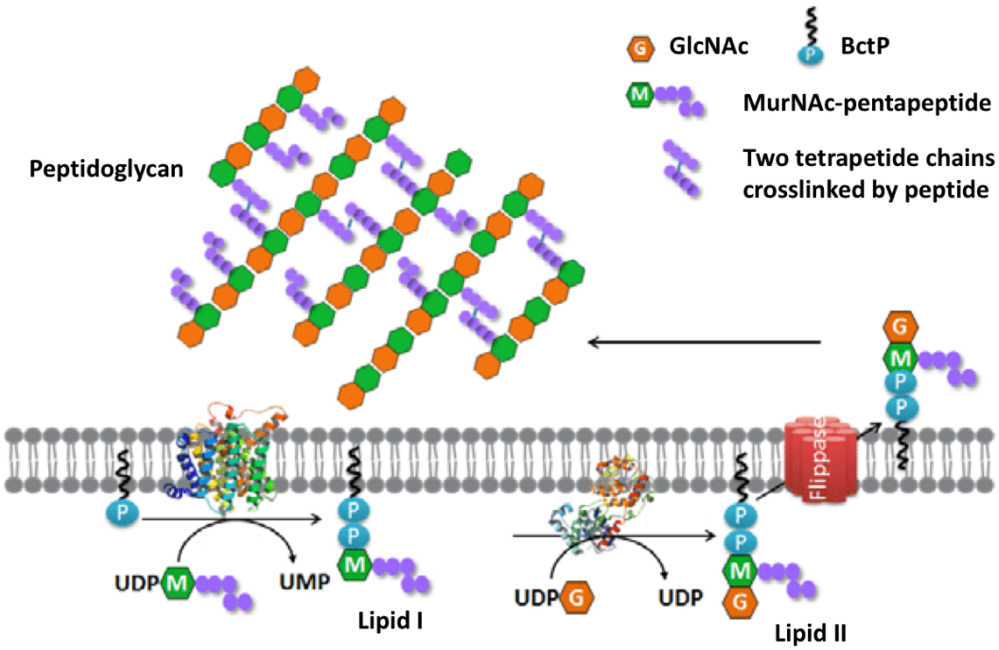

Figure 7 : Peptidoglycan synthesis pathway steps at the IM. In *E. coli*, PG is composed of polysaccharides of N-acetylglucosamine (NAG or GlcNAc) and N-acteylmruamic acid (NAM or MurNAc) subunits The PG precursor Lipid II, presenting two glycan subunits (NAG and NAM, depicted by G and M, respectively), is synthesized on the cytosolic leaflet and binds through its phosphate to the BctP. The lipid II is then flipped in the IM thanks to MurJ. (Modified from Liu & Breukink, 2016).

3.1.6. Outer membrane proteins and their interaction with other components of the membrane

Outer membrane proteins (Omp) present in the OM of bacteria are mostly β-barrel proteins or lipoproteins that widely vary in function. Examples of functions are nutrient intake, chemical exchange or detection of chemical signals among others (Wang G., 2008).

In the *Brucella* genus, Omp can be divided into three separate groups depending on their molecular weight. Group 1 contains proteins of molecular weight of 88 or 94 kDa (Moreno & Moriyón, 2006). Omp1 (BamA) and LptD are proteins from this group and are known to be required for activities inside transport machineries (Bialer *et* al., 2019; Sperandeo *et al*., 2017; Chng *et al.,* 2010). Group 2 contains two porins, channel proteins allowing passive diffusion, named *omp2a* and *omp2b* and of 36-38 kDa, which can be found in all *Brucella* species. Omp2b is a porin located in the OM that interacts with the peptidoglycan layer. Due to its localization, the porin manifestly spans the OM, further contributing to the membrane's permeability. Regarding their function, it is known that small hydrophilic molecules can enter the periplasm by passing through Omp2 porins (Moreno & Moriyón, 2006). The Omp2b porin is heterogeneously distributed at the OM (Vassen *et al.,* 2019). Interestingly, the membrane presenting Omp2b where shown to be enriched for R-LPS, suggesting a tight interaction between both molecules (Vassen *et al.,* 2019). Moreover, it is known that these cationic proteins additionally neutralize the negative charges of the LPS, represent the majority of the OM surface (Moreno & Moriyón, 2006) and that LPS molecules show strong binding to outer membrane proteins through the lipid A (Cardoso *et al.,* 2006). It is possible that interaction with R-LPS favors activity of Omp2b, giving a potential explanation for the presence of this LPS type for example by favoring diffusion to the porin by the absence of O-chains.

Group 3 contains proteins (31-34 kDa and 25-27 kDa) called Omp31, Omp3a (or Omp25) and Omp3b (or Omp22), suggested to play an unknown structural role. While Omp31 is absent in *B. abortus*, Omp25, or Omp3a, are highly conserved among *Brucella* species. The proteins coded by *omp3a* and *omp3b* families present a molecular weight surrounding 26 kDa and were suggested to interact firmly with the peptidoglycan layer, as well as the LPS (Moreno & Moriyón, 2006). This interaction was suggested by extraction procedures a few decades ago (Moriyón & López-Goñi, 1998). Experimental data supporting this idea was presented with discoveries of covalent linkage of PG and Omps in *Brucella* spp. (Godessart *et al.,* 2021).

3.2. PG synthesis and function

The PG layer located in the periplasm is crucial to the bacteria as it allows adaptation to osmotic pressure, it is an anchoring site for various proteins and it is involved in cell division (Slade *et al.,* 2019). Moreover, it plays a major role in maintaining the bacterial shape. The PG layer structure is referred to as 'sacculus' and is formed of chains of glycans connected by short peptides. The synthetized PG sacculi further interact with proteins located in the OM to allow stability. Briefly, PG precursors, called Lipid II, are synthetized in the cytosol under the control of various proteins and are constituted of two glycan units, short peptide stems and a phosphate (*Figure 7*). The phosphate enables a diphosphate binding to the BctP on the inner leaflet of the IM. The lipid II-BctPP is flipped to the periplasmic side of the IM. There, peptidoglycan glycosyltransferases enable polymerization of the glycan units to form a glycan chain. At the same time, transpeptidases are in charge of crosslinking the peptides (Egan *et al.,* 2020).

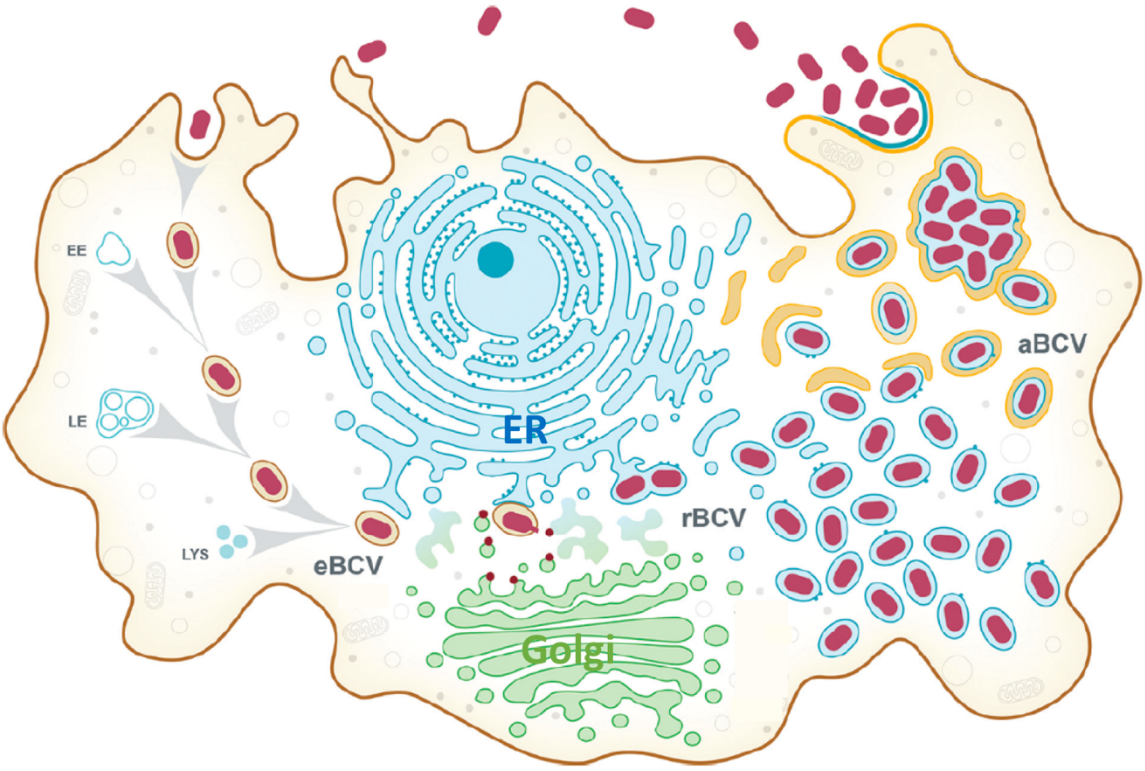

Figure 8 : Intracellular trafficking of *Brucella* inside host dendritic cells. After internalization through membrane ruffling, until 8h PI, the bacteria reside in a BCV that follows the endosomal pathway, interacting with early (EE) and late (LE) endosomes and progressively maturating into an eBCV. This eBCV is acidified and expression of the VirB T4SS is induced, enabling release of effector proteins (red dots) that allow interaction of the BCVs with the ER and the Golgi (from 8 to 12h PI). Inside this rBCV, bacteria replicate extensively 12 to 48h PI. Afterwards, rBCVs become aBCVs by being captured in autophagosome-like structures, that enable extracellular release of the bacteria (Celli J., 2019).

In *Brucella*, the glycan chains are formed of disaccharides of NAG and NAM, synthetized starting from fructose-6-phosphate (Godessart *et al.,* 2021). It was proposed the interaction with the OM are greater in *Brucella,* suggesting a greater stiffness of this genus compared to other Gram-negative bacteria. Indeed, it was observed that heat inactivation led to the degradation of the IM; yet the OM kept its morphology (Rubbi C., 1991). One possible explanation for this observation could be a significant association of the Omps with the peptidoglycan layer, as well as the long fatty acid chains of the Lipid A (Moreno & Moriyón, 2006).

While these interactions with Omps are non-covalent in bacteria such as *E. coli* (Egan *et al.,* 2020), it was shown that the PG sacculi bind covalently to certain Omps in *B. abortus*. In fact, the PG sacculi are crosslinked to the N-terminal part of Omp25 and Omp2b. Such an interaction was as well observed in *Agrobacterium tumefaciens* and its homologous proteins of Omp25 and Omp2b, suggesting that this PG-OM organization could be shared by the Rhizobiales (Godessart *et al.,* 2021).

4. *Brucella* infection

4.1. *Brucella*: intracellular facultatively extracellular pathogens

The natural niche of *Brucella* spp. are mammalian host cells. However, the bacteria are able to proliferate *in vitro* in rich culture medium. They can thereby be characterized as intracellular facultatively extracellular pathogens (Moreno & Moriyón, 2006). Bacteria enter the host cell in various infection ways, such as through skin abrasions or through mucosal surfaces either from the digestive or respiratory tract. *Brucella* starts its infection by entering host macrophages or dendritic cells, both being phagocytic cells. Once infected, a fraction of these cells is able to migrate to regional lymph nodes and thereby cause systemic infection by bacterial spreading. Finally, the disease becomes chronic by the bacteria staying inside the myeloid lineage cells, for example macrophages in the liver and spleen (Atluri *et al.,* 2011). Moreover, during pregnancy, persisting bacteria found in the lymph nodes and the spleen are able to enter the bloodstream and subsequently the gravid uterus. Thereby, *Brucella* is able to invade trophoblastic cells and proliferate in placental trophoblasts. This infection of pregnant females is behind the spontaneous abortions characterizing brucellosis (Atluri *et al.,* 2011).

4.2. The intracellular life cycle of *Brucella* species

Brucella species have coevolved with their specific mammalian hosts over a long period of time which has favored the bacteria to develop adaptations to intracellular environment. In fact, these microorganisms manage to control their intracellular trafficking, create a replication niche inside host macrophages and enable evasion from the host immune system (Celli, J., 2006). Infection of placental trophoblasts by *Brucella* follows the association with the endosomal-RE pathway, similar to macrophage invasion (Atluri *et al.,* 2011; Salcedo *et al*., 2013).

Brucella survive inside the macrophage by staying inside a membrane-bound compartment that is formed during the internalization of the bacteria (*Figure 8*), called *Brucella*-containing vacuole (BCV) (Celli, J., 2006). The internalization is generated by membrane ruffling engulfing the bacteria by macropinocytosis (Watarai *et al.,* 2002). During this first stage of the intracellular cycle (0 to 8 hours postinfection (PI), depending on the cell type infected), the BCV traffics along the unaltered endocytic pathway. Therefore, it was named endosomal BCV (eBCV). This eBCV acquires early and late endosomal markers, such as respectively EEA1 (early endosomal antigen 1) (Celli J., 2019) and the Rab7 GTPase (Starr *et al.,* 2008), a small GTPase, on its journey upon interaction with endosomes. These transient interactions are

followed by interactions with lysosome and acidification of the vacuole to a pH of 4.5, together with the acquisition of the lysosomal associated-protein 1 (LAMP1), similar to the maturation of phagolysosomes during the usual endocytic pathway. However, *Brucella* inhibits fusion of the vacuole with terminal digestive lysosomes, avoiding lysosomal degradation. In tight connection to the acidification of the BCVs, contribution of Rab7 is as well needed to promote expression of the VirB type IV secretion system (T4SS) (Celli J., 2019).

Between 8 to 12 hours PI, the vacuole heads to the endoplasmic reticulum (ER), losing its endosomal markers which are replaced by ER-membrane associated markers. Mediated by the effector proteins translocated by the VirB T4SS, eBCVs interact with ER exit sites and acquire ER and Golgi apparatus-derived membranes (*Figure 8*). These changes are accompanied with the acquisition of structural and functional ER features. At this point, 12 to 48 hours PI, fusion between BCVs and ER leads to the establishment of a bacterial replication niche, thereby the BCV were named replicative BCV (rBCV) (Celli J., 2006). It is suggested that bacterial growth and replication are promoted by intracellular conditions provided by the rBCV and an important reorganization of the ER network of the host. Recent data suggests that rBCVs are closely interacting with the host secretory pathway, as these vacuoles connect to the ER and interact with the Golgi apparatus vesicular traffic. The T4SS is essential for virulence and intracellular replication, as deleting the *virB* operon leads to the inability to convert eBCVs into rBCVs. *Brucella* is thereby unable to establish a replication niche and is degraded in the phagolysosome after a period of survival. Taking this into consideration, the T4SS plays a role as a major virulence factor in *Brucella* (Celli J., 2019).

Between 48 to 72 hours PI, the BCVs turn into so-called autophagic BCVs (aBCVs) that are surrounded by membrane structures in a T4SS-dependent manner, leading to the formation of multimembrane vacuoles containing the newly replicated bacteria. These aBCVs interact with the host cell membrane, followed by bacterial release from infected cells (*Figure 8*). These bacteria can then infect new host cells, completing the *Brucella* intracellular cycle (Celli J., 2019).

4.3. The LPS type influences intracellular trafficking

The LPS type present on the bacterial surface influences the macrophage phagocytosis. Indeed, during early infection, bacteria enter the cell through a lipid raft-mediated way. It has been proposed that one of the macrophage receptors accountable for *Brucella* uptake is the Class A scavenger receptor (SR-A) (Atluri *et al*., 2011), which interacts with the S-LPS and allows the bacteria relocation in BCVs (Celli, J., 2006). It has been noted that the periplasm of *Brucella* contains soluble components, such as high amounts of cyclic β-glucans (Moreno & Moriyón, 2006). Interestingly, it is suggested that cyclic-β-1,2-glucans (CβGs) play a role during the intracellular trafficking, as mutants lacking these polymers showed a reduced intracellular replication. CβGs are believed to present a lipophilic cavity, enabling them to extract cholesterol from membranes; cholesterol being a major component of lipid rafts (Haag *et al.,* 2010). It is proposed that due to their impact on lipid rafts present on phagosomes, CβGs may affect maturation along the endocytic pathway, possibly avoiding fusion with lysosomes, and allow directing of the BCVs to the ER (Celli J., 2006; Haag *et al.,* 2010).

In case of rough mutants, entry is not mediated by lipid rafts, but by simple phagocytosis. This could enable a faster introduction of the bacteria inside the macrophage compared to the lipid raft-mediated entry (Haag *et al.,* 2010). However, these R-LPS type bacteria find themselves inside BCVs lacking lipid raft markers usually associated with a wild type strain. Rough mutants can thereby be trafficked through the physiological degradative endocytic pathway and targeted by terminal digestive lysosomes, leading to fusion of both

organelles and lastly degradation of the bacteria (Celli, J., 2006). Therefore, R-LPS type bacteria present a greater entry in macrophages, but a reduced survival (Haag *et al.,* 2010). The S-LPS is thereby fundamental regarding infection and is thus major virulence factor (Salvador *et al*., 2018). Indeed, recognized smooth-type *Brucella* are known for their stronger virulence and ability to infect human beings. Whilst rough-type species show a low pathogenicity (Tsolis *et al.,* 2009; Atluri *et al*., 2002).

OBJECTIVES

The general objective of this master thesis was to try to identify the potential O-chain ligase(s) of *B. abortus* by focusing on two putative candidates obtained by PFAM domain similarities, *waaL* and *wadA*. Thereby, markerless deletion mutants for those two genes (Δ*waaL* and Δ*wadA*) will be constructed by allelic replacement in a WT background and characterized for S-LPS and R-LPS phenotype. This characterization will be executed by using Western blotting and immunofluorescence microscopy, both with antibodies recognizing the two forms of LPS. Moreover, it will be pursued by the analysis of bacterial morphology, growth profile in rich liquid culture medium and survival during infection. Considering the first results we obtained when working on *wadA*, i.e. its essentiality in *B. abortus*, we decided to widen the work by constructing and characterizing a Δ*wadA* mutant in *B. melitensis* as well. By such means, this work includes data obtained on the two species *B. abortus* and *B. melitensis*. Our plan was also to analyze domain composition of the putative O-antigen ligase(s), as well the generation of catalytically dead mutant. Overall, the objective of this work is to identify the main missing enzyme in the S-LPS biosynthesis pathway, and to initiate its characterization.

```
Escherichia coli      ------------------------------------------------------------  0
Brucella abortus      MSNIVTRTRTDARMPDATGPQARIRRIALVIASVIFGVLLISFRPFTPAGGAETETGGDI  60

Escherichia coli      ------------------------------------------------------------  0
Brucella abortus      INQLGFSCVGAVALASMAMFANLRKLAGIIRPGWLVMLVFLFASIFASSDPATAVRGVLL  120

Escherichia coli      ------------------------------------------------------------  0
Brucella abortus      TTVGIVAIIAVLVLPQDGDGYSALLVSVASVVIVISYAGVVLLPSLGTHGADAIEPQNSF  180

Escherichia coli      ------------------------------------------------------------  0
Brucella abortus      LWRGVFSHKNIAGPVMAVFAFAGLYLWRRGWKTSGLLIGLSALGFVSQTGSKTTMALVPF  240

Escherichia coli      ------------------------------VGTLGVEFIPPFKAYITENMPDFTYTGRTQL  31
Brucella abortus      AMLLVVLPGLMGLRKLTAGLIFAIQLAFATFTFGVVLFEPIRRLVENMDVDATFTGRVSI  300
                                                    . *:** :: *::  : :   * *:***.::

Escherichia coli      WRFVSELIAQRPWTGFGFESVWGSPTVRDTYPAFDQTWDVRGIVNAHNGYLDIAVTMGLP  91
Brucella abortus      WKFALEALSKRPWTGYGYESFWSSAYARHAARPYYLDWDVRGIVHGHNSYLDVAMTMGIP  360
                      *:*. * :::*****:*:**.*.*  .*.:   :   *******:.**.***:*:***:*

Escherichia coli      ALALACIAMMIVPAIDYLRVPKRRENIYLSDLFMMMIFFGAQNAFLESFFFKRAEPVWLL  151
Brucella abortus      ALLCAIAVIIVMPLVHYARCRPVRENMLLADFFLMIVLFGTLNAMMESFFFRRMDPVWLT  420
                      **  *  .::::* :.* *    ***: *:*:*:*:::**: **::*****:* :****

Escherichia coli      FFLAAFGMRYAARFPLKSPGEK    173
Brucella abortus      LILAIFGLGMTAKVVIPKRSV-    441
                      ::** **:  :*:. : . .
```

Figure 9: Sequence alignment between the WaaL sequence in *E. coli* (EFG6100940; BLASTp) and the WaaL homolog (BAB2_0106) found in *B. abortus*. The *(asterisk) indicates positions which have a fully conserved residue. The : (colon) indicates conservation between groups of strongly similar properties, roughly equivalent to scoring > 0.5 in the Gonnet PAM 250 matrix. The . (period) indicates conservation between groups of weakly similar properties, roughly equivalent to scoring =< 0.5 and > 0 in the Gonnet PAM 250 matrix.

```
intermedia      MSNIATRTRTDARSDVAAQANVRATVRTIALVIATITFCILLISFRPFNPLSAAASGDAS  60
ovis            MSNIVTRTRTDARMPDAT--GPQARIRRIALVIASVIFGVLLISFRPFTPAGG---AETE  55
vulpis          MSNIATRTRTDASMPDAT--GPQARIRRIALVIASVIFGVLLISFRPFTPAGG---AETE  55
inopinata       MSNIVTRTRTDARMPDAL--GPQARIRRIALVIASVIFGVLLISFRPFTPAGG---AETE  55
abortus         MSNIVTRTRTDARMPDAT--GPQARIRRIALVIASVIFGVLLISFRPFTPAGG---AETE  55
melitensis      MSNIVTRTRTDARMPDAT--GPQARIRRIALVIASVIFGVLLISFRPFTPAGG---AETE  55
canis           -------------MPDAT--GPQARIRRIALVIASVIFGVLLISFRPFTPAGG---AETE  42
                                  *   . :* :* ******:: * :********.* ..   .::.

intermedia      GGGDAINQLGFGCLGAVSLLSLAMFADPKKVAKIVSPGWLLMFAFLLASVFASPDPATAI  120
ovis            TGGDIINQLGFSCVEAVALASMAMFTNLRKLAGIIRPGWLVMLVFLFASIFASSDPATVV  115
vulpis          TGGDIINQLGFSCVGAVALASMAMFANLRKLAGIIRPGWLVMLVFLFASIFASSDPATAV  115
inopinata       TGGDIINQLGFSCVGAVALASMAMFANLRKLASIIRPGWLVMLVFLFASIFASSDPATAV  115
abortus         TGGDIINQLGFSCVGAVALASMAMFANLRKLAGIIRPGWLVMLVFLFASIFASSDPATAV  115
melitensis      TGGDIINQLGFSCVGAVALASMAMFANLRKLAGIIRPGWLVMLVFLFASIFASSDQATAV  115
canis           TGGDIINQLGFSCVGAVALASMAMFANLRKLAGIIRPGWLVMLVFLFASIFASSDPATAV  102
                 *** ******.*: **:* *:***:: :*:* *: ****:*:.**:**:*** * **.:

intermedia      RGVLLTMIGILTVIAVLSLPQDGDAYSAMLVTVASIVIVVSYAGVVLLPNLGTHGADALE  180
ovis            RGVLLTTVGIVAIIAVLVLPQDGDGYSALLVSVASVVIVISYAGVVLLPSLGTHGADAIE  175
vulpis          RGVLLTTVGIVAIVAVLALPQDGDGYSALLVSVASVVIVVSYAGVVLLPSLGTHGADAIE  175
inopinata       RGVLLTTVGIVAIIAVLVLPQDGDGYSALLVSVASVVIVVSYAGVVLLPSLGTHGADAIE  175
abortus         RGVLLTTVGIVAIIAVLVLPQDGDGYSALLVSVASVVIVISYAGVVLLPSLGTHGADAIE  175
melitensis      RGVLLTTVGIVAIIAVLVLPQDGDGYSALLVSVASVVIVISYAGVVLLPSLGTHGADAIE  175
canis           RGVLLTTVGIVAIIAVLVLPQDGDGYSALLVSVASVVIVISYAGVVLLPSLGTHGADAIE  162
                ****** :**::::*** ******.***:**:***:***:*********.*********:*

intermedia      PQNAYLWRGVFTHKNIAGPVMAAFSFAGVYLWRRGWRVSGFLIAVSALVFVSQTGSKTTA  240
ovis            PQNSFLWRGVFSHKNIAGPVMAVFAFAGLYLWRRGWKTSGLLIGLSALGFVSQTGSKTTM  235
vulpis          PQNSFLWRGVFSHKNIAGPVMAVFAFAGLYLWRRGWKTSGLLIGLSALGFVSQTGSKTTM  235
inopinata       PQNSFLWRGVFSHKNIAGPVMAVFAFAGLYLWRRGWKTSGLLIGLSALGFVSQTGSKTTM  235
abortus         PQNSFLWRGVFSHKNIAGPVMAVFAFAGLYLWRRGWKTSGLLIGLSALGFVSQTGSKTTM  235
melitensis      PQNSFLWRGVFSHKNIAGPVMAVFAFAGLYLWRRGWKTSGLLIGLSALGFVSQTGSKTTM  235
canis           PQNSFLWRGVFSHKNIAGPVMAVFAFAGLYLWRRGWKTSGLLIGLSALGFVSQTGSKTTM  222
                ***:*******:**********.*:***:*******:.**:**.:*** **********

intermedia      ALVPLAMLLVITPGLFGLRFLAPVAVFTIQFLLALFTFGTVLFEPMHQLVLQLDVDPTFT  300
ovis            ALVPFAMLLVVLPGLMGLRKLTAGLIFAIQLAFATFTFGVVLFEPIRRLVENMDVDATFT  295
vulpis          ALVPFAMLLVVLPGLMGLRKLTAGLIFAIQLAFATFTFGVVLFDPIRRMVENMDVDATFT  295
inopinata       ALVPFAMLLVVLPGLMGLRKLTAGLIFAIQLAFATFTFGVVLFEPIRRMVENMDVDATFT  295
abortus         ALVPFAMLLVVLPGLMGLRKLTAGLIFAIQLAFATFIFGVVLFEPIRRLVENMDVDATFT  295
melitensis      ALVPFAMLLVVLPGLMGLRKLTAGLIFAIQLAFATFTFGVVLFEPIRRLVENMDVDATFT  295
canis           ALVPFAMLLVVLPGLMGLRKLTAGLIFAIQLAFATFTFGVVLFEPIRRLVENMDVDATFT  282
                ****:*****: ***:*** *:   :*:**: :* * **.***:*::::* ::*** ***

intermedia      GRTSIWAFAVEALSQRPWTGFGYESFWGTPIAKQAANPYYLDWDVRGIVHGHNGYLDIAL  360
ovis            GRVSIWKFALEALSKRPWTGYGYESFWSSAYARHAARPYYLDWDVRGIVHGHNSYLDVAM  355
vulpis          GRVSIWKFALEAQSKRPWTGYGYESFWSSAYARHAARPYYLDWDVRGIVHGHNSYLDVAM  355
inopinata       GRVSIWKFALEALSKRPWTGYGYESFWSSAYARHAARPYYLDWDVRGIVHGHNSYLDVAM  355
abortus         GRVSIWKFALEALSKRPWTGYGYESFWSSAYARHAARPYYLDWDVRGIVHGHNSYLDVAM  355
melitensis      GRVSIWKFALEALSKRPWTGYGYESFWSSAYARHAARPYYLDWDVRGIVHGHNSYLDVAM  355
canis           GRVSIWKFALEALSKRPWTGYGYESFWSSAYARHAARPYYLDWDVRGIVHGHNSYLDVAM  342
                **.*** **:** *:*****:******.:  *::**.*****************.***:*:

intermedia      SMGVPALICAILVIIVM----------PLVNYARCRPVRENLLLADFFLMVVFFGTLNAM  410
ovis            TMGIPALLCAVQAGAREHAAGRLLFDDRLVRNAQCHDG--------KFFLPAHGPGLAH--  406
vulpis          TMGIPALLCAIAVIIVM----------PLVHYARCRPVRENMLLADFFLMIVLFGTLNAM  405
inopinata       TMGIPALLCAIAVIIVM----------PLVHYARCRPVRENMLLADFFLMIVLFGTLNAM  405
abortus         TMGIPALLCAIAVIIVM----------PLVHYARCRPVRENMLLADFFLMIVLFGTLNAM  405
melitensis      TMGIPALLCAIAVIIVM----------PLVHYARCRPVRENMLLADFFLMIVLFGTLNAM  405
canis           TMGIPALLCAIAVIIVM----------PLVHYARCRPVRENMLLADFFLMIVLFGTLNAM  392
                :**:***:**: .               **. *:*:         .***     *  :

intermedia      LESFFFRRMDPVWLTLVFAIFGLRLTAKIIIPKR--    444
ovis            TYPCHFRPWHDGKSRHPEAICLIGVTS----------   433
vulpis          MESFFFRRMDPVWLTLILAIFGLGMTAKVVIPKRSV    441
inopinata       MESFFFRRMDPVWLTLILAIFGLGMTAKVVIPKRSV    441
abortus         MESFYFRRMDPVWLTLILAIFGLGMTAKVVIPKRSV    441
melitensis      MESFFFRRMDPVWLTLILAIFGLGMTAKVVIPKRSV    441
canis           MESFFFRRMDPVWLTLILAIFGLGMTAKVVVPKRSV    428
                    .**  .       **  : :*:
```

Figure 10: Sequence alignment of WaaL (BAB2_0106) in different species of the *Brucella* genus: *B. intermedia, B. ovis, B. vulpis, B. inopinate, B. abortus, B. melitensis* and *B. canis*

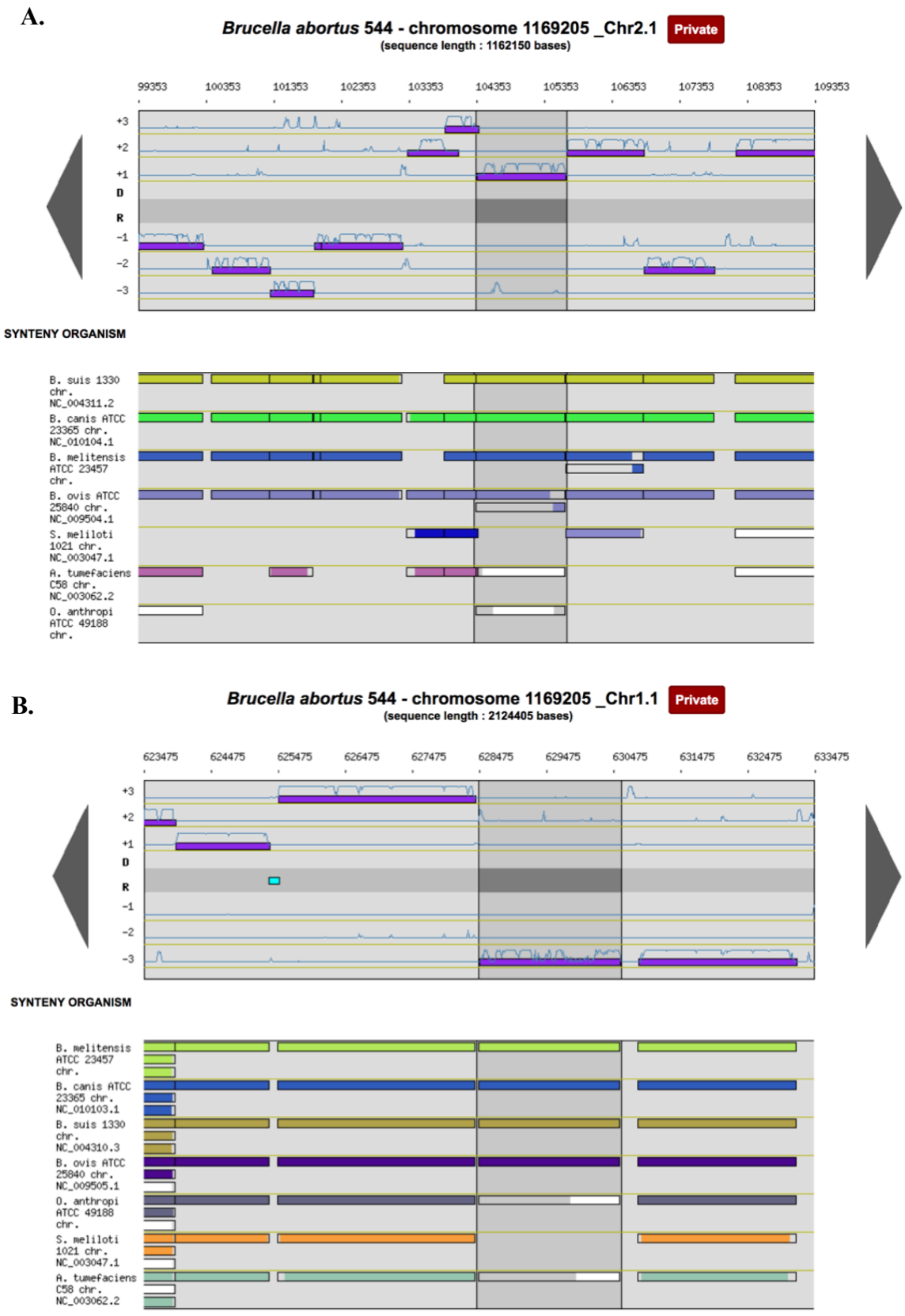

Figure 11: Synteny analysis of A. *waaL* (BAB2_0106) and B. *wadA* (BAB1_0639) in *B. abortus* 544 with different species of the *Brucella* genus (*B. ovis, B. melitensis* and *B. canis)* and other Rhizobiales (*Sinorhizobium melioti, Agrobacterium tumefaciens, Ochrobactrum anthropi*). Colored domains represent conserved sequences at similar localization in the genome compared to neighboring genes. White domains present similar sequences but at a different region of the genome. Grey/non-colored domains indicate non-conserved sequences (Vallenet *et al*., 2006; Vallenet *et al*., 2019).

A.

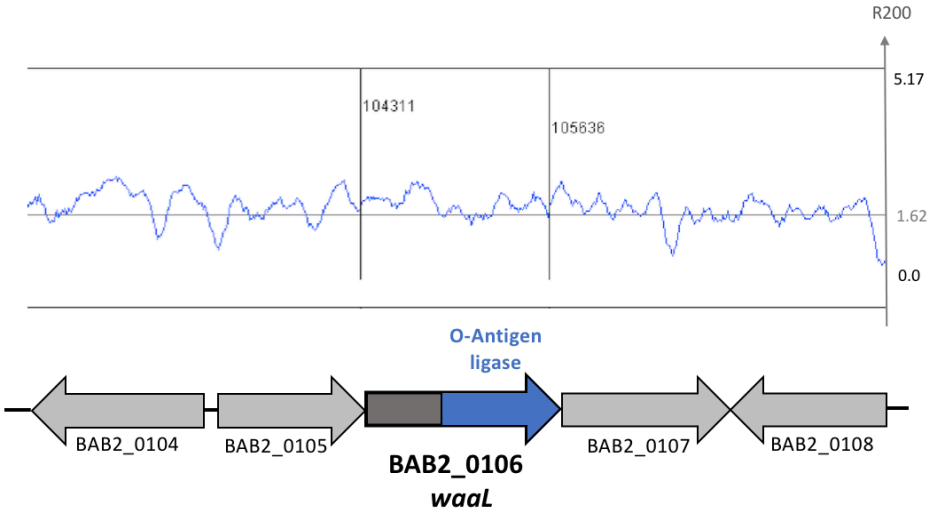

B.

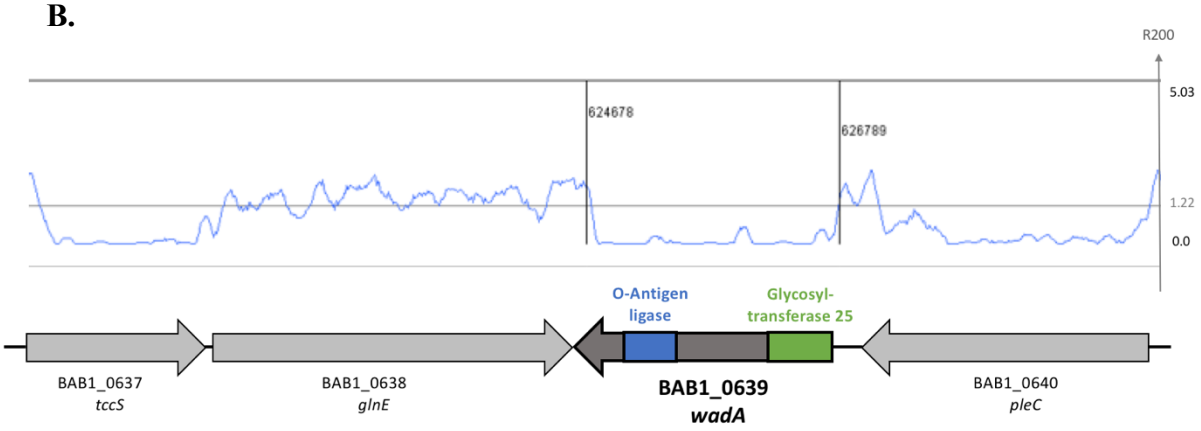

Figure 12: A. Tn-seq analysis of *waaL* (BAB2_0106) in TSB medium. A library of mutants was constructed for *B. abortus* 2308, and their growth on plates (rich medium) was analyzed. The blue line represents the mean of the transposon insertion in the genome (R200, $\log_{10}$ of the number of mini-Tn*5* insertion(s)+1 computed in a sliding window of 200 bp). If the R200 is above the thin grey line representing the mean of insertion in the whole genome, it means that bacteria can grow with an insertion in that gene, and that the gene is not essential under the tested conditions. If the line is below, it means that the global fitness is affected by the insertion and that the gene is important for the bacterial growth. If the blue line is at zero, it means that the gene is essential for growth. Domain predictions are written above the genes. **B. Tn-seq analysis of *wadA* (BAB1_0639) in TSB medium.** The predicted protein WadA presents two predicted domains: one O-antigen ligase domain and one glycosyltransferase 25 domain, both predicted as essential for growth in rich medium in *B. abortus* according to the analysis.

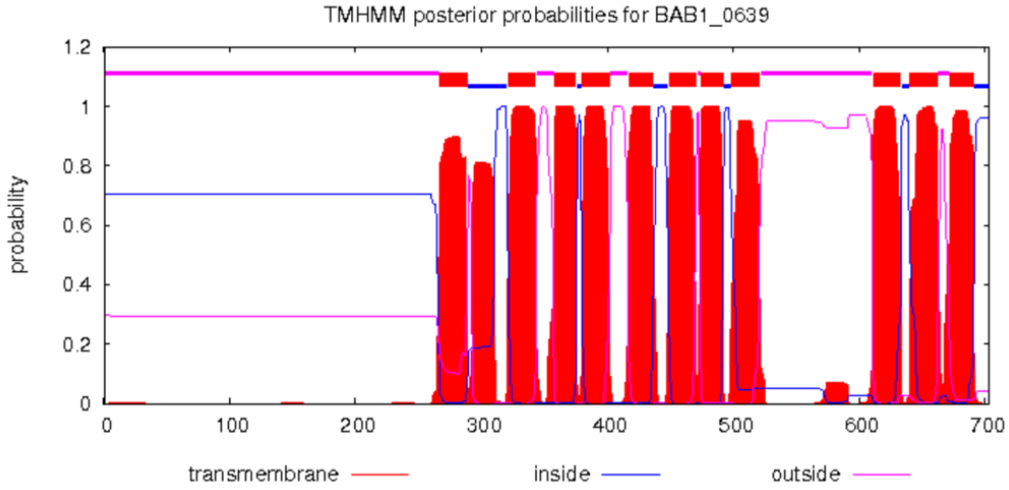

Figure 13: Prediction of transmembrane segments for WadA (BAB1_0639) from *B. abortus*. Prediction were done using the TMHMM tool (Krogh *et al.,* 2001). Putative transmembrane domains are represented red, cytosolic domains in blue and periplasmic domains in pink. The GT domain was predicted to be localized form amino acids 45 to 186 and is predicted to be inside in the cytoplasm since it needs an activated sugar (UDP-glucose) for its activity. The OAg ligase domain is believed to be localized from amino acids 445 to 615 and is predicted to be located in the cytoplasmic membrane and the periplasm.

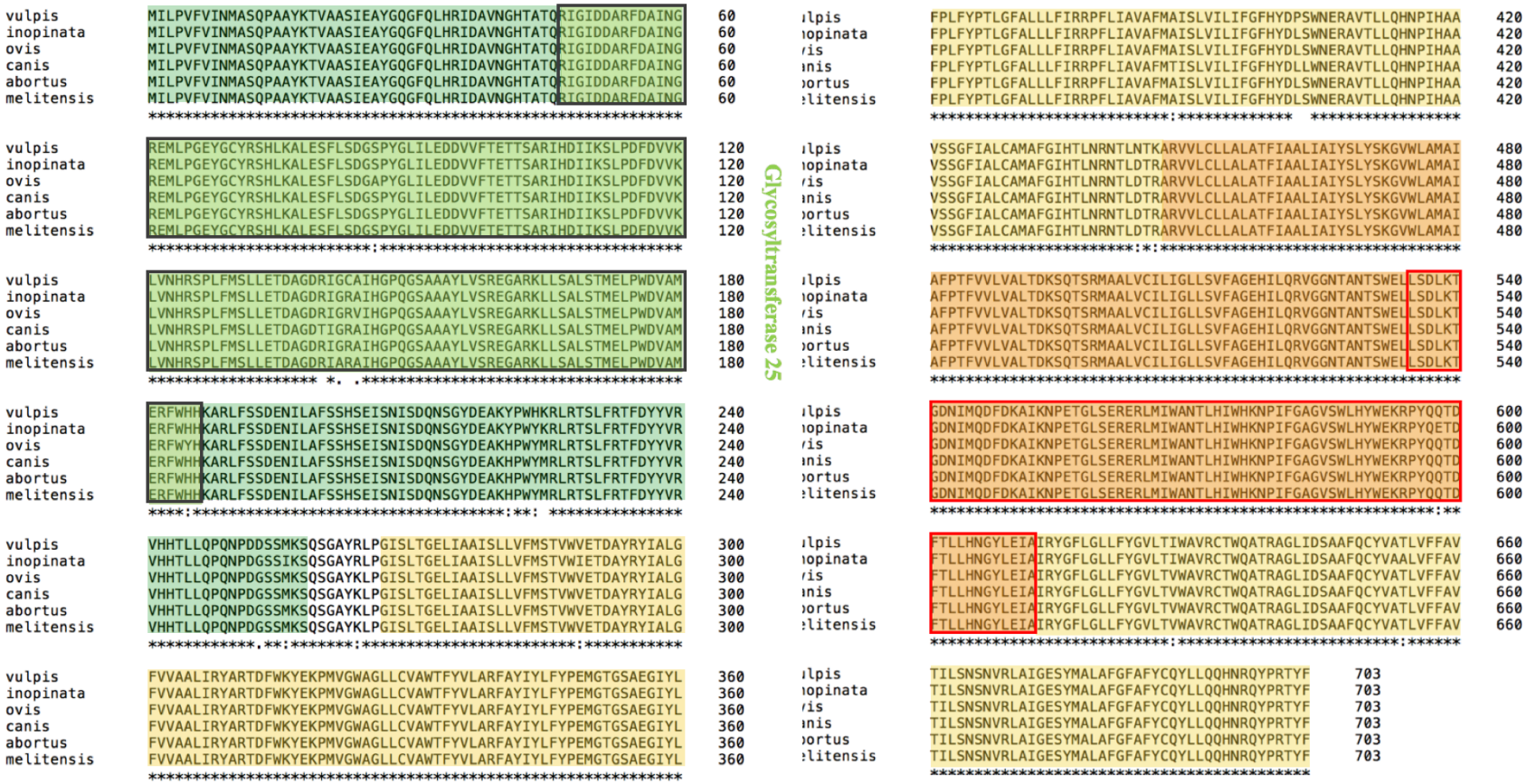

Figure 14: Sequence alignment of WadA (BAB1_0639) predicted proteins between species of *Brucella* genus*: B. vulpis, B. inopinata, B. canis, B. canis, B. ovis, B. abortus, B. melitensis.* Predicted domains are represented as well with one Glycosyltransferase 25 domain (light green) and one O-Chain ligase domain (orange). The black boxes delimit the sequence deleted in the GT deletion mutants. The red boxes delimit the sequence deleted for the OAg deletion mutants. Sequences incorporated in a replicative pBBR plasmid for complementation are marked in dark green for GT complementation and in yellow for OAg complementation.

RESULTS

1. *In silico* analysis

Two potential candidates as O-chain ligase in *B. abortus* were identified by similarity to established or putative O-chain ligases. More precisely, the research was made based on predicted proteins annotated as "ligase" from the *B. abortus* 2308 genome using the similarity to PFAM domains (PFAM Database, 2006) (Suarez & Guzman-Verri, personal communication).

The first candidate found was BAB2_0106, a homolog of *waaL,* also known to be the O-chain ligase in multiple other bacterial species as previously mentioned in the Introduction. Sequence alignment of the WaaL predicted proteins from *E. coli* (EFG6100940) and *B. abortus* showed a highly conserved region with an e-value of $3e^{-44}$ (BLASTp), the only difference being that the protein appeared longer in *B. abortus* (*Figure 9*). Prediction of transmembrane domains in the protein sequence using TMHMM (Krogh *et al.,* 2001), suggested the presence of twelve transmembrane domains and a small and a large periplasmic loop in *B. abortus* (*Figure S1*), similar to the characterized WaaL in *E. coli* (Q9ZIT0-1; UniProt (*Figure S2*)) (*Figure S1*). The conserved part seen on sequence alignment (*Figure 9*) represents the predicted large periplasmic loop, followed by three transmembrane domains. Interestingly, this BAB2_0106 gene seems conserved throughout the *Brucella* genus, even in the known R-LPS species *B. canis,* with the exception of the *B. ovis* showing different amino acid sequence at the C-terminal part of the protein (*Figure 10*). Similar results were shown by synteny analysis[2] with BAB2_0106 being conserved within the *Brucella* species tested, while in other Rhizobiales such as *Agrobacterium tumefaciens* and *Ochrobactrum anthropi* a big part of the gene is conserved but located at another position in the genome (*Figure 11.A.*).

Moreover, using a transposon sequencing (Tn-seq) experiment, a high throughput experiment highlighting essential genes for growth in rich medium, we observed that this gene is not essential for the bacterial growth in rich culture medium (*Figure 12.A.*).

As a second candidate, we identified *wadA* (BAB1_0639), previously annotated as *wa***. Using TMHMM (Krogh *et al.,* 2001), WadA was predicted to present twelve transmembrane domains, as well as a large periplasmic loop. In addition, the presence of a large cytosolic domain was also suggested (*Figure 13*). Moreover, domain prediction analysis on the predicted protein revealed a putative O-chain ligase (OAg) domain at the C-terminal part of the protein and also a Glycosyltransferase (GT) domain at the N-terminal part, predicted to be part of the glycosyltransferase family 25. Synteny analysis showed that the gene and the putative domains are highly conserved within the *Brucella* genus, but not in other Rhizobiales such as *Agrobacterium tumefaciens* and *Ochrobactrum anthropi* where only a homologous GT domain is predicted to be found elsewhere in the genome (*Figure 11.B.*). Furthermore, alignment of the amino acids sequences of *Brucella* spp. showed that the sequence is highly conserved (*Figure 14)*. While the Tn-seq analysis suggested that the whole *wadA* gene is essential for bacterial growth in *B. abortus* (*Figure 12.B.*), González *et al.* managed to obtain a *wadA* deletion mutant in *B. melitensis* (González *et al.,* 2008).

[2] Synteny analysis provides information about the conversation of homologous genes and the gene order between genomes of different species (Liu *et al*., 2018)

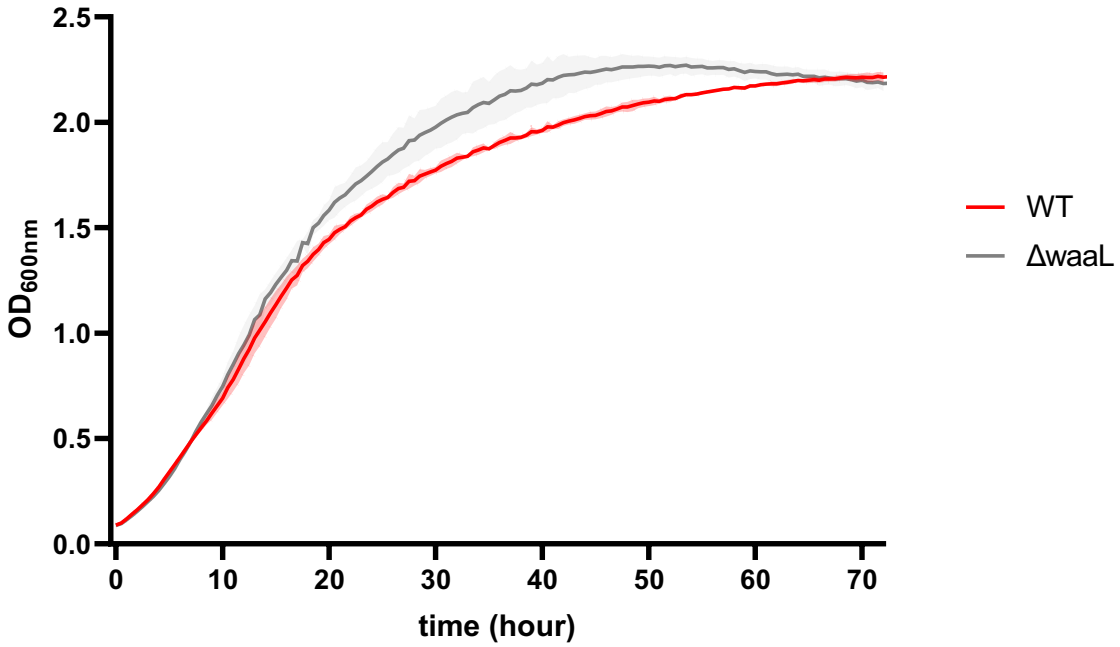

Figure 15: Growth curve of the WT (red) and Δ*waaL* (grey). The growth was performed in TSB rich medium for 72h at 37°C, with OD measurements taken at 600 nm every 30 min. (N=3)

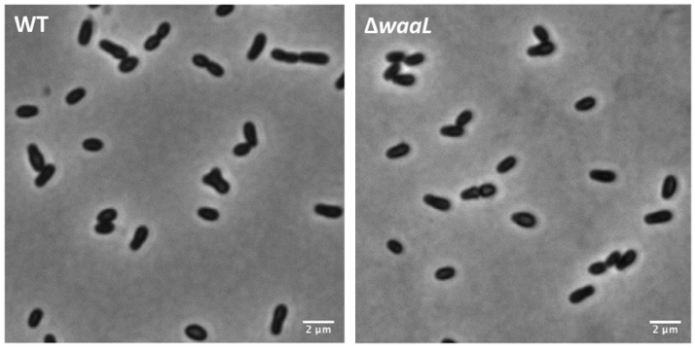

Figure 16: Microscopy images on *B. abortus* 544 WT and Δ*waaL* in late exponential phase (DO_{600} ~ 0.7).

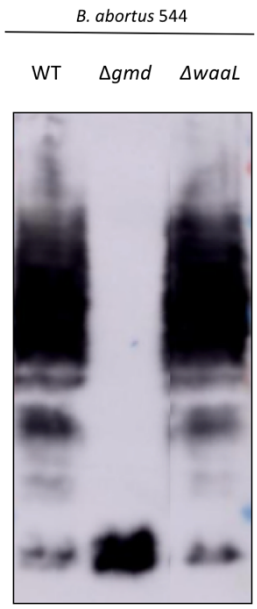

Figure 17: Western Blot of different *B. abortus* strains (WT, *Δgmd, ΔwaaL)* labeled with A68/24D08/G09, an anti-R-LPS antibody. This antibody binds to the LPS core, thereby enabling to visualize signal given from R-LPS (down) and signal given from S-LPS (up). WT strains are S-LPS phenotype controls, while Δ*gmd* is a R-LPS phenotype control. (Original image *Figure S3)*

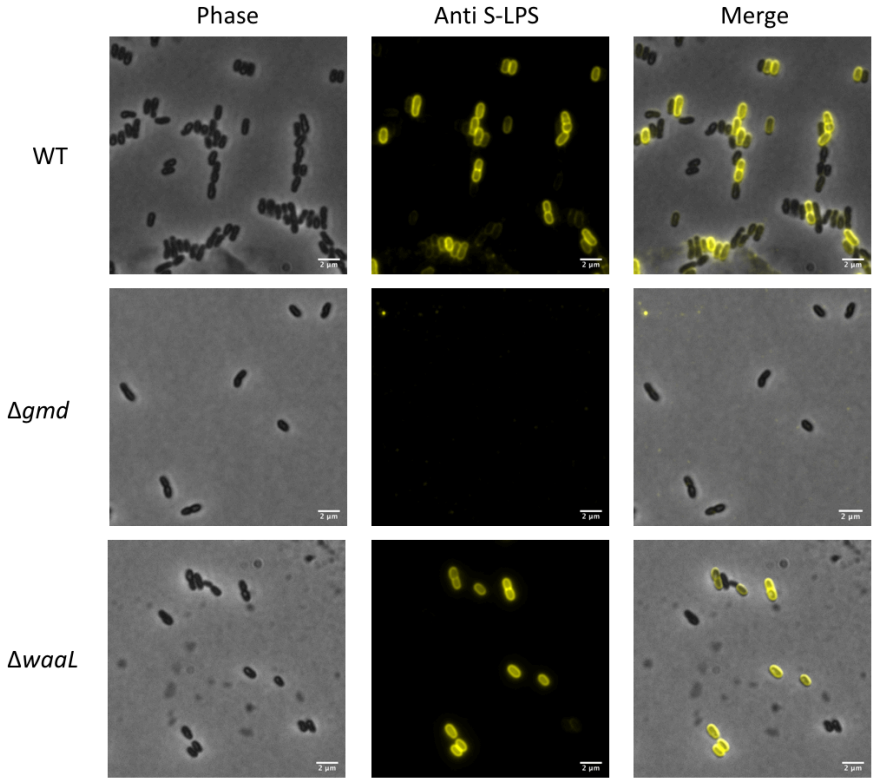

Figure 18: Immunofluorescence microscopy on WT, Δ*gmd* and Δ*waaL* mutant in *B. abortus*. Bacteria were labeled with anti-S-LPS antibody A76/12G12 as a primary antibody. Goat anti-mouse IgG H+L AlexaFluor 514 was used as a secondary antibody (YFP channel).

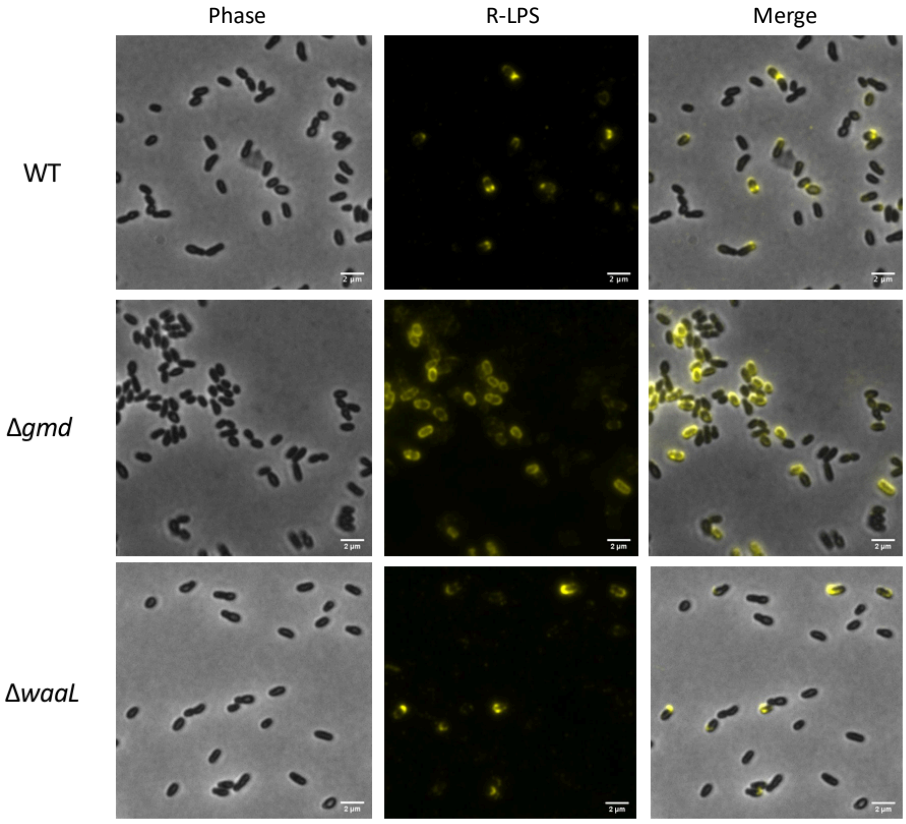

Figure 19: Immunofluorescence microscopy on WT, Δ*gmd* and Δ*waaL* mutant in *B. abortus*. Bacteria were labeled with anti-R-LPS antibody A68/03F03/D05 as primary antibody. Goat anti-mouse IgG2b AlexaFluor 488 was used as a secondary antibody (YFP channel).

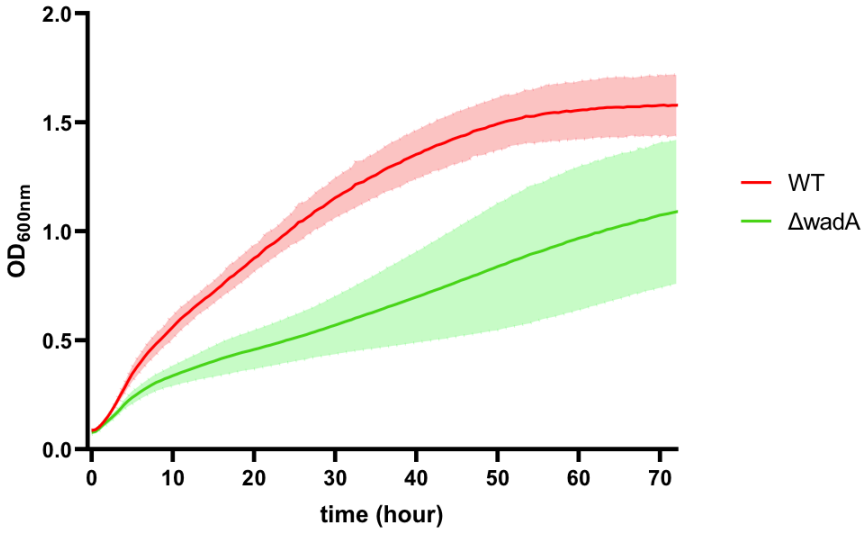

Figure 20: Growth curve of different *B. melitensis* strains (WT, Δ*wadA*). The growth was performed in 2YT medium for 72h at 37°C, with OD measurements taken every 30 min. (N=3)

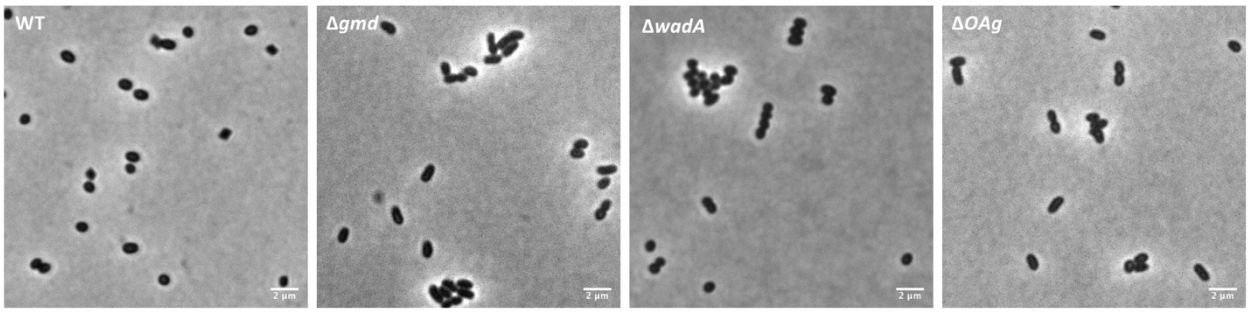

Figure 21: Microscopy images on WT, Δ*gmd*, Δ*wadA* and Δ*OAg* in *B. melitensis* 16M in exponential phase (DO_{600} ~ 0.7). WT bacteria seem to be dispersed, while Δ*gmd* bacteria tend to form aggregates. The Δ*wadA* and Δ*OAg* mutants also seem to form aggregates (*Figure S4*).

2. Δ*waaL* mutant presents a S-LPS phenotype in *B. abortus*

We started by deleting BAB2_0106 (*waaL)* in the WT background. The Δ*waaL* deletion mutant was easily obtained, and its growth in liquid rich medium was assessed by optical density (OD) measurements taken every 30 min through 72h. At the start of the experiment, the bacteria were in exponential phase. The experiment was performed three times in order to obtain a replicate. As seen on *Figure 15,* this mutant showed no noticeable changes of growth compared to the control WT *B. abortus* 544. We could observe an exponential phase of growth where bacteria multiply, followed by a plateau without growth also called "stationary phase". By microscopy, the morphology of the bacteria was observed during exponential phase of growth, and no noticeable difference was observed compared to the WT (*Figure 16*). The bacteria presented a rod-shaped morphology and did not seem to present issues to divide.

In order to investigate the presence of S- LPS on the surface of Δ*waaL*, a WB was performed on samples taken at exponential phase (*Figure 17*). Two controls were used, the WT known to present S-LPS and R-LPS simultaneously, and the mutant Δ*gmd* known to present only R-LPS on the surface. The labeling was made using an anti-R-LPS antibody (A68/24D08/G09). Thereby, samples with a rough phenotype presented a single R-LPS signal, as seen for Δ*gmd*. While samples with a smooth phenotype present signals for both types of LPS, as seen for the WT. *Figure 17* indicates a labeling of the Δ*waaL* mutant identical to the WT phenotype, suggesting a smooth phenotype for the deletion mutant.

To further investigate the presence of R-LPS or S-LPS on the Δ*waaL* mutant surface, immunofluorescence (IF) microscopy was performed on this mutant with the corresponding antibodies. Labeling with an anti-S-LPS antibody (A76/12G12) showed a homogenous labeling of the Δ*waaL* bacteria, similar to the WT; while the negative control Δ*gmd* showed no signal (*Figure 18).* As Gmd is one of the first proteins intervening in the O-chain synthesis, the deletion of *gmd* leads to bacteria lacking the O-chain. When labeling with an anti-R-LPS antibody (A68/03F03/D05) (*Figure 19)*, Δ*waaL* presented a phenotype similar to the WT with a non-homogenous labeling, while Δ*gmd* mutant was homogeneously labelled by the primary anti-R-LPS antibody. These images revealed that the Δ*waaL* mutant presents a phenotype similar to the WT strain.

The WB results and by IF images show that Δ*waaL* presents a S-LPS phenotype, thereby implying that WaaL (BAB2_0106) is not the primary O-chain ligase in *B. abortus.*

3. The Δ*wadA* mutant in *B. melitensis* presents a R-LPS phenotype

As a rough mutant was obtained by González *et al.* when deleting *wadA* in *B. melitensis*, while they were working on WadA being a glycosyltransferase, we first wanted to reproduce their results by constructing a deletion mutant (Δ*wadA*) in *B. melitensis* 16M. We first aimed to characterize this mutant for growth, morphology and for S-LPS or R-LPS phenotype.

We managed to construct the strain, suggesting that *wadA* is not essential in *B. melitensis*. Even though this was expected, it will be important to consider for the next experiments. We then wanted to assess the fitness of this construction by studying the growth and morphology of the mutant compared to the 16M WT strain. The growth profile was evaluated by measuring culture OD for 72h with intervals of 30 min in rich (2YT) medium. *Figure 20* indicates a slower growth represented by a flattened curve of the Δ*wadA* mutant compared to the WT. We observed bacteria in late exponential phase using optical microscopy and we could notice that the Δ*wadA* bacteria tend to form aggregates, while the WT bacteria did not (*Figure 21*).

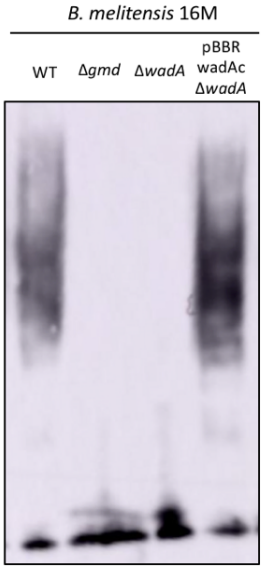

Figure 22: Western Blot of different *B. melitensis* strains (WT, *Δgmd*, *ΔwadA,* pBBR wadAc *ΔwadA)* labeled with A68/24D08/G09, an anti-R-LPS antibody. This antibody binds to the LPS core, thereby enabling to visualize signal given from R-LPS (down) and signal given from S-LPS (up). WT strains are S-LPS phenotype controls, while Δ*gmd* is a R-LPS phenotype control.

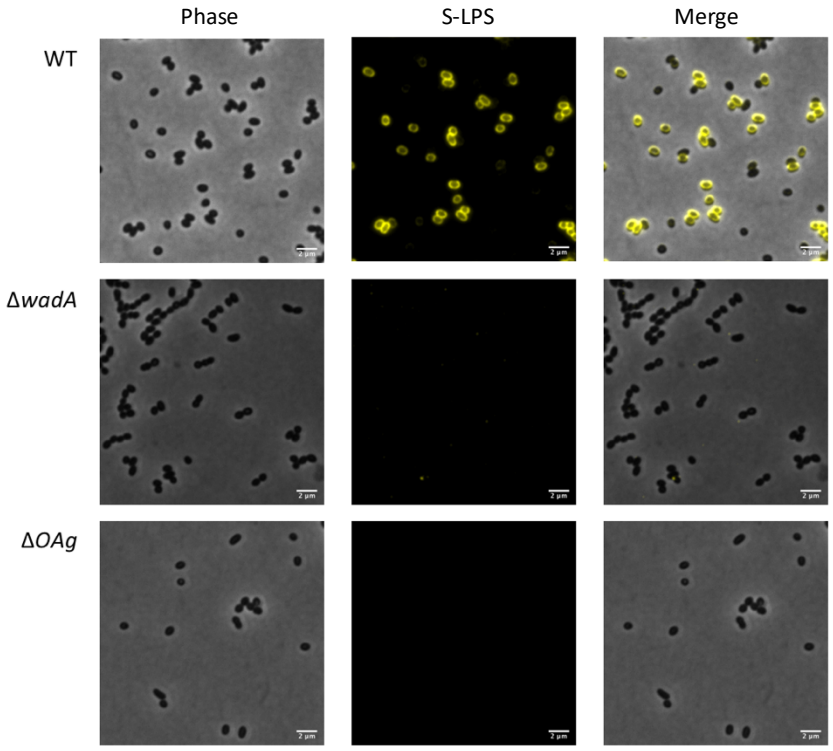

Figure 23: Immunofluorescence microscopy on WT, Δ*wadA* and Δ*OAg* mutant in *B. melitensis.* Bacteria were labeled with anti-S-LPS antibody A76/12G12 as a primary antibody. Goat anti-mouse IgG H+L AlexaFluor 514 was used as a secondary antibody (YFP channel).

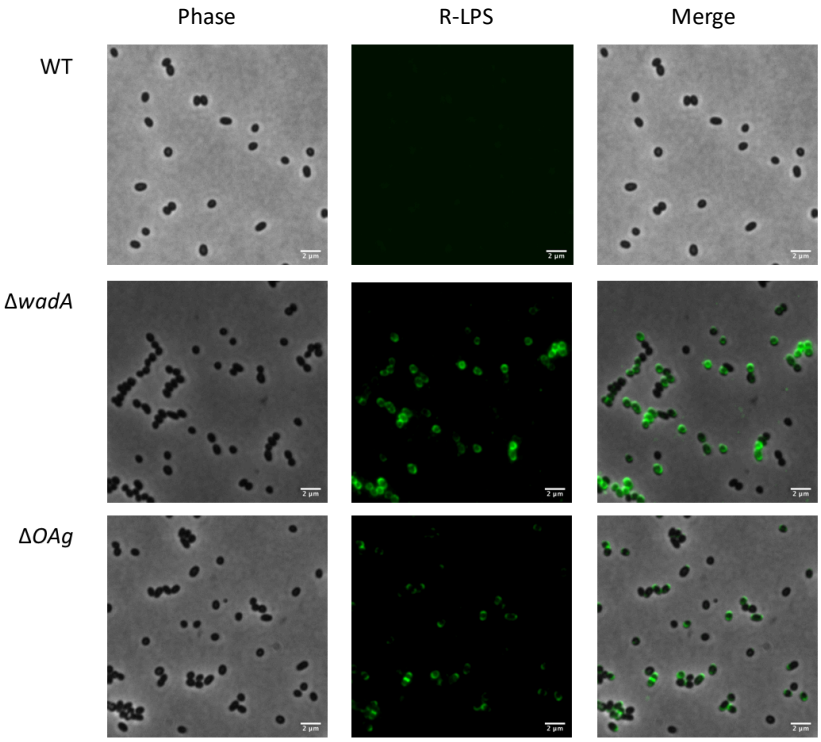

Figure 24: Immunofluorescence microscopy on WT, Δ*wadA* and Δ*OAg* mutant in *B. melitensis.* Bacteria were labeled with anti-R-LPS antibody A68/03F03/D05 as primary antibody. Goat anti-mouse IgG2b AlexaFluor 488 was used as a secondary antibody (FITC channel).

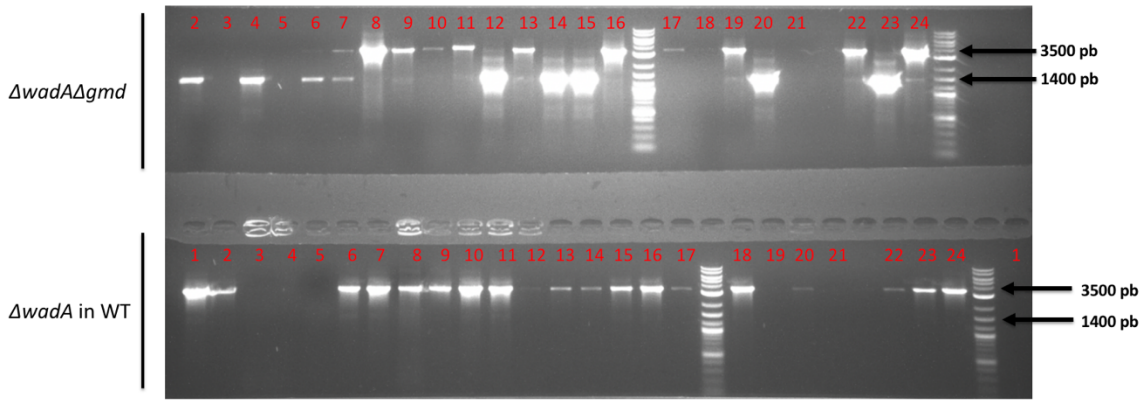

Figure 25: Migration profile of the diagnostic PCR of 24 streaks out of 150 putative Δ*wadA* in WT and 24 streaks of putative Δ*wadA*Δ*gmd* after conjugation and selection. WT strains are expected to have an amplification of 3500 pb, while deletion mutants for *wadA* are expected to show an amplification of 1400 pb.

The rough control Δ*gmd* tend to form aggregates as well. Interestingly, aggregation is a phenotype that has previously been reported for *Brucella* rough strains (Bello *et al.,* 2015).

Characterization of this mutant was performed via a WB using a monoclonal antibody (A68/24D08/G09) able to recognize the core (attached or not to the O-chain), thereby allowing to simultaneously detect rough and smooth LPS separated by electrophoresis. The results show that while 16M WT strain simultaneously presented R-LPS and S-LPS signals, the rough control Δ*gmd* only displayed R-LPS signal (*Figure 22*). Regarding the Δ*wadA* mutant, it exclusively displayed R-LPS signal, further confirming González *et al.* results. This was further supported by restoring S-LPS signals when complementing the mutant with a copy of the whole *wadA* gene on a replicative plasmid (pBBR), under the control of the promotor of *wadA* (P*wadA*) (*Figure 22)*. The backbone of this plasmid is pBBR1-derived, with a copy number of 10 per cell (Elzer *et al*., 1994).

Moreover, labelling with an anti-S-LPS antibody (A76/12G12) resulted in no visible signal on Δ*wadA*, while the WT strain presented a homogenous labelling of the bacterial surface (*Figure 23*). Additionally, when labelling with an anti-R-LPS antibody (A68/03F03/D05), the Δ*wadA* mutant displayed fluorescent signal, in contrast to the smooth control (WT strain) (*Figure 24*).

Taken together, the data found by phase contrast microscopy, IF and WB suggest a R-LPS type phenotype for the Δ*wadA* mutant in *B. melitensis.* We can therefore propose that we could reproduce the observations made by González *et al.* Nevertheless, the growth assessment revealed a reduced fitness of this rough mutant that has not been reported before.

4. *wadA* is essential in *B. abortus*

Since the Δ*wadA* deletion mutant was viable in *B. melitensis*, we attempted to construct the deletion strain in *B. abortus* 544*,* both species being very closely related, the average amino acid sequence identity being greater than 99% (Halling *et al.,* 2005). Following our protocol for the construction of a Δ*wadA* mutant, we screened about 150 deletion candidates in three biological replicates by diagnostic PCR but no clone turned out to be deleted for the gene (*Figure 25*). As we were not able to delete the gene, we hypothesize that *wadA* is essential in *B. abortus* in rich medium, which would correlate with the Tn-seq data previously obtained (*Figure 12.B.*).

One explanation for the essentiality of *wadA* in *B. abortus* could be linked to the accumulation of the O-chain to the lipid carrier bactoprenol (BctP), thereby impeding the essential peptidoglycan precursor from binding to the BctP and being transported to the periplasmic space, as data in *E. coli* showed that the two pathways use the same BctP pool (Jorgenson & Young, 2016). Indeed, as the O-chain is not essential, the absence of S-LPS on the surface is not sufficient to explain the inability to obtain the mutant.

Taken that *B. melitensis* doubling time is about 4 h, while *B. abortus* multiplies in 2 h 45, we proposed that the non-toxicity of a potential accumulation of O-chain to the BctPP could be related to the slower growth of *B. melitensis.* Indeed, slower growth might enable a rate of recycling of the BctPP intervening in the O-chain and peptidoglycan synthesis pathways, thereby allowing the synthesis of the PG layer even in absence of WadA. Another hypothesis could be that the BctPP release from the O-chain is more efficient in *B. melitensis*.

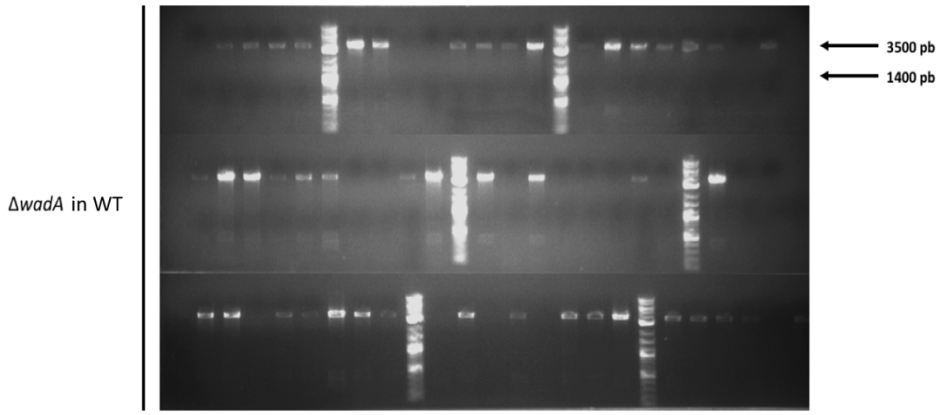

Figure 26: Migration profile of the diagnostic PCR of 64 streaks out of 150 putative Δ*wadA* in WT with growth at 30°C. WT strains are expected to have an amplification of 3500 pb, while deletion mutants for *wadA* are expected to show an amplification of 1400 pb.

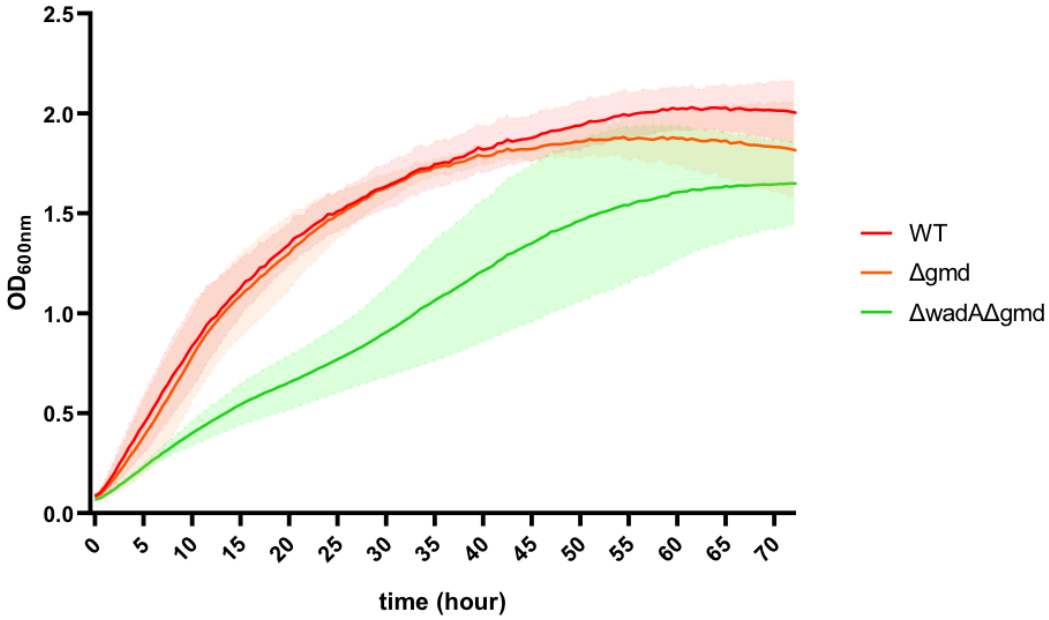

Figure 27: Growth curve of different *B. abortus* strains (WT, Δ*gmd*, Δ*wadA*Δ*gmd)* in TSB medium for 72h at 37°C, with OD measurements taken every 30 min. (N=3)

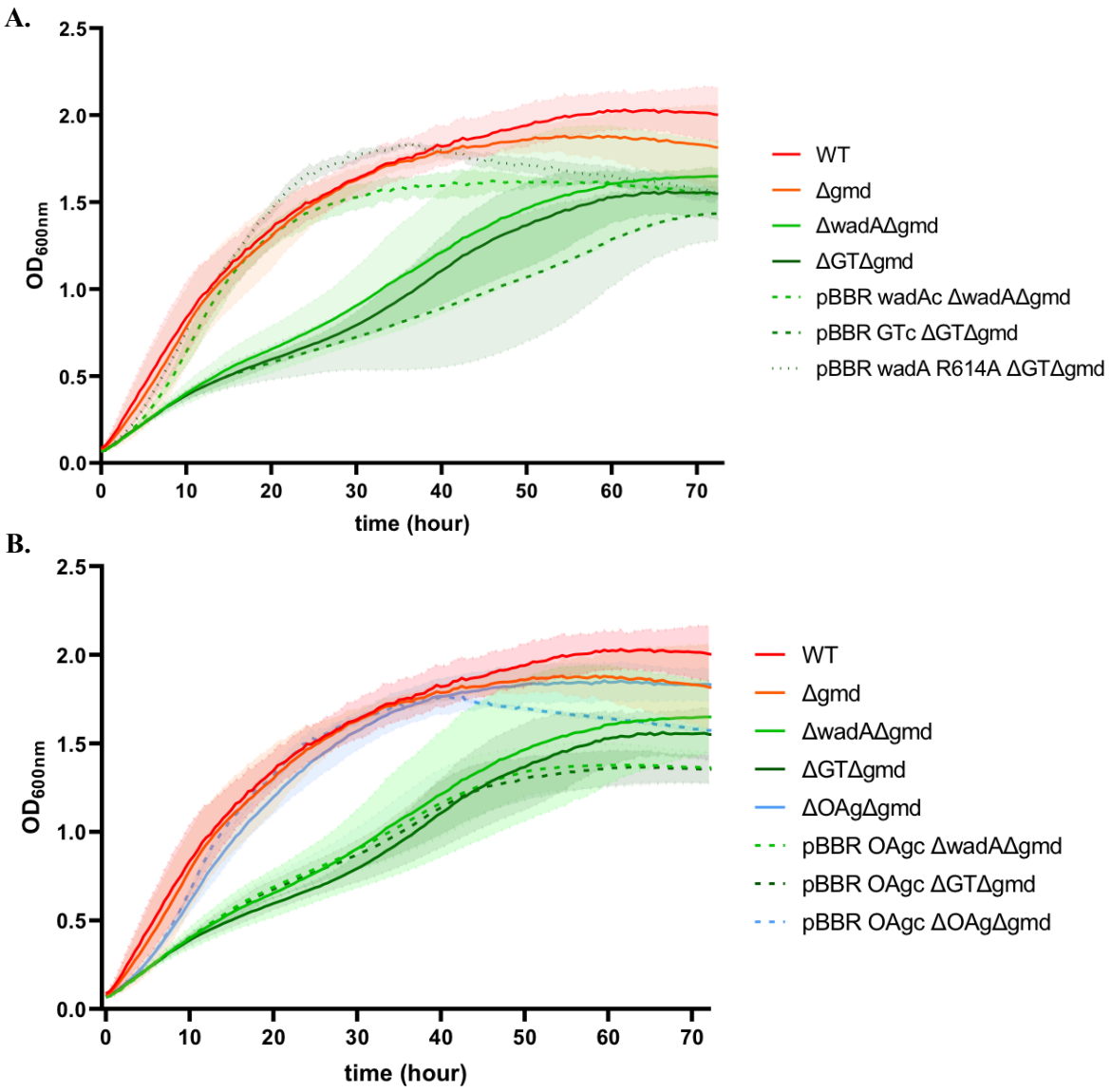

Figure 28: Growth curve of different *B. abortus* strains (WT, Δ*gmd*, Δ*wadA*Δ*gmd*, Δ*GT*Δ*gmd*, Δ*OAg*Δ*gmd*) and the complementation strains A. pBBR wadAc Δ*wadA*Δ*gmd*, pBBR GTc Δ*GT*Δ*gmd*, pBBR *wadA* R614A Δ*GT*Δ*gmd*; B. pBBR OAgc Δ*wadA*Δ*gmd*, pBBR OAgc Δ*GT*Δ*gmd*, pBBR OAgc Δ*OAg*Δ*gmd*; in TSB medium for 72h at 37°C, with OD measurements taken every 30 min. Complementation strains were grown in TSB supplemented with Chloramphenicol (Cm). (N=3)

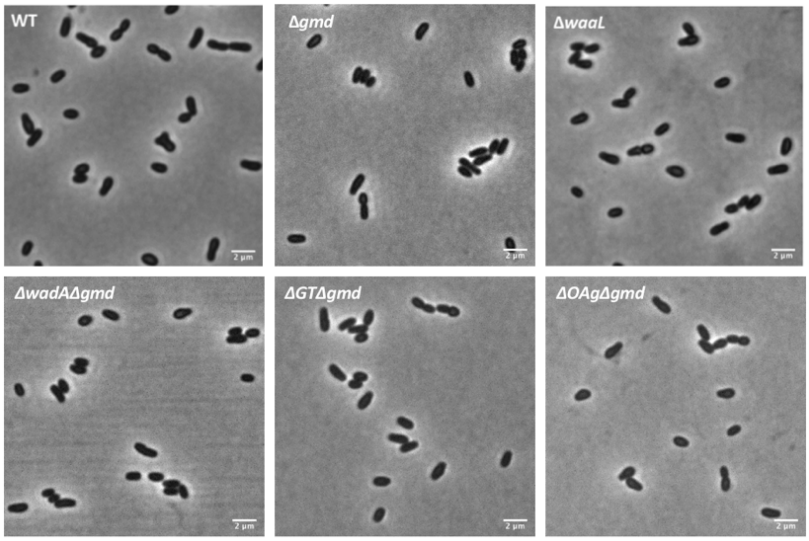

Figure 29: Microscopy images on *B. abortus* 544 WT, Δ*gmd*, Δ*waaL*, Δ*wadA*Δ*gmd*, Δ*GT*Δ*gmd* and Δ*OAg*Δ*gmd* in late exponential phase (DO_{600} ~ 0.7). Please note that the WT picture is identical to the one shown on *Figure 14*. Scale bar represents 2 µm. (*Figure S4* presents microscopy images after minimal resuspension)

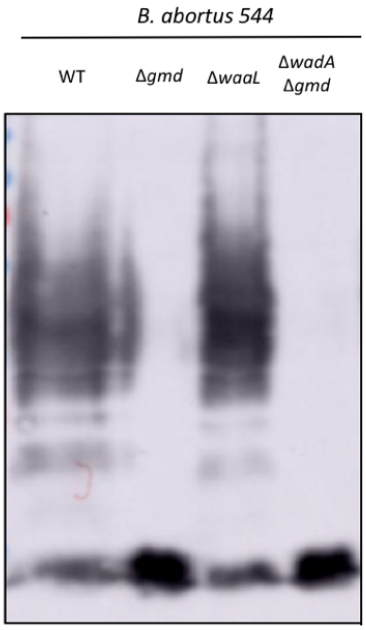

Figure 30: Western Blot of different *B. abortus* strains (WT, Δ*gmd*, Δ*waaL*, Δ*wadA*Δ*gmd)* labeled with A68/24D08/G09, an anti-R-LPS antibody. This antibody binds to the LPS core, thereby enabling to visualize signal given from R-LPS (down) and signal given from S-LPS (up). WT strains are S-LPS phenotype controls, while Δ*gmd* is a R-LPS phenotype control.

We therefore performed a conjugation in order to delete *wadA* in *B. abortus*, but this time the cultures were incubated at 30°C with the aim to slow down bacterial growth. Slower growth was achieved, as plates had to be incubated for 5 to 7 days to allow growth, compared to 4 days at 37°C. Similar to the results found for conjugation at 37°C, screening of 150 putative candidates grown at 30°C revealed no deletion mutant for *wadA*. *Figure 26* presents 64 of these candidates tested by diagnostic PCR. We thereby report that slow growth, at least in these conditions, does not allow deletion of the essential gene *wadA*.

5. The double Δ*wadA*Δ*gmd* mutant is viable

5.1. The double Δ*wadA*Δ*gmd* mutant shows growth defects

Since a Δ*gmd* mutant, unable to synthesize the O-chain, was available in the *B. abortus* 544 background (Vassen et al., 2019), we performed a conjugation to obtain a double mutant Δ*wadA*Δ*gmd* with the hope to bypass the toxic effect of O-chain-linked BctPP saturation. This double mutant construction turned out to be successful and viable (*Figure 25*), revealing the possibility to delete *wadA* in the absence of the O-chain production and supporting the hypothesis of a toxicity due the sequestration of the BctPP pool by the O-chains.

Interestingly, when assessing the growth of the mutants, Δ*wadA*Δ*gmd* displayed a distinct growth profile compared to the WT and the Δ*gmd* curves (*Figure 27*). Indeed, the Δ*gmd* mutant did not display a decreased fitness as its curve was similar to the WT. However, Δ*wadA*Δ*gmd* exhibited growth defects. The elongated time needed to reach stationary phase revealed a reduced fitness of the double mutant. The observation of growth defects of the Δ*wadA*Δ*gmd* double mutant was supported by the ability to return to a standard growth curve by complementing with a medium copy replicative plasmid (pBBR) containing the entire *wadA* gene, under to control of its own promotor (P*wadA*) in order to allow an expression as closed as possible to the WT (Δ*wadA*Δ*gmd*::pBBR*wadA*) (*Figure 28.A.*).

From a morphological point of view, the Δ*wadA*Δ*gmd* mutant showed no obvious morphological defect (*Figure 29*) compared to the WT or Δ*gmd* bacteria. As expected and similarly to Δ*gmd* bacteria, Δ*wadA*Δ*gmd* bacteria showed a tendency to aggregate. Besides, when performing a WB on this double mutant with an anti-R-LPS antibody (A68/24D08/G09), Δ*wadA*Δ*gmd* presented a rough phenotype, similar to the Δ*gmd* control (*Figure 30*). These results correlate with the fact that we are in a Δ*gmd* background, and therefore in any case in absence of an O-chain.

5.2. Both WadA domains are essential in *B. abortus*

As domain prediction for WadA suggested the presence of two separate domains, we attempted to delete these domains individually. This should help us identify if one domain in particular is essential.

Concerning the O-chain ligase domain (OAg), we first attempted to partially delete this domain in a WT background. The idea was to exclusively delete the large periplasmic loop of the OAg domain, thought to hold the catalytic sites of the domain, in order to keep the rest of the protein structure as intact as possible and not alter the activity of the remaining protein. By using *Figure 13,* we determined the sequence to be deleted without impacting the transmembrane domains and marked this sequence by a red box on *Figure 14*. A screening of 100 putative candidates revealed no deletion mutant for this periplasmic loop (data not shown).

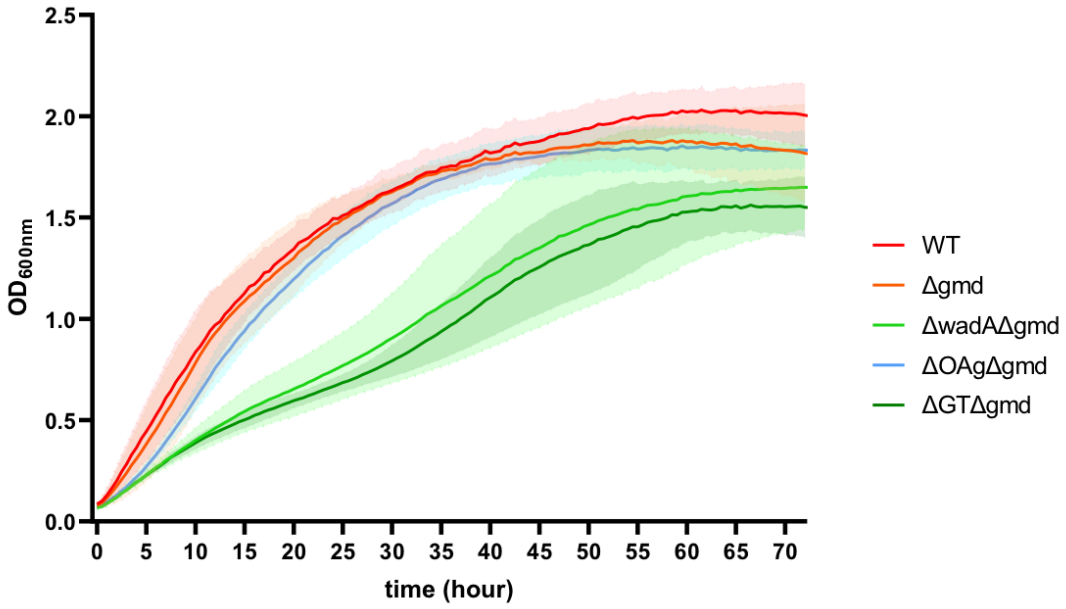

Figure 31: Growth curve of different *B. abortus* strains (WT, Δ*gmd*, Δ*wadA*Δ*gmd*, Δ*OAg*Δ*gmd*, Δ*GT*Δ*gmd*) in TSB medium for 72h at 37°C, with OD measurements taken every 30 min. (N=3)

However, a Δ*OAg*Δ*gmd* could easily be obtained, which reinforces our hypothesis of a toxicity related to the O-chain. The growth of the Δ*OAg*Δ*gmd* mutant was assessed, and it displayed a growth curve similar to the WT and Δ*gmd* strains with an exponential phase and a stationary phase (*Figure 31*). This mutant presented a morphology similar to the WT but tend to form aggregates (*Figure 29*).

An attempt of complementation was done by adding a copy of the coding sequence for the entire OAg domain, as well as the sequence coding for the remaining transmembrane domains of *wadA* (*Figure 13 + Figure 14, yellow mark*) on a medium copy replicative plasmid (pBBR) under to control of its own promoter (P*wadA*) (Δ*Oag*Δ*gmd*::pBBR*Oagc*). We could observe a standard growth curve for this complementation, but a slight growth defect after 40 h (*Figure 28.B.*). Moreover, when complementing the Δ*wadA*Δ*gmd* mutant with the same pBBR plasmid (Δ*wadA*Δ*gmd*::pBBR*OAg*), we were not able to restore growth (*Figure 28.B.*), indicating an inability of the OAg domain on itself to complement the deletion mutant. These results suggest the growth defects to be related to an activity of the Glycosyltransferase (GT) domain.

A deletion mutant for the GT domain was as well constructed in a Δ*gmd* background by deleting exclusively the coding sequence for the GT domain (*Figure 14, light green mark*), without impacting the transmembrane domains and in order to reduce risk of misfolding of the remaining protein. It presented a tendency to form aggregates, but the bacteria showed a normal morphology (*Figure 29*). OD measurements revealed a reduced growth for this Δ*GT*Δ*gmd* mutant with an elongated time to reach stationary phase, just as the Δ*wadA*Δ*gmd* deletion mutant (*Figure 31*). This observation suggests that the growth defects can be appointed to the absence of the GT, rather than the absence of the complete *wadA* gene, unless the remaining fragment of WadA would not be functional for O-chain ligation. We attempted to complement this phenotype of the Δ*GT*Δ*gmd* mutant by adding a copy of the coding sequence of the predicted cytosolic domain containing the GT domain (*Figure 13 + Figure 14, dark green mark*) on a medium copy replicative plasmid (pBBR) under the control of its own promoter (P*wadA*) in order to allow its expression as close as possible to the WT (Δ*GT*Δ*gmd*::pBBR*GTc*). However, we did not succeed to restore the WT phenotype with this construction (*Figure 28.A.*). When complementing with a similar pBBR plasmid containing a copy of the *OAg* domain (*Figure 14, yellow mark*) (Δ*GT*Δ*gmd*::pBBR*OAgc*), we were not able to restore growth (*Figure 28.B.*). This suggests that, if pBBR*OAgc* encodes a functional O-chain ligase (which seems to be the case in *B. melitensis*, see section 6.2.), it is not the absence of this activity that is responsible for the growth defect of the Δ*GT*Δ*gmd* mutant.

In order to explain the Δ*GT*Δ*gmd*::pBBR*GTc* result, we propose that the cytosolic GT domain on itself is in incapacity to reach its protein structure, leading to an inability to be functional. The pBBR GTc Δ*GT*Δ*gmd* strain would thereby keep a reduced growth. Yet we were able to complement this Δ*GT*Δ*gmd* mutant with a pBBR plasmid containing a functional GT domain, but a mutated OAg domain (pBBR *wadA* R614A) (*Figure 28.A.*) (see section 7.). This construction showed a standard growth curve, suggesting a complementation of the GT domain. Additionally, we also verified the ratio between OD measures and colony forming units (CFU) for the three double mutants (Δ*wadA*Δ*gmd*, Δ*Oag*Δ*gmd*, Δ*GT*Δ*gmd*). This method is used to estimate the number of viable bacteria in a sample. When comparing the three mutants, we did not observe any difference in the CFU count (*Figure S5*).

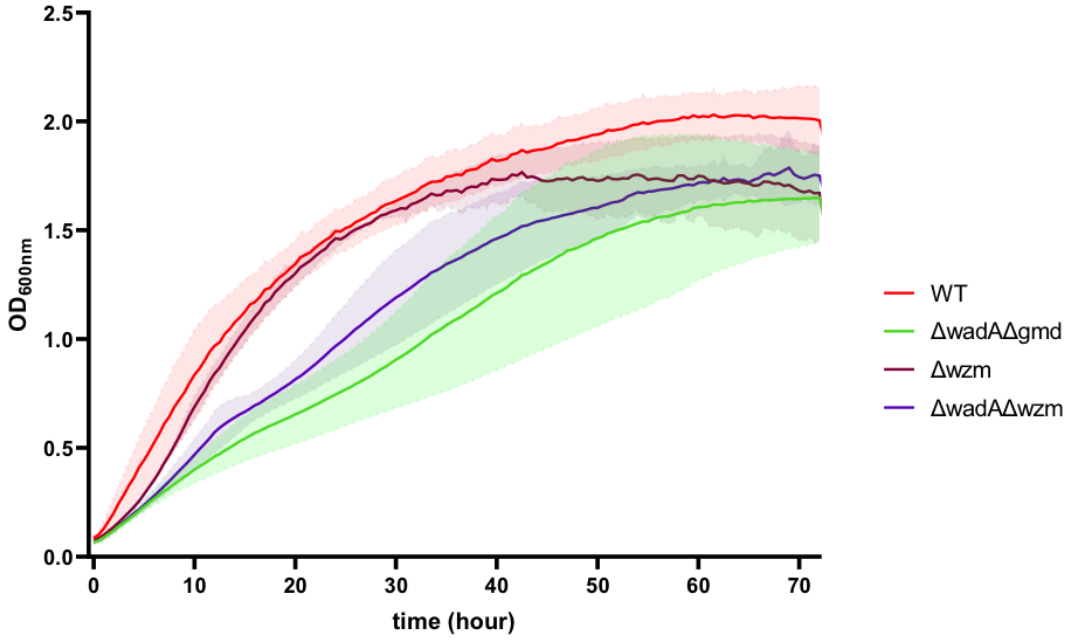

Figure 32: Growth curve of different *B. abortus* strains (WT, Δ*wadA*Δ*gmd*, Δ*wzm*, Δ*wadA*Δ*wzm*) in TSB medium for 72h at 37°C, with OD measurements taken every 30 min. (N=3)

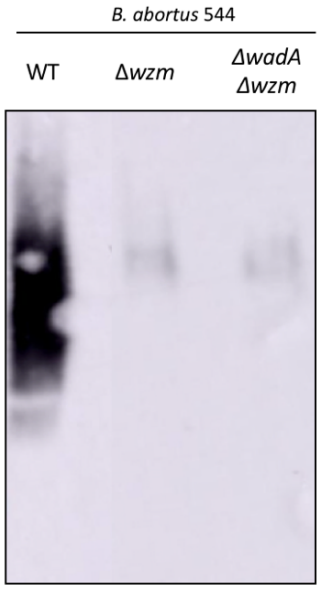

Figure 33: Western Blot of different *B. abortus* strains (WT, Δ*wzm*, Δ*wadA*Δ*wzm*) labeled with A76/12G12, an anti-S-LPS antibody. This antibody binds to the O-chain, displaying signal given from S-LPS or BctPP-linked O-chains.

5.3. WadA can also be deleted in a Δ*wzm* background

Since we expect that a Δ*wadA* deletion strain cannot be obtained due to toxic sequestration of the BctPP by the O-chain, we wanted to know whether this toxicity was due to cytoplasmic or periplasmic O-chain accumulation. That question could be answered by deleting the ABC transporter able to flip the O-chain from the cytoplasmic leaflet to the outer leaflet, Wzm/Wzt. Fortunately, a *B. abortus* Δ*wzm* mutant was available in our team (Vassen V., 2018), that is proposed to be unable to translocate the O-chain linked to the BctPP from the cytosolic leaflet to the periplasmic leaflet of the IM. The ability to obtain Δ*wadA* in a Δ*wzm* background would suggest that the toxic effects generated by the BctPP accumulation would be dependent of the localization of this accumulation. Indeed, it would mean that this accumulation would be toxic when happening in the periplasm. However, considering the O-chain saturates the BctPP pool on the cytosolic leaflet of the IM, the Δ*wadA*Δ*wzm* construction would suggest the possibility to recycle the BctPP at the cytosolic leaflet.

The attempt to delete *wadA* in this Δ*wzm* background succeeded. It is to mention that both Δ*wzm* and Δ*wadA*Δ*wzm* mutants had a sticky growth on agar plates and tend to form aggregates in liquid culture. Assessment of the growth revealed the Δ*wzm* had a standard growth rate, as compared to the WT. However, Δ*wadA*Δ*wzm* presented a reduced growth (*Figure 32*), similar to what has been observed for the Δ*wadA*Δ*gmd* double mutant (*Figure 27*). It can therefore be stated that the absence of WadA is responsible for growth defects.

In order to confirm that the O-chain was still produced in a Δ*wzm* background, a WB was performed. We performed the WB using a monoclonal antibody (A76/12G12) labeling the O-chain. We could find signal for both mutants Δ*wzm* and Δ*wadA*Δ*wzm*. However, this signal was reduced compared to the WT strain and the signal suggested a reduction in O-chain heterogeneity (*Figure 33*). We will elucidate these observations later on in the Discussion (2.1).

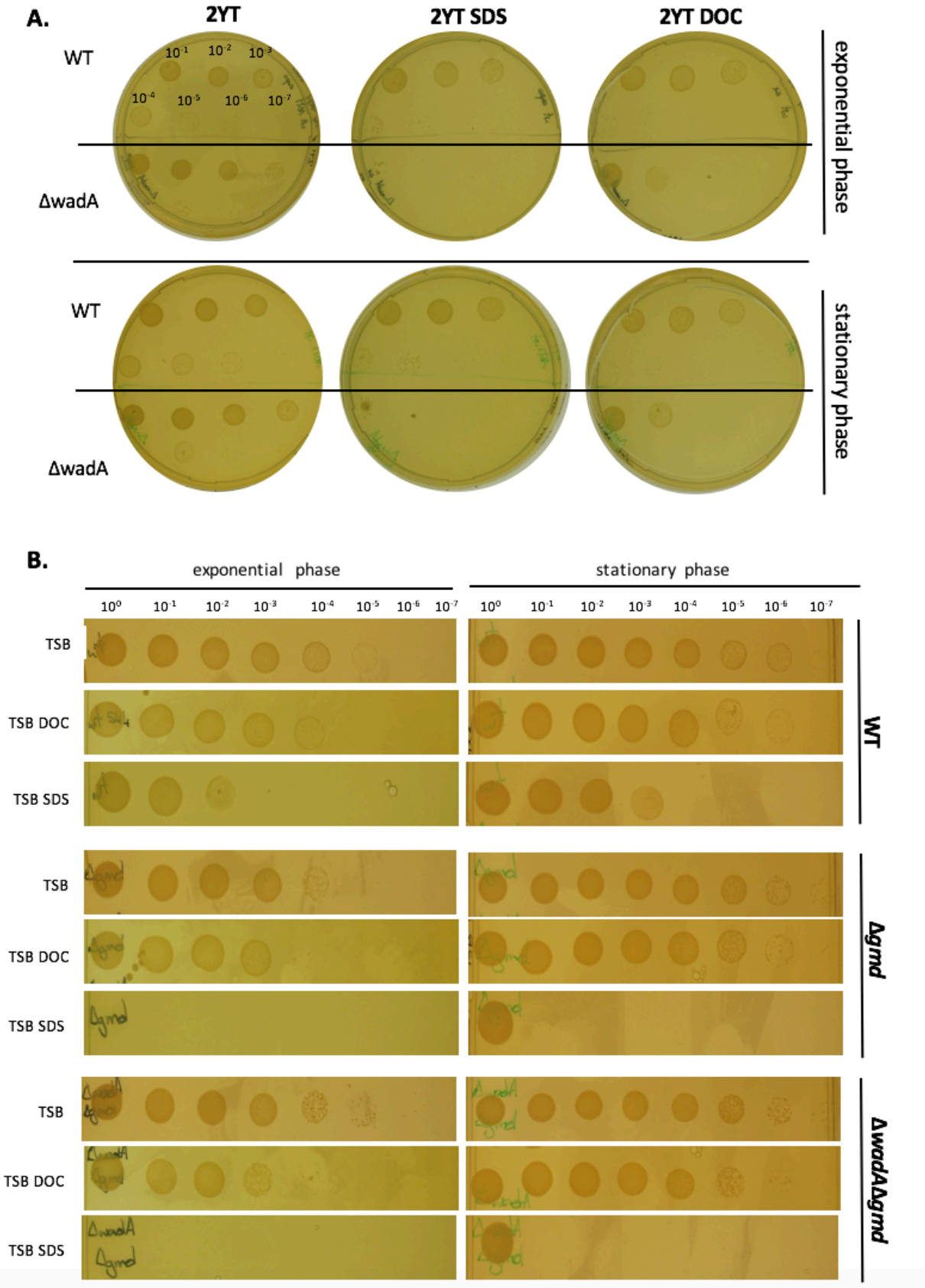

Figure 34: Spot assay on plate containing 0.001% SDS or 0.015% DOC with A: *B. melitensis* (WT, *ΔwadA*) and B: *B. abortus* (WT, *Δgmd, ΔwadAΔgmd*). Bacterial culture in exponential and in stationary phase were diluted (10-fold dilutions) and plated rich medium supplemented with SDS or DOC.

5.4. The double Δ*wadA*Δ*gmd* mutant presents outer membrane defects

As depicted on *Figure 31,* both our double mutants Δ*wadA*Δ*gmd* and Δ*GT*Δ*gmd* presented reduced growth. However, the Δ*OAg*Δ*gmd* double mutant did not alter in growth rate. We proposed that the growth defect only observed in Δ*wadA*Δ*gmd* and Δ*GT*Δ*gmd* were due to the absence of the last core sugar (Glc), that would impair OM integrity. To answer this question, we tested our mutants under different OM stressors, such as sodium deoxycholate (DOC) and sodium dodecyl sulfate (SDS), two anionic detergents; the first one being a mild and second one being a strong detergent. The WT and deletion strain for *gmd* were used as controls. Overnight exponential and stationary phase cultures were diluted by 10-fold dilutions and plated on TSB agar plates, supplemented with sublethal concentration of DOC (0.015%) or SDS (0.001%). After incubation, growth in the dilution drops was observed.

The milder detergent DOC enabled us to identify variations between the mutants. Indeed, while the Δ*gmd* mutant had similar CFUs to the WT strain, the Δ*wadA*Δ*gmd* double mutant presented a reduction ($x10^{-1}$) in CFU count when exposed to DOC (*Figure 34.B.*). These observations suggest a reduced membrane integrity in the Δ*wadA*Δ*gmd* double mutant more pronounced than the Δ*gmd* mutant. On the other hand, we could observe a reduction ($x10^{-3}$) in CFU for the Δ*gmd* and Δ*wadA*Δ*gmd* mutants under SDS stress compared to the WT strain (*Figure 34.B.*), suggesting that SDS was too strong of a detergent to see small differences between the two mutants. The same results were observed when *B. melitensis* WT and Δ*wadA* were subjected to the same membrane stresses. As depicted in *Figure 34.A.,* the Δ*wadA* mutant showed a strong reduction of CFUs when exposed to SDS. Regarding DOC exposure, the Δ*wadA* mutant presented a reduction ($x10^{-1}$) in CFUs compared to the WT strain, which correlate with the findings in *B. abortus*.

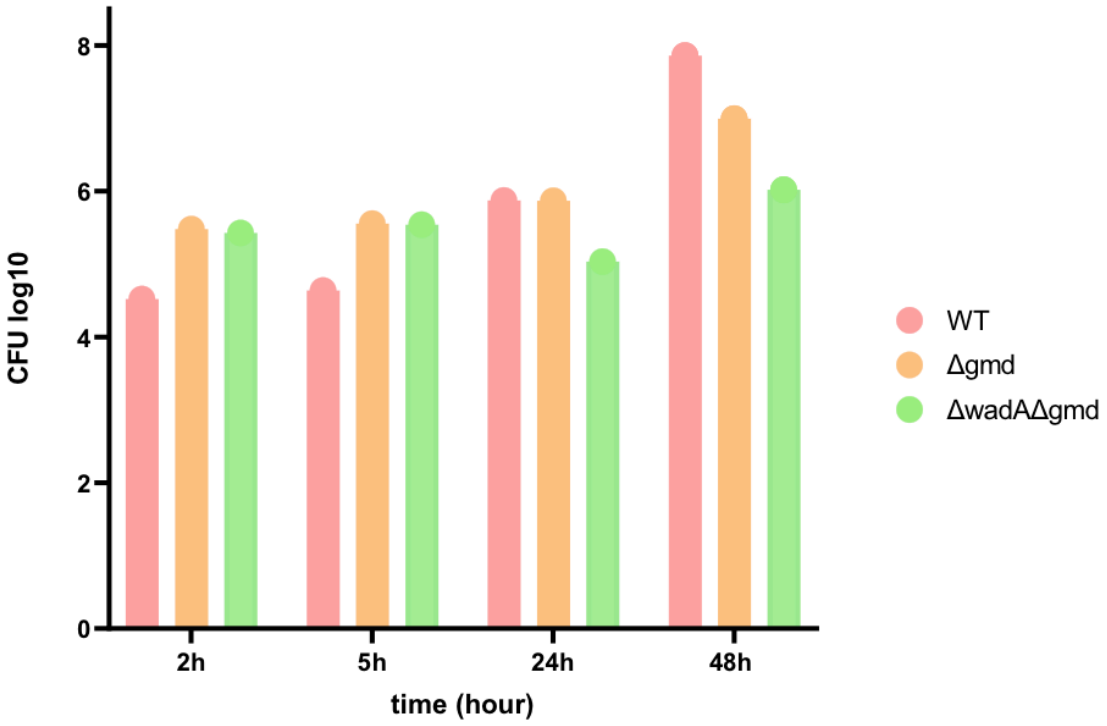

Figure 35: CFU after infection of J774.A1 macrophages with WT, Δ*gmd* and Δ*wadA*Δ*gmd B. abortus* mutants. CFU log_{10}/ml (normalized at OD_{600}=1) were obtained at time 2h, 5h, 24h and 48h PI. (N=1)

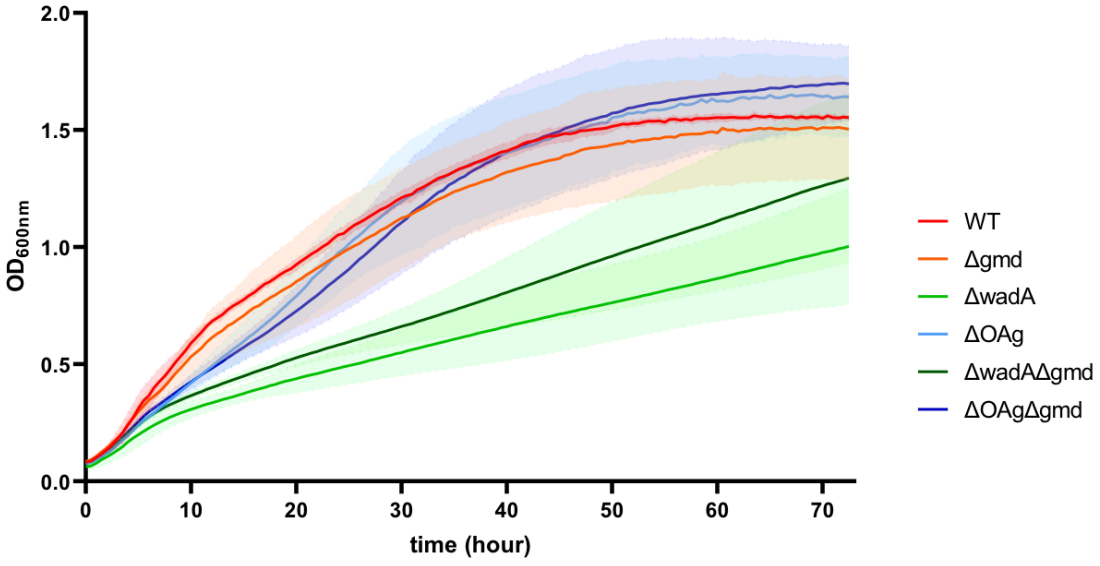

Figure 36: Growth curve of different *B. melitensis* strains (WT, Δ*gmd*, Δ*wadA*, Δ*OAg*, Δ*wadA*Δ*gmd*, Δ*OAg*Δ*gmd*) in 2YT medium for 72h at 37°C, with OD measurements taken every 30 min. (N=3)

5.5. J774.A1 macrophage infection with the double mutant Δ*wadA*Δ*gmd*

As we observed growth defects in rich medium for the Δ*wadA*Δ*gmd* double mutant, as well as under membrane stress conditions, we wanted to assess if this mutant is capable of surviving and proliferating during infection. Indeed, deleting the last core sugar could impact intracellular survival, as reports suggest that mutants presenting issues in membrane integrity show an attenuation in infection (Verdiguel-Fernández *et al.,* 2017).

Intracellular survival and growth of the Δ*wadA*Δ*gmd* double mutant (*B. abortus*) was assessed through macrophage infection. J774.A1 macrophages were infected with the WT, Δ*gmd* and Δ*wadAΔgmd* and the CFU were obtained for different stages of infection. At 2 h post-infection (PI), we could observe a lower CFU count for the WT, compared to Δ*gmd* and Δ*wadAΔgmd* (*Figure 35*). This is classical for Rough strains of *B. abortus* and *B. melitensis* (Porte *et al*., 2003). However, the WT control showed a gradual increase in CFU over time (from 5 to 48 h), correlating with its entry in macrophages followed by intracellular replication (*Figure 35*). Regarding the Δ*wadA*Δ*gmd* double mutant, CFU counts at 5 h PI were similar to the rough Δ*gmd* mutant, presenting a higher CFU compared to the WT. Yet, at 48 h PI, the CFU for Δ*gmd* was lower than the WT (*Figure 35*). These observations correlate with the theory aspect of infection. Indeed, the rough mutant are known to present a better entry in macrophage, followed by a reduction in intracellular replication (Porte *et al*., 2003). The Δ*wadA*Δ*gmd* CFU count at 24 h PI was reduced compared to 5 h PI, suggesting an intracellular killing of the Δ*wadA*Δ*gmd* double mutant between these two time points. Furthermore, we could observe a slight increase at 48 h PI. However, CFU remained lower than the WT and Δ*gmd* controls (*Figure 35*). However, it has to be noted that the experiment was performed one single time, such that biological replicates still need to be performed.

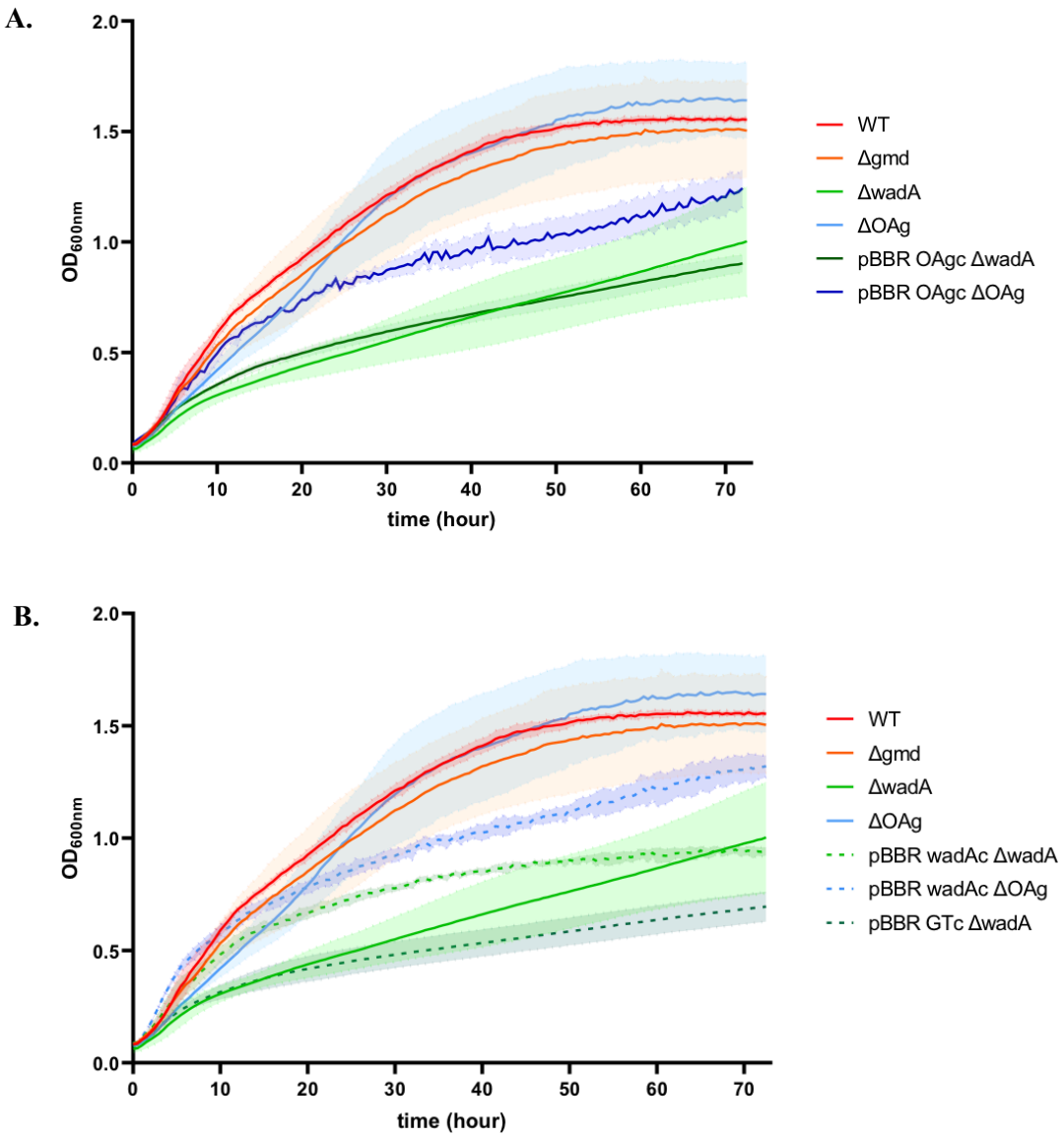

Figure 37: Growth curve of different *B. melitensis* strains (WT, Δ*gmd*, Δ*wadA*, Δ*OAg*) and the complementation strains (A. pBBR OAgc Δ*wadA*, pBBR OAgc Δ*OAg;* B. pBBR wadAc Δ*wadA*, pBBR wadAc Δ*OAg*, pBBR GTc Δ*wadA*) in 2YT medium for 72h at 37°C, with OD measurements taken every 30 min. Complementation strains were grown in 2YT supplemented with Cm. (N=3)

6. The O-antigen ligase domain deletion mutant in *B. melitensis* is viable and presents a rough phenotype

6.1. The Δ*OAg* deletion mutant in *B. melitensis* shows no growth defects

To further study WadA as the O-chain ligase, and since the *wadA* gene is not essential in *B. melitensis*, we decided to delete the OAg domain in that strain. Therefore, we attempted to delete the large periplasmic loop of this putative domain. The conjugation was performed in a WT and in a Δ*gmd* background. Both Δ*OAg* and Δ*OAg*Δ*gmd* deletion mutants were viable and revealed a standard growth curve (*Figure 36*), in contrast to the Δ*wadA* and Δ*wadA*Δ*gmd* mutants that presented a flattened curve suggesting growth defects (*Figure 36*). These results correlate with the findings of the Δ*wadA*Δ*gmd* and Δ*OAg*Δ*gmd* double mutants in *B. abortus* (see section *5.2.*).

In order to confirm that these results were due to an absence of the OAg domain, complementation strain was constructed in the Δ*OAg* deletion mutant by adding a copy of the coding sequence of the OAg domain (*Figure 14, yellow mark*) on a medium copy replicative plasmid (pBBR) under to control of its own promoter, P*wadA* (Δ*OAg*::pBBR*OAgc*). Surprisingly, this construction led to a decrease of fitness (*Figure 37.A.*). This plasmid was also used to complement the Δ*wadA* deletion mutant (Δ*wadA*::pBBR*OAgc*), resulting in a growth curve similar to the uncomplemented Δ*wadA* deletion mutant with reduced growth (*Figure 37.A.*).

A complementation strain was constructed with a pBBR plasmid containing an entire *wadA* coding sequence under the P*wadA* promoter. Complementing the Δ*OAg* deletion mutant with a full-length copy of *wadA* led to a decrease of fitness (Δ*OAg*::pBBR*wadAc*), while this growth defect was not observed in the uncomplemented Δ*OAg* deletion mutant (*Figure 37.B.*). Additionally, we observed that when complementing the Δ*wadA* deletion mutant with the whole gene of *wadA* (Δ*wadA*::pBBR*wadAc),* a partial complementation was observed, as the complemented version was not able to reach OD as high as the WT in the same time.

Finally, a complementation strain was constructed by adding a copy of the cytosolic domain with the GT coding sequence (*Figure 14, dark green mark*) on a pBBR plasmid under the P*wadA* control. This construction (Δ*GT*::pBBR*wadAc)* presented reduced growth without an exponential and a stationary phase (*Figure 37.B.*), suggesting a loss of functionality when expressing the GT domain on its own.

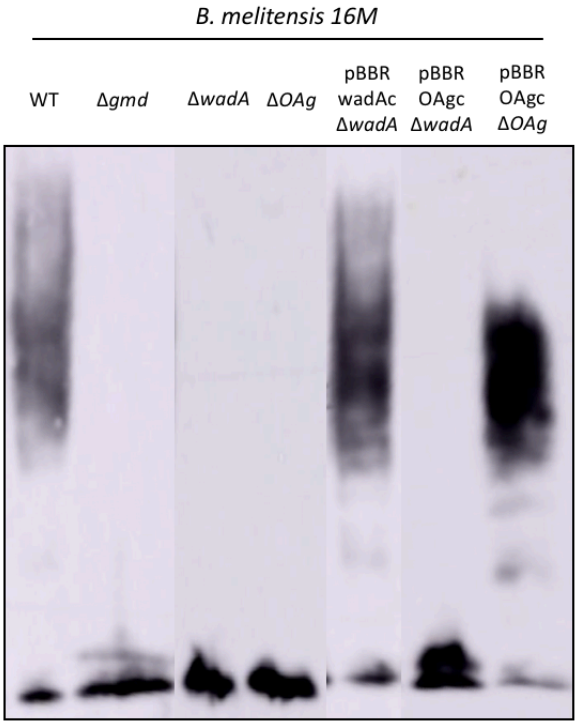

Figure 38: Western Blot of different *B. melitensis* strains (WT, *Δgmd, ΔwadA, ΔOAg)* and the complementation strains (pBBR *wadAc ΔwadA,* pBBR *OAgc ΔwadA*, pBBR *OAgc ΔOAg*) labeled with A68/24D08/G09, an anti-R-LPS antibody. This antibody binds to the LPS core, thereby enabling to visualize signal given from R-LPS or signal given from S-LPS. WT strain is a S-LPS phenotype control, while Δ*gmd* is a R-LPS phenotype control. (Original images: *Figure S6)*

6.2. The Δ*OAg* mutant in *B. melitensis* presents rough LPS

A WB was performed using an anti-R-LPS antibody (A68/24D08/G09) that interacts with the LPS core. While the positive smooth control WT presented signals for R-LPS and S-LPS, the negative rough control (Δ*gmd*) presented signal exclusively for R-LPS. Similar to the previous results found for the Δ*wadA* deletion mutant, the Δ*OAg* deletion mutant displayed solely R-LPS signal (*Figure 38*).

In order to confirm that the results we obtained are due to the absence of the O-chain ligase domain, the Δ*OAg*::pBBR*OAgc* complementation strain was tested. This complementation enabled the restoration of S-LPS bands when performing a WB with the anti-R-LPS antibody (A68/24D08/G09) (*Figure 38*). However, adding this copy to the Δ*wadA* deletion mutant (Δ*wadA*::pBBR*OAgc*) was not sufficient to restore smooth signal (*Figure 38*), which is perfectly consistent with the requirement of a glucose on the core to anchor the O-chain.

As the WB showed the presence of S-LPS when complementing with the plasmids containing the *wadA* and *OAg* genes, we can affirm that the constructs enable a functional expression of the protein and the OAg domain. It also indicates that the glycosyltransferase activity of WadA in the ΔOAg is at least partially conserved.

Furthermore, IF images obtained on the mutant supported this result. Indeed, when labeling with an anti-S-LPS antibody (A76/12G12), the Δ*OAg* deletion mutant showed no labelling signal on its surface, similar to the Δ*wadA* deletion mutant, suggesting an absence of S-LPS (*Figure 23*), compared to the WT strain that presented a homogenous labeling of its surface (*Figure 23*). Moreover, labeling with an anti-R-LPS antibody (A68/03F03/D05) indicated fluorescent signal for the Δ*OAg* deletion mutant, similar to the Δ*wadA* deletion mutant, while the WT strain presented no signal (*Figure 24*).

Figure 39: Sequence alignments of BAB1_0639 of *B. abortus* and other α-proteobacteria with highlighting of two conserved amino acids (red) believed to represent the catalytic sites of the OAg domain. The sequences were found by BLAST. Identification of the two putative catalytic sites were carried out by taking the data found by Jorgenson & Young (2016) and locate similar amino acids in the large periplasmic loop of OAg. We predicted R614 and H605 to represent the potential catalytic sites in *B. abortus*. (Enlarged representation can be found under *Figure S7).*

7. Identification of amino acids necessary for the OAg domain activity

7.1. H605 and R614 are two conserved residues in the alpha proteobacteria

As mentioned in the Introduction, Jorgenson & Young managed to identify some amino acids which seem to represent the catalytic sites of the O-chain ligase activity of WaaL in *E. coli*. Interestingly, these amino acids were positively charged, suggesting an importance of positively charged amino acids for the ligase activity to liberate the O-chain from the BctPP. Mutations of these amino acids with non-charged amino acids resulted in an incapacity to perform the ligase activity.

Considering these findings, we blasted *wadA* looking for the closest homologs in other α-proteobacteria. Interestingly, we only found few species inside α-proteobacteria presenting homologs for *wadA*. After aligning these sequences (*Figure 39*), we looked for positively charged amino acids conserved in all the species identified. More precisely, we searched for these residues around the amino acids believed to form the large periplasmic loop of the OAg domain. As Jorgenson & Young precisely identified an Arg and a His residue, we searched for similar residues. We were able to detect a conserved His residue, H605 in *B. abortus*, and a conserved Arg residue, R614 in *B. abortus* (*Figure 39*), which were predicted to be located on the putative periplasmic loop according to TMHMM prediction (*Figure 13*). We therefore propose that these residues could represent sites necessary for the ligase activity.

It is to note that the residue position within the sequence varies between species on this alignment. The annotation for *B. melitensis* seen in *Figure 39* would be H651 and R660. However, to facilitate further descriptions, we are going to keep the annotation H605 and R614 for both *B. abortus* and *B. melitensis*.

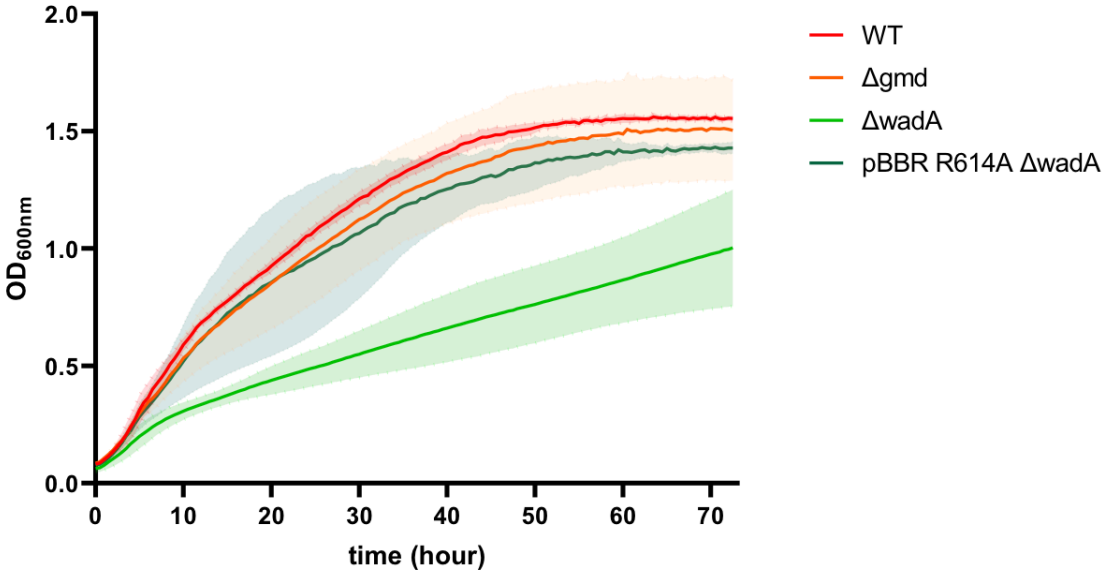

Figure 40: Growth curve of different *B. melitensis* strains (WT, Δ*gmd*, Δ*wadA*, Δ*OAg*) and two complementation strains pBBR R614A Δ*wadA* in 2YT medium for 72h at 37°C, with OD measurements taken every 30 min. Complementation strains were grown in 2YT supplemented with Cm. (N=3)

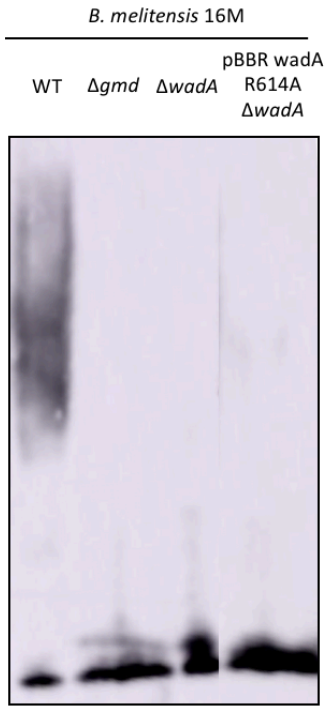

Figure 41: Western Blot of different *B. melitensis* strains (WT, *Δgmd*, *ΔwadA*, pBBR wadA R614A in *ΔwadA)* labeled with A68/24D08/G09, an anti-R-LPS antibody. This antibody binds to the LPS core, thereby enabling to visualize signal given from R-LPS or signal given from S-LPS. WT strains are S-LPS phenotype controls, while Δ*gmd* is a R-LPS phenotype control. (Original images *Figure S6)*

7.2. R614A point mutation in *B. melitensis* leads to a rough phenotype

Regarding the potential residues found in *B. melitensis*, we attempted to test the hypothesis that arginine 614 (R614) is required for O-chain ligase activity (we did not test histidine 605 because the timing of the master thesis did not allow it). The idea was to attempt to complement the Δ*wadA* deletion mutant with a pBBR replicative plasmid containing a copy of *wadA* displaying a point mutation of the catalytic residue. If R614 is required for the O-chain ligase activity, complementation should not be obtained, while the complementation with the wild type allele was obtained with the pBBR*wadAc* plasmid in the *B. melitensis* Δ*wadA* strain (see *Figure 38*). The R614 was mutated to an alanine *(*Δ*wadA*::pBBR*wadA*-R614A), a neutral amino acid (small, uncharged, that does not impose or permit torsions in the main chain). By characterizing this complemented mutant, we should be able to identify the presence or absence of S-LPS and thereby discover if this mutated *wadA* copy still presents a ligase activity.

First of all, the growth of the complemented candidate was assessed by measuring the OD over 72 h. The growth curves suggest a return to a standard curve, similar to the WT strain (*Figure 40*). Therefore, we can affirm that the point mutation did not alter the ability of the *wadA* copy to complement the deletion mutant and restore WT growth rate, suggesting that the WadA-R614A variant is at least partially functional and thus folded.

A WB was performed with an anti-R-LPS antibody (A68/24D08/G0) with the Δ*wadA*::pBBR*wadA*-R614A strain. In *Figure 41*, this strain displayed an absence of O-chain for the complemented mutant, as exclusively rough signal could be detected, in contrast to the WT control. This result suggests that in the absence of the positively charged Arg residue, the O-chain ligase activity of WadA is disrupted, supporting the hypothesis that the OAg domain performs the ligation of the O-chain to the LPS core.

7.3. Deletion of *wadA* in *B. abortus* cannot be achieved in presence of a R614A point mutation in the genome of the bacteria

The strategy used in *B. melitensis* was not possible in *B. abortus* as we were only in possession of the double mutant Δ*wadA*Δ*gmd*, ultimately lacking the O-chain. Therefore, we used another strategy where we first added an external copy of *wadA* containing R614A in the *B. abortus* WT strain and then attempted to delete the genomic copy of *wadA* by allelic replacement. The replicative plasmid used was of medium copy (pBBR) and the mutated *wadA* copy was under the control of its P*wadA* promotor (WT::pBBR*wadA*-R614A). Following the conjugation of the pBBR *wadA* R614A, we attempted to delete *wadA* in the genome of the bacteria by using an integrative plasmid (pNPTS), able to perform recombination. However, we added a constant selective pressure by supplementing the culture with Cm to ensure the maintenance of the replicative plasmid with the point mutation within the bacteria. 50 putative candidates were screened by diagnostic PCR and no Δ*wadA* deletion mutant appeared under these conditions (data not shown). We can therefore propose that the R614A point mutation disrupts the putative O-chain ligase activity, impeding the possibility to delete *wadA*. In other words, it seems like the R614 residue is essential in *B. abortus* and that this residue indeed represents an essential site of the ligase activity. However, we are in absence of a control construct. It should be tested if we can carry out the deletion of *wadA* in a Δ*gmd* strain containing the plasmid (Δ*gmd*:: pBBR*wadA*-R614A).

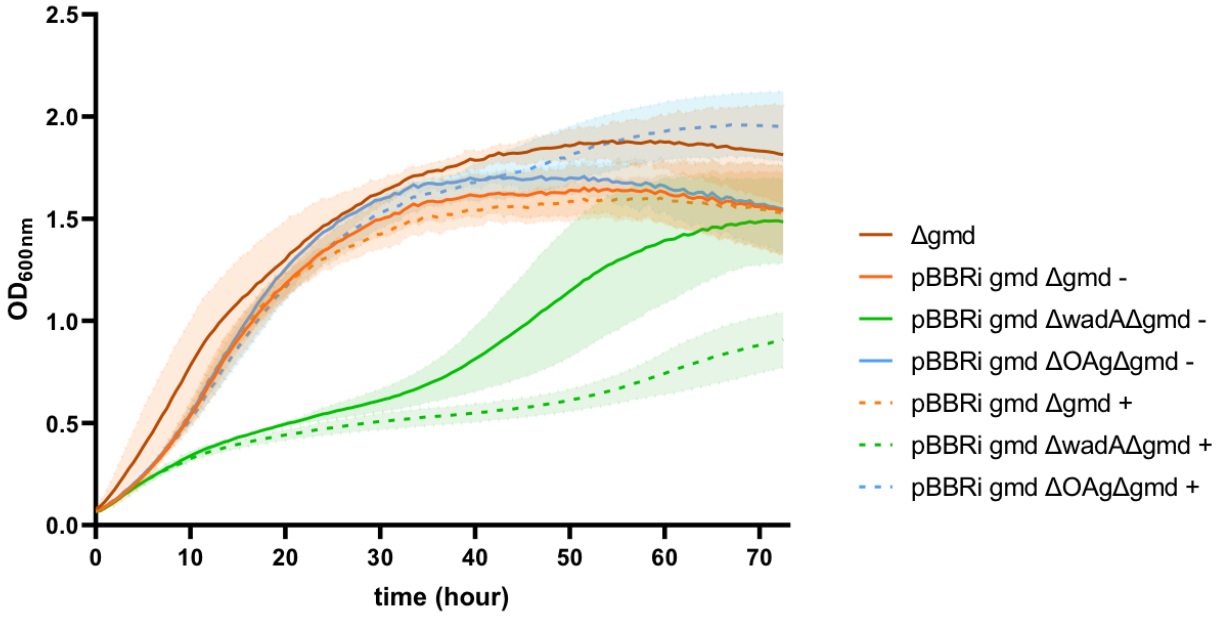

Figure 42: Growth curve of different *B. abortus* strains (Δ*gmd,* pBBRi gmd Δ*gmd* pBBRi gmd Δ*wadA*Δ*gmd* and pBBRi gmd Δ*OAg*Δ*gmd)* without (-) and with (+) induction of *gmd* expression, in TSB medium (supplemented with Cm) for 72 h at 37°C, with OD measurements taken every 30 min. IPTG was added at time 0h. (N=3)

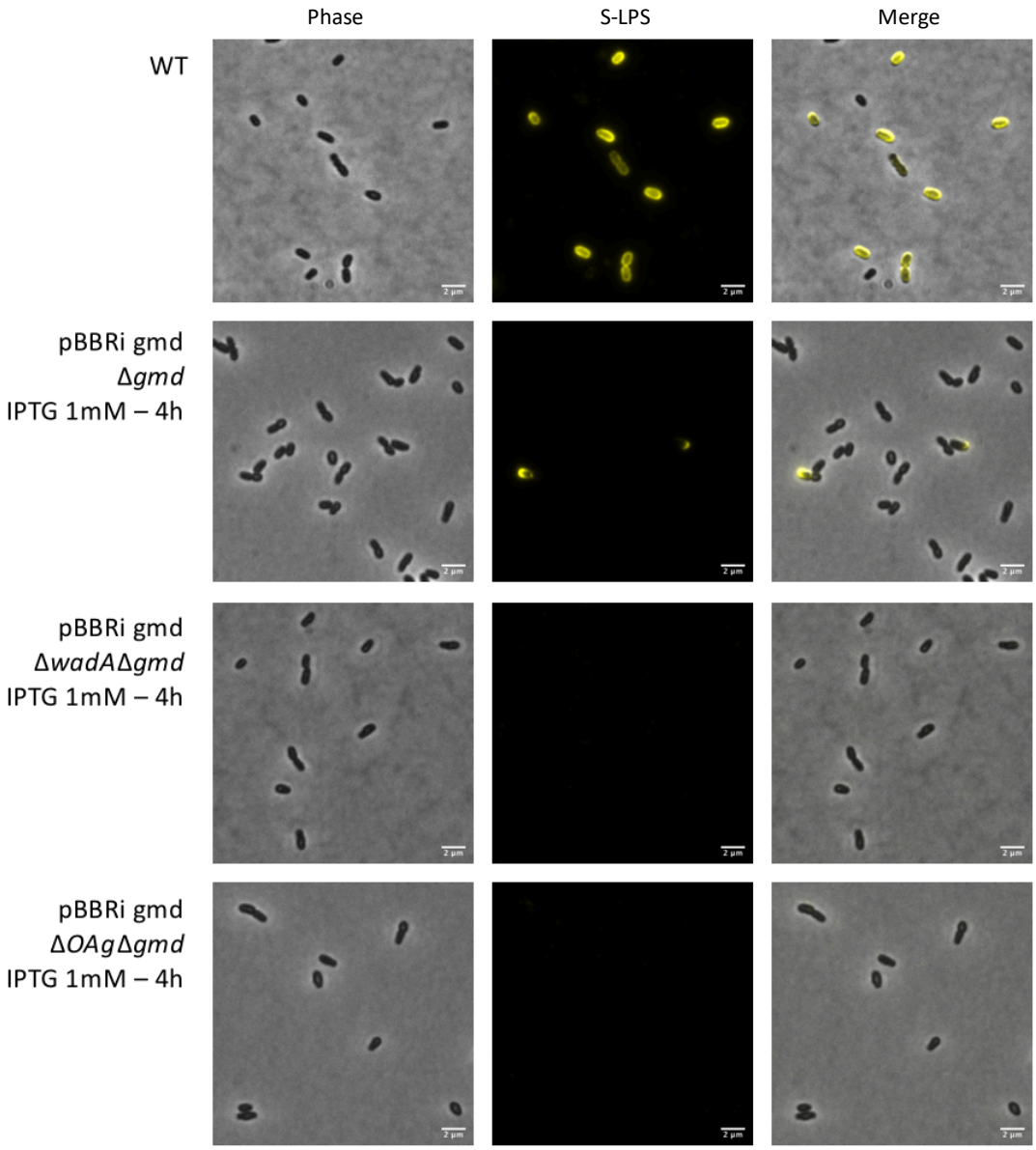

Figure 43: Immunofluorescence microscopy images on wt, Δ*gmd*, Δ*wadA*Δ*gmd and* Δ*OAg*Δ*gmd* after 4h induction of pBBRi gmd. Bacteria were labeled with anti-S-LPS antibody A76/12G12 as a primary antibody. Goat anti-mouse IgG H+L AlexaFluor 514 was used as a secondary antibody (YFP channel).

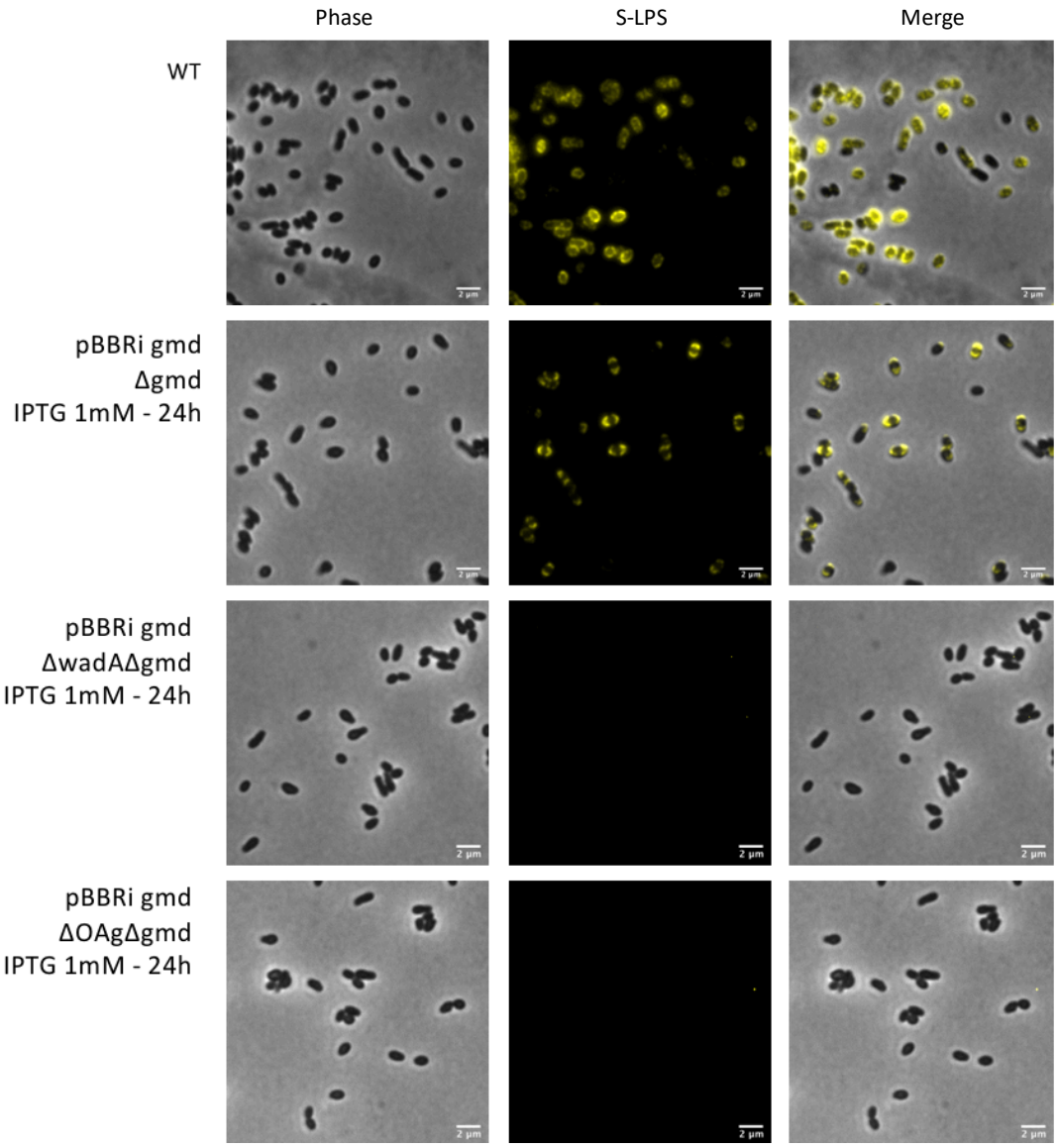

Figure 44: Immunofluorescence microscopy images on wt, Δ*gmd*, Δ*wadA*Δ*gmd and* Δ*OAg*Δ*gmd* after 24h induction of pBBRi gmd. Bacteria were labeled with anti-S-LPS antibody A76/12G12 as a primary antibody. Goat anti-mouse IgG H+L AlexaFluor 514 was used as a secondary antibody (YFP channel).

8. Inducible expression of Gmd in the double mutants Δ*wadA*Δ*gmd and* Δ*OAg*Δ*gmd*

We wondered if controlled expression of gmd could restore S-LPS production on the surface in the presence of Δ*wadA* or Δ*OAg* mutations in *B. abortus*, which should not be the case if the OAg domain is indeed the O-chain ligase in *B. abortus*. Using an IPTG-inducible replicative plasmid pBBRi (*Material & methods - Induction of S-LPS with IPTG*), we constructed strains where we were able to induce the expression of *gmd* in a Δ*wadA*Δ*gmd* and Δ*OAg*Δ*gmd* background. This controlled induction of *gmd* expression should not impede the cultures to grow as potential O-chain-linked BctPP saturation should not be reached. However, we should be able to detect the presence of S-LPS on the surface of the bacteria in presence of the O-chain ligase activity.

These constructions were first assessed for their growth by measuring OD over 72 h. As depicted on *Figure 42*, inducing *gmd* expression in a Δ*wadA*Δ*gmd* background led to even more pronounced growth defects compared to the uninduced Δ*wadA*Δ*gmd* mutant. Regarding the Δ*OAg*Δ*gmd* mutant, *gmd* expression did not alter the growth profile as the induced strain presented a similar exponential phase to the uninduced strain and the WT strain. However, after around 40 h, we could observe a shift of the curve with an amplification of the OD measurements. Indeed, the induced Δ*OAg*Δ*gmd* strain seemed to achieve similar OD measurements as the WT strain. Interestingly, a slight shift could also be observed for the induced Δ*wadA*Δ*gmd* strain after 50 h.

In order to characterize the double mutants after *gmd* induction, we performed IF microscopy after different times of induction. At first, we labeled the strains 4 h after adding IPTG with an anti-S-LPS antibody (A76/12G12). The positive control WT presented a homogenous labeling of its bacterial surface. Our positive control for *gmd* expression was the induced Δ*gmd*::pBBRi *gmd* strain, which displayed a signal at few poles (*Figure 43*), indicating the incorporation of S-LPS on the growing poles. Therefore, we can suggest that the *gmd* expression was successful in a fraction of the cells. Regarding the pBBRi *gmd* Δ*wadA*Δ*gmd* and pBBRi *gmd* Δ*OAg*Δ*gmd* strains, none presented S-LPS signal on their surface after 4 h induction (*Figure 43*). Identical labeling with the anti-S-LPS antibody was performed after 24 h induction. Yet again, the WT control presented a homogenous labeling. The pBBRi *gmd* Δ*gmd* strain induced for 24 h displayed an increased labeling of its surface (*Figure 44*) compared to the results found after 4 h induction (*Figure 43*), suggesting a rise in S-LPS incorporation, correlating with an increased synthesis of O-chain likely due to the presence of Gmd. However, neither of the pBBRi *gmd* Δ*wadA*Δ*gmd* and pBBRi *gmd* Δ*OAg*Δ*gmd* strains presented S-LPS signal (*Figure 44*). We can therefore suggest that *wadA* is necessary for the incorporation of the O-chain to the LPS core in *B. abortus* as well. And even more precisely, the OAg domain would have been needed for this ligase activity (if the residual WadA deleted for the OAg domain is functional).

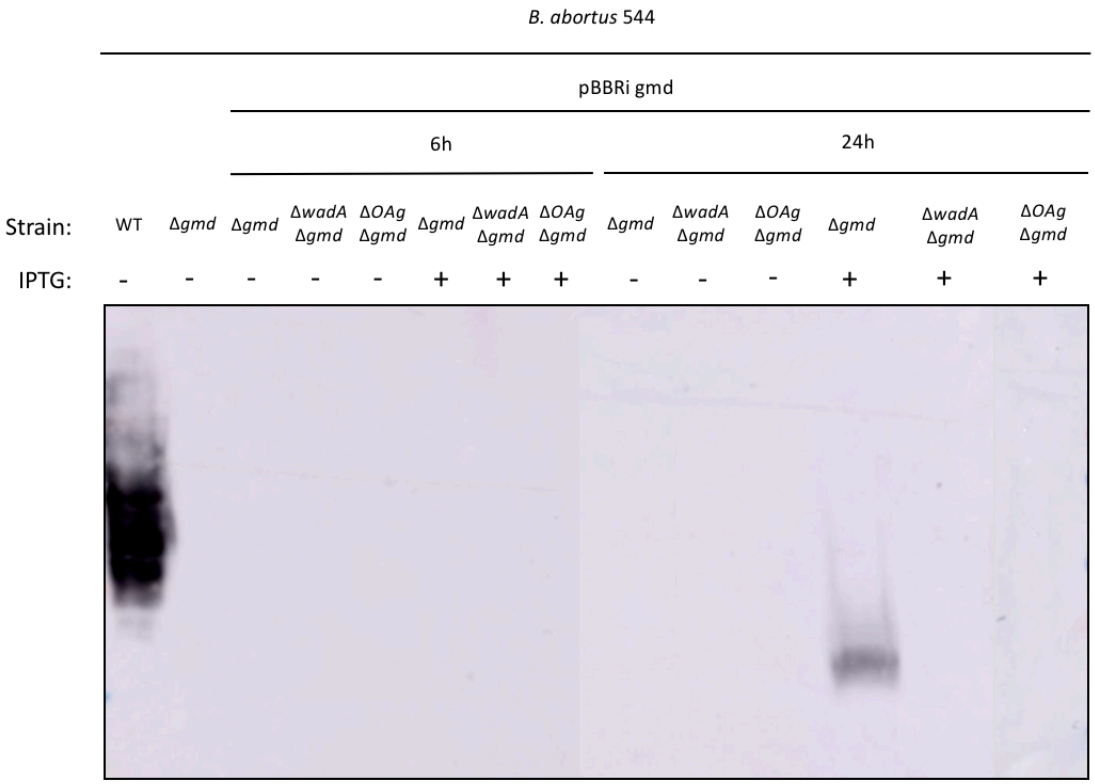

Figure 45: Western Blot of different *B. abortus* strains (WT, Δ*gmd)* and strains containing a pBBRi gmd copy labeled with A76/12G12, an anti-S-LPS antibody. This antibody binds to the O-chain, displaying a signal in the presence of S-LPS (or BctPP-O-chain). Gmd expression was (+) or was not (-) induced by adding IPTG to the culture for 6h or for 24h. (N=2)

In the absence of the large periplasmic domain of the putative OAg domain, there is no incorporation of S-LPS on the bacterial surface, despite the presence of Gmd. However, we have to check if Δ*wadA* and Δ*OAg*-carrying strains analyzed here are still able to produce the O-chain. We therefore performed WB on these *gmd* uninduced or induced strains. Induced strains tested after 6 h and 24 h. Labeling was performed using an anti-S-LPS antibody (A76/12G12) able to recognize the O-chain but not the core of the LPS, as seen for our positive control WT (*Figure 45*). While our negative control Δ*gmd* displayed no signal. None of our uninduced strains displayed signal, indicating an absence of O-chain, explained by the lack of Gmd. Strains induced during 6 h with IPTG presented no S-LPS signal. However, the pBBRi *gmd* Δ*gmd* strain induced for 24 h presented a signal, but of lower molecular weight compared to the WT strain. Regarding the pBBRi *gmd* Δ*wadA*Δ*gmd* and pBBRi *gmd* Δ*OAg*Δ*gmd* strains induced for 24 h, we could not detect O-chain signal (*Figure 45*). Therefore, we cannot conclude that the absence of S-LPS on induced strains carrying the Δ*wadA* or Δ*OAg* mutations is due to the absence of O-chain ligase activity; we have to consider that O-chain synthesis is impaired in these strains.

DISCUSSION AND PERSPECTIVES

The LPS is a major component of the OM of Gram-negative bacteria. This essential molecule is estimated to represent 75% of the bacterial surface (Lerouge & Vanderleyden, 2002). While some species are called smooth as they present S-LPS and R-LPS, some species like *B. ovis* exclusively present R-LPS and are named rough species. This work focused on two smooth *Brucella* species, mainly *B. abortus* and *B. melitensis*. While the majority of the synthesis pathway of the LPS has been characterized, the O-chain ligase, necessary to add the O-chain to synthesize the S-LPS molecule, has not yet been identified in *Brucella*. Through *in silico* analysis, we found two potential candidates: *waaL* and *wadA*. We thereby focused our research on these two candidates with the goal to identify the putative O-chain ligase in *Brucella* spp.

1. Investigation of WaaL (BAB2_0106)

In *E. coli,* WaaL has been reported as the O-chain ligase and many homologs have been found in other bacterial species such as *Pseudomonas, Salmonella, Myxococcus* and *Vibrio* (Pérez-Burgos *et al.,* 2019; Schild *et al.,* 2005; Islam *et al*., 2010). While some papers refer to WaaL as the O-chain ligase in *B. abortus*, evidence supporting this assumption has never been found (Moriyón *et al*., 2004; Haag *et al.,* 2010).

In *B. abortus* 2308, BAB2_0106 appears as a homolog of *E. coli waaL*. Synteny analysis suggests a conservation of BAB2_0106 (*waaL*) in the *Brucella* genus, while homologs of this gene seem to be present at another position of the genome in other alphaproteobacteria (*Figure 11.A.*). Transmembrane domain prediction analysis suggests a structure with twelve transmembrane domains and two periplasmic loops (*Figure S1*), similar to *E. coli* (Pérez *et al*., 2008). However, WB and IF analyses have shown that a deletion mutant for this gene in *B.abortus* (Δ*waaL*) displayed a S-LPS phenotype. This deletion mutant presented neither morphological abnormalities, nor any growth defects. IF images showed signals similar to WT strains with a homogenous labeling of S-LPS on the bacterial surface (*Figure 18*). While for the WT strain, we could observe rough signal on the poles only, labeling of R-LPS in a rough control was homogeneous (*Figure 19*). The Δ*waaL* mutant showed R-LPS signals on the division sites exclusively, similar to the WT (*Figure 19*). Considering that *Brucella* present a unipolar growth, synthesis of new cell envelope occurs at the growing pole and division sites. It is suggested that newly incorporated material is easily recognized by the antibodies targeting the R-LPS, while accessibility to old R-LPS molecules might be sterically hindered, for example by the O-chains of the S-LPS molecules present on the remaining bacterial surface.

Based on the presence of S-LPS signal on the Δ*waaL* deletion mutant, we propose that WaaL is probably not the main O-antigen ligase in *B. abortus* in rich medium. Of course, we cannot exclude redundancy with another O-chain ligase. Indeed, a second protein might be able to perform the ligation activity and compensate for the absence of the O-chain ligation activity by WaaL, so that we would not detect a rough phenotype in the Δ*waaL* deletion mutant.

Moreover, different O-chain ligases could be involved in the S-LPS synthesis depending on the environmental conditions. In this case, we could expect reduced *waaL* expression in the tested condition, being growth in a rich medium, if an O-chain ligase distinct from WaaL is active. However, we could suggest that in other environmental conditions, for example growth in poor medium or in presence of certain stresses, the bacteria might favor the synthesis of another type of S-LPS requiring WaaL. Indeed, we cannot exclude that another type of O-chain, never described so far in *Brucella*, could be the substrate of WaaL.

In order to identify if *waaL* is transcribed when bacteria are cultured in rich medium, the expression of *waaL* could be assessed by RTq-PCR (Reverse Transcription quantitative Polymerase Chain Reaction). This technique enables detection of mRNA. If no expression of *waaL* is detected, it can be proposed that WaaL is not active in *Brucella* spp. and that another gene is responsible for the O-chain ligase under the tested conditions. In case we can detect *waaL* expression, the expression of WaaL could be analyzed through Western blotting in order to determine if the mRNA is translated.

The O-chain being the component varying the most between the two classes of bacteria, but also between two species of the same phylum, it is not surprising that the O-chain ligase might vary between *E. coli* and *Brucella* spp. We therefore proposed that another protein could play this role in the *Brucella* genus.

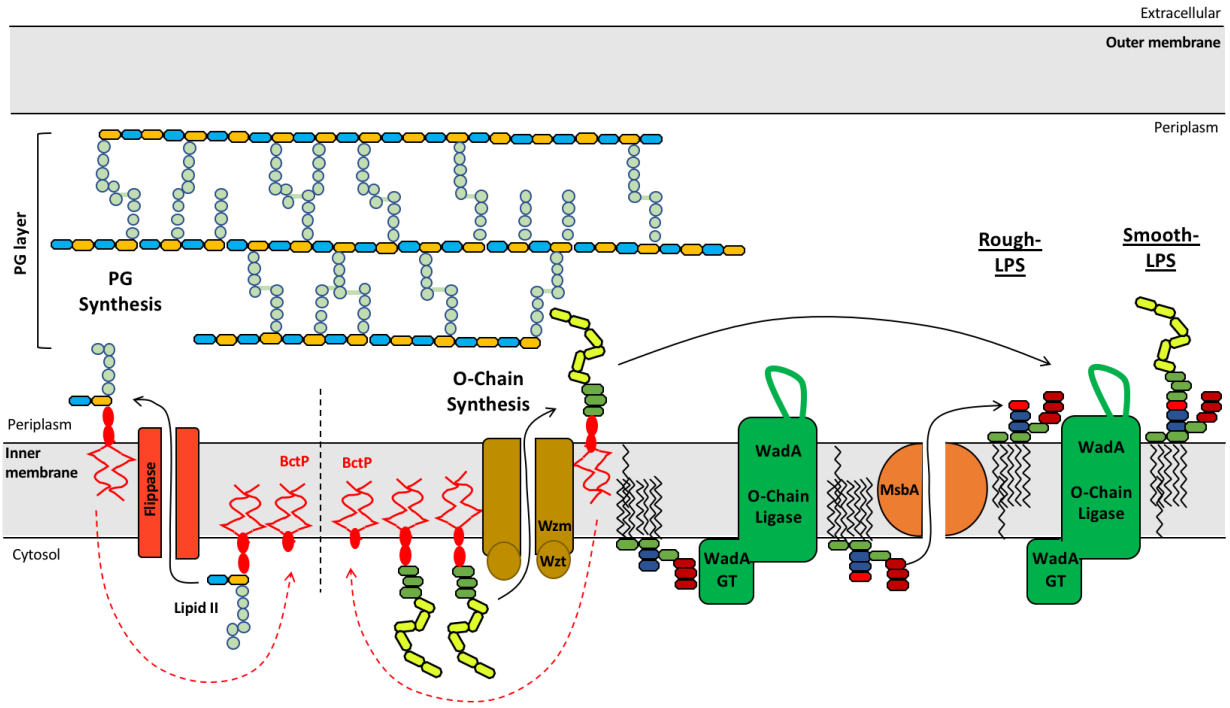

Figure 46: Schematic representation of the LPS synthesis pathway and the PG synthesis pathway using the same BctP pool. During the LPS synthesis, the O-chain binds to BctPP in order to be translocated to the periplasmic leaflet. After O-chain ligation to the LPS core, the BctP is flipped and returns to the cytosolic leaflet. Regarding the PG synthesis, the precursor, lipid II, binds to the BctPP in order to be translocated to the periplasmic leaflet. This lipid A is composed of a disaccharide and a peptide chain. Once freed from the lipid II, the BctP returns to the inner leaflet. We propose that a unique BctP pool present on the IM is necessary for both synthesis pathways as it binds to the O-chain and to the lipid II. In this manner, in a condition were the O-chain is not ligated to the LPS core, the O-chains stay bound to the BctPP, reducing the BctP pool able to enter the PG synthesis pathway and consequently leading to a decrease in PG synthesis.

2. Investigation of WadA (BAB1_0639)

2.1. *wadA* is essential in *B. abortus* 544

WadA has been previously shown to be a glycosyltransferase involved in the LPS core synthesis by adding the last core sugar in *B. melitensis*. This last sugar is essential for the O-chain to be ligated to the core. Indeed, a deletion mutant was constructed in *B. melitensis* and presented R-LPS on the surface (González *et al.,* 2008). Interestingly, two domains were predicted for that gene, the glycosyltransferase and the O-chain ligase domain. TMHMM analysis of *wadA* gave the prediction of twelve transmembrane domains and a large periplasmic loop (*Figure 13*), similar to WaaL in *E. coli* (*Figure S1*) (Pérez *et al*., 2008). Moreover, TMHMM analysis suggested the *wadA* glycosyltransferase domain, absent in *waaL* in *E. coli,* would be located in the cytoplasm, where it would add the last sugar to the core of the R-LPS before being translocated, and the O-chain ligase was predicted to be in the periplasmic space (*Figure 13*). This prediction of localization correlates with other ligases that have been shown to be active in the periplasmic space (Han *et al.,* 2012).

B. abortus was supposed to be the main species of this work, but surprisingly we could not obtain the Δ*wadA* mutant, while the construction of other deletion mutants was clearly feasible. The possibility to obtain a viable Δ*wadA* in *B. melitensis* discovered by González *et al*. inclined us to generate a Δ*wadA* mutant in this species, which was successful. We postulate that this gene is essential for growth in rich medium in *B. abortus*. In order to explain this essentiality, we proposed that toxic effects occur due to an accumulation of O-chain in absence of the O-chain ligase. Therefore, we aimed to delete *wadA* in a strain unable to produce O-chains. As Gmd is a protein necessary during O-chain synthesis, a Δ*gmd* deletion mutant fulfills this requirement. Interestingly, the construction of the Δ*wadA*Δ*gmd* double mutant succeeded, supporting our hypothesis of toxic O-chain accumulation. Similar results were obtained when attempting to delete the *GT* and the *OAg* domains individually, as the construction had to be performed in a Δ*gmd* background; these data suggest that both domains are essential.

It can be imagined that when deleting the O-chain ligase, the unligated O-chains stay bound to their lipid carrier, the BctPP and lead to these toxic effects. Indeed, the O-chain precursor is synthesized on the cytosolic leaflet of the IM on the lipid carrier BctP (see section 3.1.4. of the Introduction). This precursor is then translocated to the periplasmic leaflet through the ABC transporter Wzm/Wzt. During this translocation, the O-chain stays bound to the BctPP, before detaching itself to be ligated to the LPS core by the O-chain ligase. Once the BctPP is freed from the O-chain, it is suggested to be dephosphorylated (BctP) before being flipped via a protein-assisted mechanism to the cytosolic leaflet (Manat *et al*., 2014) and is able to reenter the synthesis pathway (*Figure 46*). In this manner, the BctP is required for S-LPS synthesis. However, the lipid carrier is also involved it other synthesis pathways, such as the essential PG (see section 3.2. of the Introduction). Indeed, the PG layer of the periplasm needs to be constantly synthesized as the bacteria grow. During their synthesis, the PG precursors bind to the BctP to give the so-called lipid II (*Figure 46*) (Egan *et al.,* 2020). The lipid carrier BctP is thereby essential for both S-LPS and PG syntheses. It can thereby be proposed that an O-chain-linked BctPP saturation leads to growth defects due to an inability to produce the PG layer as the BctP pool present on the cytosolic leaflet could decrease, thus leading to growth inhibition and hindering the construction of a Δ*wadA* deletion mutant in *B. abortus*. Experimental data supporting the hypothesis of BctPP saturation by O-chains has been obtained in *E. coli,* where accumulation of BctPP-linked intermediates, and thereby BctPP sequestration, led to morphological defects (Jorgenson & Young, 2016).

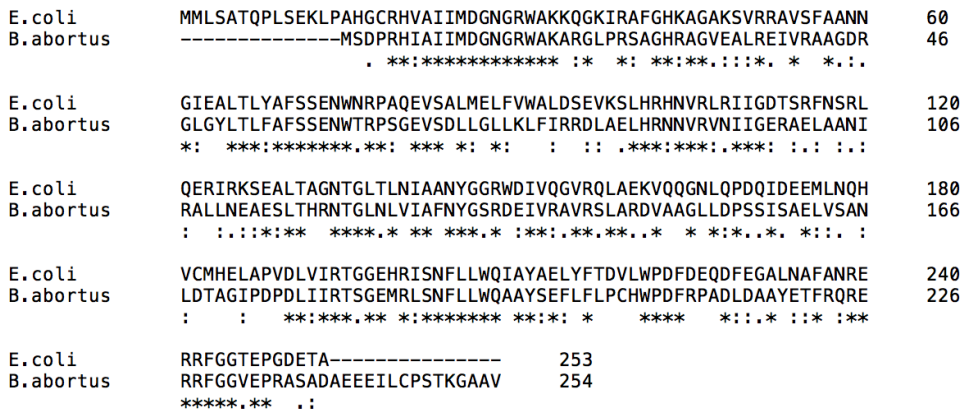

Figure 47: Sequence alignment of UppS in *E. coli* and the homolog found in *B. abortus* (BAB1_1180) identified using BLAST.

It was demonstrated that alteration in the O-chain synthesis resulted in alteration in the PG biogenesis. For instance, deletion mutants for the O-chain ligase WaaL presented morphological defects with the bacteria growing 40% wider and 62% longer compared to WT bacteria. These alterations were shown not to be simply due to lack of the O-chain, as the deletion of one of the proteins intervening in the early stages of biosynthesis (*wecA*) resulted in bacteria lacking the O-chain but presenting a normal morphology. Moreover, the double deletion mutant for *waaL* and *wecA* presented a standard morphology, meaning that inhibiting O-chain synthesis in Δ*waaL* reduced the toxic effects (Jorgenson & Young, 2016). This supported the concept of morphological alterations being generated by an accumulation of BctPP-linked intermediates, instead of absence of S-LPS, and resulting in an impairment of the PG synthesis and consequently to growth defects. This hypothesis was further supported after overexpression of the gene coding for the undecaprenyl pyrophosphate synthase (UppS) in the *ΔwaaL* mutant (Jorgenson & Young, 2016). UppS catalyzes the formation of BctPP, which is later transformed into BctP by undecaprenyl pyrophosphate phosphatase (UppP) in order to enter the synthesis pathways. Thereby, overexpressing UppS leads to an increase in BctP molecules (El Ghachi *et al*., 2004). It was shown that increasing the BctP pool in the *ΔwaaL* mutant reduces defects created by O-chain-linked BctPP accumulation, as the return to a standard morphology was observed. This supports that the two pathways, LPS and PG syntheses, share the same BctP pool, and that decreased availability in BctP due to sequestration of the carrier by one of the pathways impacts the second biosynthesis pathway (Jorgenson & Young, 2016). Through sequence "blasting ", we managed to identify an UppS homolog in *B. abortus*, BAB1_1180 (*Figure 47*). Increasing the pool of BctP by overexpressing BAB1_1180 should allow deletion of *wadA* in a *B. abortus* WT background and is a perspective for this work to support this BctPP sequestration hypothesis.

However, we were still wondering if the localization, cytosolic or periplasmic, of this BctPP saturation had an impact on growth. Therefore, an attempt to delete *wadA* in a Δ*wzm* background was performed, as this deletion mutant should present synthesis of O-chain precursors, but unable to be translocated to the periplasmic leaflet of the IM, the precursors remain on the cytosolic leaflet. The construction of this Δ*wadA*Δ*wzm* double mutant succeeded, indicating that toxic effects could be due to accumulation of the BctPP on the periplasmic leaflet specifically.

It is to mention for the Δ*wzm* and Δ*wadA*Δ*wzm* mutants that the WB revealed presence of O-chain. However, the migration profile of these two mutants was altered, as we could observe that the signals for Δ*wzm* and Δ*wadA*Δ*wzm* were reduced in intensity compared to the WT strain (*Figure 33*). This WB was initially performed to determine the presence or absence of O-chain, considering results previously described (Vassen V., 2018). Indeed, Vassen *et al*. pointed out that their Δ*wzm* mutant presented no detectable amount of intracellular O-chain, suggesting that there might be a negative feedback loop inducing a reduction of O-chain synthesis, the remaining molecules being under the WB threshold. Interestingly, opposed results were found in a Δ*wzm/wzt* mutant in *B. melitensis*, where an intracellular accumulation of O-chain was reported, of reduced heterogeneity, yet of similar intensity compared to the WT control (Godfroid *et al.,* 2000). This observation further revealed differences between the two species with, potentially, non-identical BctP recycling. In this work, the WB results in *B. abortus* suggest presence of O-chain, but at a reduced quantity, supporting the idea of a negative feedback. It is maybe this decrease in O-chain quantity that enables to delete *wzm* and *wadA* without causing important toxic effects due to BctPP saturation, even with the O-chain synthesis still being performed on the BctP molecules. The small O-chain quantity could permit a sufficient level of BctP able to enter the PG synthesis pathway. Another possible explanation to the ability to delete *wzm* could be that BctPP linked to O-chain, on the cytosolic leaflet would

be easier to recycle then when located in the periplasmic leaflet. Yet the protein enabling recycling of the BctPP when on the periplasmic leaflet could be less active or absent in *B. abortus*, explaining why we are unable to delete *wadA* individually in this species.

Moreover, the WB suggested a reduced variability of the O-chain in the the Δ*wzm* and Δ*wadA*Δ*wzm* mutants compared to the WT (*Figure 33*), an observation correlating with the reduced heterogeneity observed in the Δ*wzm/wzt* mutant in *B. melitensis* (Godfroid *et al.,* 2000). These differences could be explained by the distinct carrier of the O-chain for the mutants in contrast to the WT. Indeed, while this polysaccharide is bound to the lipid A-core in the WT strain, the two mutants present the O-chain on the BctPP. It can be proposed that bound to this lipid carrier, the O-chain reaches a chain structure of 96 to 100 Per subunits and trapped in the cytosolic leaflet, it manages to keep this structure. While we could suggest that when translocated through the compartments to reach the OM, the O-chain structure is affected and thereby presents a greater heterogeneity (*Figure 33*).

Even if this BctPP saturation hypothesis is correct, one question remains: why would *wadA* be essential in *B. abortus*, but not in *B. melitensis*? We suggested that, as it shows a slower growth, *B. melitensis* might have time to establish BctPP recycling in the Δ*wadA* mutant, sufficient to the synthesis of the PG layer and therefore allow bacterial growth. However, as *B. abortus* naturally grows faster, this BctPP recycling is not sufficient. Thereby, we proposed that forcing *B. abortus* to grow slower might allow deletion of *wadA.* Considering that we were not able to delete *wadA* in *B. abortus* even at a slower growth rate (30°C incubation), we suggest that something else is responsible for the non-essentiality in *B. melitensis*. Indeed, *B. melitensis* might hold a protein recycling the BctPP that would be absent in *B. abortus.* Interestingly, the Δ*wadA*Δ*gmd* mutant in *B. abortus* did not present morphological defects, similar to the Δ*waaL*Δ*wecA* mutant in *E. coli*, a phenotype that can be explained by the absence of O-chain synthesis, and consequently no BctPP saturation. However, if WadA is the O-chain ligase, we could expect a Δ*wadA* deletion mutant in *Brucella* spp. to present changes in morphology, similar to the Δ*waaL* deletion mutant in *E. coli* (Jorgenson & Young, 2016). Interestingly, the Δ*wadA* mutant in *B. melitensis* presented a standard morphology, in contrast to Δ*waaL* in *E. coli.* It can be proposed that this absence of morphological defects, even in absence of the O-chain ligase, could be explained by a sufficient BctPP recycling capacity in *B. melitensis*. Proposed activities for a potential protein responsible for this recycling could be a pyrophosphatase detaching the unligated O-chains from the BctPP and/or a flippase that would shuttle the BctP back to the cytosolic leaflet that might be more efficient than in other species. By doing so, the free BctP pool would increase in the cytosolic leaflet, thereby enabling growth by allowing the PG layer formation. The presence of such a protein (which could be absent in *B. abortus*) could be investigated by performing a Tn-seq analysis on *B. melitensis* WT and Δ*wadA* mutant and comparing the results of both strains. Indeed, this protein should be essential in the Δ*wadA* deletion mutant, but maybe not in the WT strain. Another possibility to explain the differences between the two species could be a negative feedback due to *wadA* deletion in *B. melitensis* leading to a decrease in O-chain synthesis or a possible increase in BctP under these conditions. These changes could reduce toxic effects from O-chain-linked BctPP accumulation and thereby allow a viable mutant. While *B. abortus* might not present the emergence of such a feedback response.

As *wadA* was revealed essential, we would suggest using the inducible CRISPRi method in order to inhibit the transcription of *wadA*, which would be equivalent to a deletion mutant in a WT background. Indeed, a single guide RNA targeting *wadA* can be constructed. A dCas9 is able to recognize this single guide. This protein then sterically blocks the RNA polymerase elongation and consequently represses *wadA* transcription. Conveniently, the different

contributors of this technique can be induced, allowing a controlled repression of *wadA* (Peters *et al.,* 2019). OD measurements could be performed on the induced construction in order to establish the growth rate. Indeed, if we observe a reduced growth of the induced mutant compared to the non-induced control, we would have further support suggesting *wadA* to be essential for *B. abortus* growth.

2.2. The GT domain is important for membrane integrity

When we assessed growth rate of the different constructions in *B. abortus*, the double mutants Δ*wadA*Δ*gmd* and Δ*GT*Δ*gmd* showed growth defects in rich liquid medium, while the mutant lacking the OAg domain exclusively (Δ*OAg*Δ*gmd*) did not present any growth defects (*Figure 31*). As it is known that membrane stability and integrity are essential for bacterial growth, we suggest that removing the last sugar of the LPS core might impact the membrane integrity and consequently lead to reduced growth. In order to establish if the membrane stability was affected in the double deletion mutants, we put them under membrane stress conditions and assessed their growth. The stress agents we used were SDS and DOC, two detergents known to be membrane stressors. During our assessment, we determined reduced survival to the membrane stresses for the Δ*gmd* mutant compared to the WT strain. This reduction of the Δ*gmd* mutant can be explained by the absence of S-LPS, as these molecules can sterically hinder the detergent in the WT strain and allow better survival. However, the Δ*wadA*Δ*gmd* double mutant showed even less survival to the stresses than the Δ*gmd* mutant (*Figure 34*), indicating an effect of the *wadA* deletion on membrane integrity. The results thereby support the proposition of reduced survival being attributed to the absence of the last core sugar due to the unavailability of the GT activity and consequently a decrease in membrane stability.

It has been previously reported that *E. coli* presents a close interaction between Omps and LPS. Indeed, copurification of the two molecules was achieved, more specifically with the porin OmpF (Schindler & Rosenbusch, 1978). It was established that OmpF can bind to LPS molecules presenting different sizes. Indeed, this interaction could be observed with unaltered S-LPS, as well as LPS mutants lacking the O-chain and the core sugars (deep rough mutant) (Arunmanee *et al*., 2016). The results additionally suggest that the OmpF interact with multiple LPS molecules (Schindler & Rosenbusch, 1978). Moreover, putative binding sites were discovered on the OmpF, amino acids though to be located near the extracellular surface facing the membrane and able to interact with the lipid A-core through numerous Van der Waals interactions. It was also described that the OmpF of *E. coli* and in the Gram-negative species *Enterobacter cloacae* its homolog OmpE36 interacted with the disaccharide lipid A backbone and the inner LPS core sugars through polar interactions, such as hydrogen bonds, in addition to the Van der Waals interactions (Arunmanee *et al*., 2016). Another report describes specific interaction patterns between LPS molecules and six different Omps in *E. coli*, suggesting the existence of interactions with the three components of the LPS, the lipid A, the core and the O-chain (Shearer *et al*., 2019). This led to the proposition that the Omp-LPS interactions are likely rigid, non-fluid structures and that this assembly could play an essential role in membrane stability and integrity. Furthermore, observed data suggests that porin biogenesis requires the presence of these interactions with LPS molecules (Arunmanee *et al*., 2016; Koplow & Goldfine, 1974).

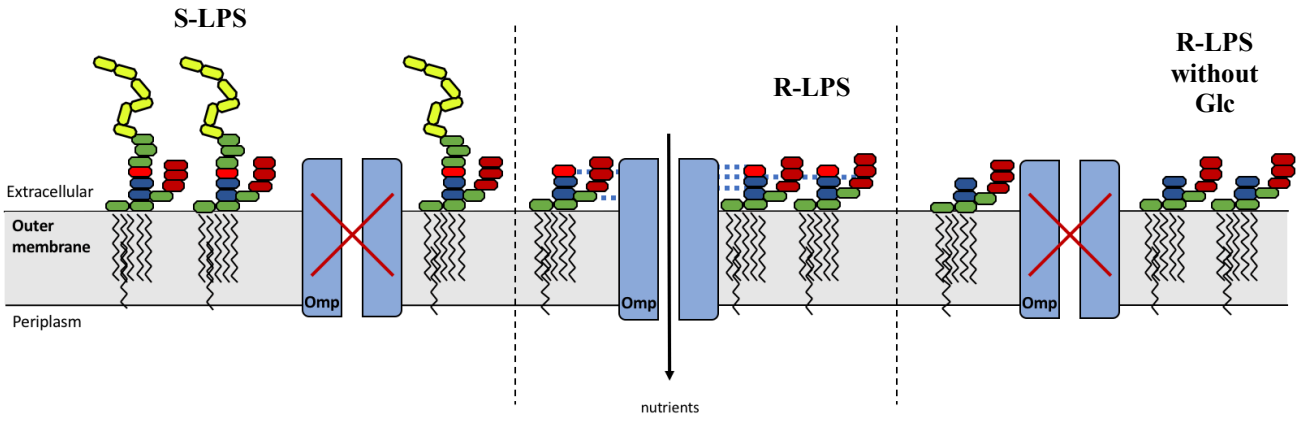

Figure 48: A. Schematic representation of the hypothetic interaction of Omps and R-LPS molecules. Considering the co-localization of Omps (Omp2b) and R-LPS clusters, we believe interaction (dots) of these components is necessary for Omps porin activity, thereby allowing entry of nutrients in the bacteria. On the contrary. S-LPS molecules spatially obstruct the Omps, inhibiting nutrient intake. Furthermore, we postulate that the LPS core in absence of the last core sugar Glc (red) presents reduced capacity to interact with Omps. In this manner, Δ*wadA* and Δ*GT* deletion mutants should present nutrimental deficiency.

Considering the discovery of a co-localization of Omp2b and R-LPS clusters (Vassen V., 2018), we propose that localization in close environment of these two components is required for the Omp2b activity (*Figure 48*). A first hypothesis explaining this co-localization would be that the chained polysaccharide sterically hinders the diffusion of nutrients from the extracellular environment to the porins, while the rough molecules allow diffusion. As these porins are believed to be essential for nutrient intake of the bacteria (Vassen *et al.,* 2019), R-LPS clusters would be crucial for survival and therefore localize around Omp2bs. Indeed, we suggest that a basal level of R-LPS is vital to allow nutrient intake and enabling bacterial growth. However, following the observation of the homologs OmpF in *E. coli* and OmpE36 in *E. cloacae* (Arunmanee *et al*., 2016), we also propose a second hypothesis with a potential interaction between the R-LPS and Omp2b, instead of just a co-localization, to activate the Omp2bs in *Brucella* spp. This could as well be imagined for other Omps, other than Omp2b, such as LptD and BamA. These Omps could interact with the LPS core, which would allow activation and diffusion of molecules through the porin (*Figure 48*).

Interestingly, it was observed in *E. coli* that rough mutants, heptose-deficient with heptose being one of the last sugars of the LPS core, presented alterations in membrane integrity. Indeed, these mutants presented a reduced quantity of Omps, as well as changes in their apparent molecular weight. It could thereby be suggested that the Omps maturation requires the presence of LPS molecules presenting an integral core (Koplow & Goldfine, 1974). Following the same idea for *Brucella* spp., we can suggest that Omps demand an intact LPS core to allow interaction between the two compounds. Thereby, we can suggest that the interactions are dependent on the presence of the last core sugar, Glc. We propose that lacking the GT domain that adds this last core sugar could impede growth by preventing Omps interaction and consequently lead to membrane instability, defects in transport machineries or insufficient nutrient intake *(Figure 48)*. The same decrease in nutrients should be responsible for slower growth during intracellular infection. Indeed, we could observe a reduced replication for our Δ*wadA*Δ*gmd* double mutant, compared to the Δ*gmd* mutant (Figure 35). This experiment should however be performed again in order to confirm these observations, as biological replicates are needed.

This hypothesis could also explain the results of the growth curve assays in the *B. abortus* complemented strains. Indeed, the pBBR *wadAc* Δ*wadA*Δ*gmd* strain presented an almost standard growth curve, but the OD stayed inferior to WT measurements (*Figure 28.A.*). At the same time, the pBBR *OAgc* Δ*OAg*Δ*gmd* strain presented a starting standard growth, followed by a small reduction after 40h (*Figure 28.B.*). Moreover, the complemented strains in *B. melitensis* presented an intermediate growth rate between the non-complemented and the WT strains (*Figure 37*). It was even noted that pBBR *OAgc* Δ*OAg* presented a reduced growth compared the Δ*OAg* mutant (*Figure 37.A.*), being a surprising discovery. However, we would suggest that these growth defects could be attributed to an overexpression of *OAg,* the pBBR plasmid being present at around 10 copies per cell (Elzer *et al*., 1994). If there would indeed be an overexpression of this domain, we could suggest an increased O-chain ligase activity, leading to an increase in S-LPS molecules. While at first this increase might not alter growth considerably, we propose that an excessive amount of surface S-LPS could lead to a decrease of R-LPS on the bacteria. Thereby, we could reach a point where the amount of R-LPS on the surface could be insufficient for interaction with Omps, which would in the end lead to a decrease in Omps activity. If the porins would decline in activity, the nutrient quantity would reduce until reaching a crucial level and finally generating a decrease in growth.

2.3. WadA is the main O-chain ligase in *B. abortus*

2.3.1. The OAg domain is necessary for the O-chain ligation activity in *B. abortus*

Using an inducible plasmid (pBBRi containing a copy of *gmd* under the control of the *Plac* inducible promoter, in strains deleted for *gmd*), we were able to induce expression of *gmd*, in order to consequently restore O-chain synthesis in a Δ*gmd* strain. We could observe O-chain signal for the induced Δ*gmd* mutant after 24h by WB (*Figure 45*) and IF (*Figure 44*), indicating presence of functional Gmd. After induction of *gmd* expression in the Δ*wadA*Δ*gmd* and Δ*OAg*Δ*gmd* mutants, we could not detect S-LPS signals when performing IF microscopy (*Figure 44*).

Interestingly, the WB signal for the induced Δ*gmd* mutant was of lower intensity and of lower molecular weight, compared to the WT strain (*Figure 45*). A potential explanation for this observation could be that the uninduced mutants, lacking *gmd*, generate a negative feedback leading to a reduction in other enzymes needed during O-chain synthesis. Thereby, after inducing *gmd*, some proteins of the synthesis pathway could still be missing or at insufficient quantity to allow the formation of an O-chain of standard length. The O-chain could thereby be of lower molecular weight, and simultaneously at lower quantity (*Figure 45*). As smooth signal was revealed by IF, we can affirm that basal levels of sugar units are present (*Figure 43*). A longer time of IPTG induction could be used to see whether the O-chain quantity increases over time. This might enable the re-expression of other enzymes, once *gmd* is expressed and allow detection of S-LPS signal similar to the WT control. Another possible explanation for the low WB signal intensity might be the affinity A76/12G12 has for the O-chain. Indeed, it has been noted that this antibody shows a lower reactivity compared to other anti-S-LPS antibodies (Laurent *et al.,* 2004). Otherwise, we can simply propose that the WB technique presents a lower sensitivity than the IF. Taking this into consideration, we cannot exclude that O-chain is synthesized in the 24h induced Δ*wadA*Δ*gmd* and Δ*OAg*Δ*gmd* mutants, but that we were unable to detect it. We could therefore recommend performing a WB using another antibody, such as 04F09 showing higher affinity (Laurent *et al.,* 2004). Yet again, we would suggest performing a WB on these mutants after 48h induction and check if then we would be able to detect a smooth signal. Taken that we were able to detect O-chain signal on *Figure 33* for Δ*wadA*Δ*wzm*, we can affirm that the inability of detection in *Figure 45* is independent of the localization of the O-chain in the cytosol or periplasm. However, as the signals on *Figure 33* were as well of low intensity, we could propose that the localization reduces the threshold of detection, supporting the idea that 24h induced Δ*wadA*Δ*gmd* and Δ*OAg*Δ*gmd* mutants might present O-chain in the cytosol but in low quantity, thereby under the limit of detection.

Growth curves of the Δ*wadA*Δ*gmd* and Δ*OAg*Δ*gmd* mutants revealed that induction of *gmd* led to changes in growth profile. Indeed, induction in the Δ*wadA*Δ*gmd* mutant provoked stronger growth defects (*Figure 42*), supporting again toxic effects due to O-chain-linked BctPP accumulation. However, induction in the Δ*OAg*Δ*gmd* mutant did not lead to a reduced growth (*Figure 42*). On the contrary, we were able to determine a slight increase in growth compared to the uninduced mutant. This observation was replicated three times. Furthermore, CFU count of these mutants revealed no noticeable changes between strains (*Figure S8*). We can thereby propose that *gmd* induction provoked a bacteriostatic effect, rather than a bactericidal effect.

Induction of *gmd* expression in a Δ*gmd* background generates S-LPS, while *gmd* induction in a Δ*OAg*Δ*gmd* background does not, in *B. abortus*. This suggests that the OAg domain of WadA is necessary for O-chain ligase activity in *B. abortus*, considering that the OAg domain

is functional in *B. melitensis* (*Figure 38*) and possibly in *B. abortus* according to the growth profile (*Figure 42*).

Additional support of WadA being the O-chain ligase was shown in *B. melitensis*, where we observed that the Δ*wadA* deletion mutant, as well as our Δ*OAg* deletion mutant, presented a rough phenotype. These observations were detected through IF microscopy where the two mutants did not present any S-LPS signal (*Figure 23*), as well as by WB where the deletion mutants presented rough signal exclusively (*Figure 38*). Moreover, the WB results show that complementation with a copy of *OAg* in the Δ*OAg* deletion mutant restored the smooth phenotype, while this complementation was unsuccessful in the Δ*wadA* deletion mutant (*Figure 38*). These complementation results suggest that **deletion of the OAg domain** (periplasmic loop) **does not impact the function of the remaining WadA protein, i.e. the GT domain, as an *OAg* copy is sufficient to restore a WT phenotype. Moreover, they suggest that the OAg domain specifically is involved in the ligation of the O-chain. It can thereby be postulated that WadA is the O-chain ligase in *B. melitensis*.**

2.3.2. The large periplasmic loop of OAg domain holds an essential amino acid for the ligase activity

Considering that the results suggest the OAg domain is required for the O-chain ligation, we wished to identify catalytic residues in this domain. Discoveries made with *E. coli* suggest an importance of some positively charged amino acids for the O-chain ligase activity of WaaL on its two periplasmic loops (Ruan *et al.,* 2012; Pérez *et al*., 2008). These amino acids are believed to be crucial for the O-chain ligation, although it is not proposed that these represent the catalytic sites themselves. In point of fact, it was proposed that these positive charges could be necessary to stabilize the phosphate groups of the BctPP after cleaving the O-chain. Thereby, the uptake of the O-chain would be dependent of these amino acids, which would explain their essentiality (Ruan *et al.,* 2012).

By sequence alignment with WadA homologs from other bacteria, we were able to identify conserved and positively charged amino acids in WadA of *B. abortus* (*Figure 39*). One identified amino acid, Arg-614, was mutated to an alanine, a small neutral residue, and this coding sequence was inserted in a pBBR plasmid. We than proceeded to place the plasmid in different strains, such as in a *B. abortus* WT background and attempted to delete *wadA* in this complemented strain (Δ*wadA*::pBBR*wadA*-R614A). This construction would give supplementary data to support the essentiality of the mutated residue. If this was indeed one of the sites necessary for the OAg activity, it should be impossible to delete *wadA* in these conditions due to the toxicity caused by O-chain accumulation on BctPP. However, if this amino acid reveals to be non-essential, the deletion should be obtained as there is no O-chain accumulation due to the presence of a functional *wadA* copy. Our results revealed an incapacity to obtain the mutant, suggesting that in the absence of the Arg-614, the OAg domain cannot fulfill its activity and would thereby indicate that this amino acid is essential. This attempted construction should however be controlled by attempting to delete *wadA* in a pBBR*wadA*-R614A Δ*gmd* deletion mutant and see if this deletion is achievable.

Additional results supporting the importance of this Arg were found in *B. melitensis*. Indeed, complementing a Δ*wadA* deletion mutant with the pBBR*wadA*-R614A plasmid led to the return to a standard growth curve (*Figure 40*), indicating a partially functional protein (GT domain). However, the WB revealed signal for R-LPS exclusively, suggesting that the point mutation impeded the O-chain ligation activity (*Figure 41*). Considering these results, we can propose that the Arg-614 is required for O-chain ligase activity, maybe as suggested for WaaL of *E. coli*, by stabilizing BctPP generated by the cleavage of the O-chain from the lipid carrier.

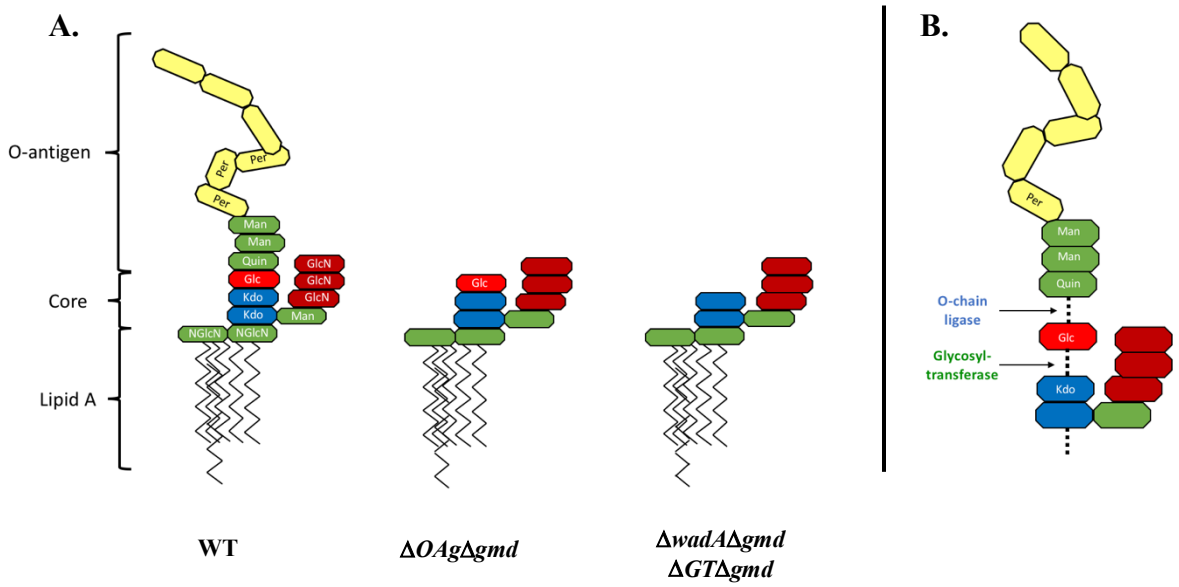

Figure 49: A. Schematic representation of the hypothetic LPS core for Δ*wadA*Δ*gmd*, Δ*GT*Δ*gmd* and Δ*OAg*Δ*gmd* double mutants in *B. abortus*. B. Site of action of the identified GT and OAg domains in *B. abortus*. The two sites of action are indicated with arrows. Man: mannose; NGlcN: diaminoglucose; GlcN: glucosamine; Kdo: 3-deoxy-D-manno-octulosonic acid; Per: N- formylperosamine ; Glc : glucose

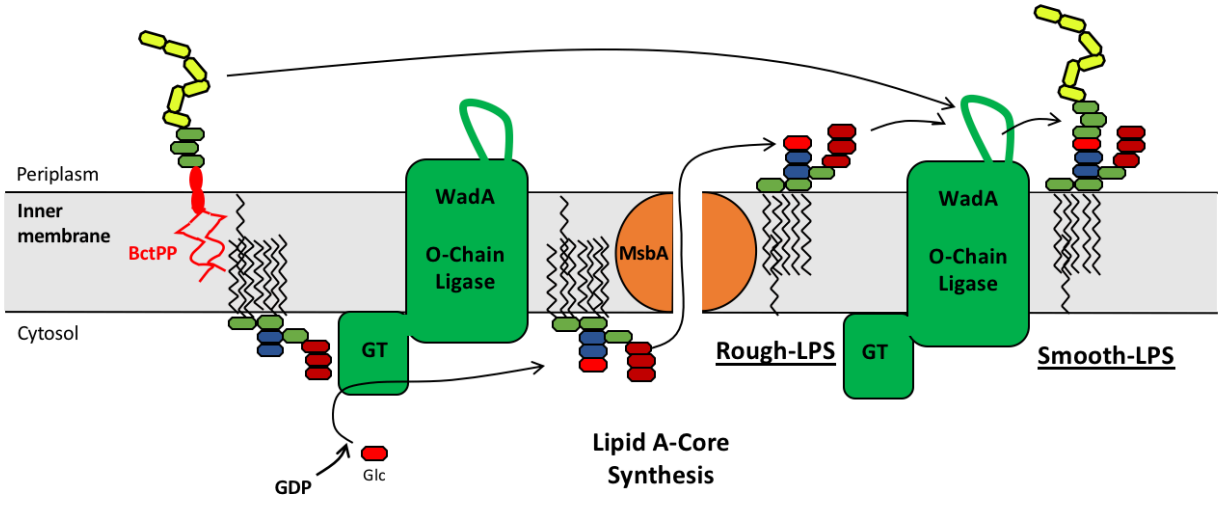

Figure 50 : The two predicted domains of WadA might be involved at different steps during the S-LPS synthesis. (Inspired by unpublished data kindly gifted by Conde R.). Taking into consideration the two predicted domains for WadA and previously published data, we suggest a hypothesis where the GT domain would add the last core sugar, before translocation of the R-LPS by MsbA. Whilst the OAg domain would act after translocation and would ligate the O-antigen from the BctPP carrier to the LPS core on the periplasmic leaflet, thereby forming the S-LPS.

Potential perspectives for this hypothesis would be a point mutation of this Arg-614 into a positively charged lysine. This would allow to prove the importance of the positive charge, rather than the amino acid side chain on itself. In fact, such a mutation in *E. coli* presented a functional protein, indicating that the charge is the crucial component (Ruan *et al.,* 2012). Moreover, we could as well proceed to the point mutation of the identified homolog His-605 (*Figure 39*) residue with a small neutral amino acid to detect a second potential decisive site.

2.3.3. WadA is a bifunctional enzyme

Given the domain prediction for *wadA*, it was proposed that WadA is involved at two steps of the LPS synthesis (*Figure 49 + 50*). Indeed, it was shown that the GT activity is necessary for the LPS core synthesis. This GT would add the last core sugar, a Glc, to the Kdo II, thereby finishing the central branch of the LPS core while in the cytosol (González *et al*., 2008). On the other hand, the putative OAg domain would act as an O-chain ligase by adding the first sugar of the O-chain, a quinovosamine, to the Glc of the LPS core. In this order, we would obtain the finished S-LPS (*Figure 49 + Figure 50*). Considering the TMHMM prediction of GT as a cytosolic domain (*Figure 13*), it is suggested that the GT activity is performed before the translocation of the LPS core to the periplasmic leaflet. After the translocation, the OAg domain would perform the O-chain ligation, indicating that the two WadA domain activities are separated in localization and in time (*Figure 50*). Our results support this bifunctional protein hypothesis, as when comparing the growth curves of the mutants, we could observe a reduced growth after deletion of *wadA*, but a standard growth in the Δ*OAg* deletion mutants, indicating that the remaining part of *wadA* carries out a second activity (*Figure 31 + 36*). Results suggesting a glycosyltransferase activity from the GT domain were mentioned earlier (2.2. The GT domain is crucial for membrane integrity)

Considering the putative activities of these two domains, we can propose the LPS core structure of our deletion mutants. Indeed, in the absence of the OAg domain, there would be no ligation of the O-chain to the LPS core. However, this would mean that the core on itself would stay intact (*Figure 49*). The last sugar of the central branch of the core would be a Glc. On the other hand, when deleting the GT domain, this last core sugar would be absent, as it would not be transferred to the core (*Figure 49*). In order to prove this hypothesis, nuclear magnetic resonance (NMR) spectroscopy could be performed on the different mutants. This would enable to determine the absence or presence of the Glc unit and confirm the predictions we made for the different mutants (*Figure 49*). A final proposition would be to assess biochemically the two activities on purified WadA and its purified substrates. Results indicating interaction between these components and synthesis of S-LPS would offer conclusive prove for WadA being the O-chain ligase. However, such an experiment would reveal laborious, considering the transmembrane localization of WadA and its lipidic substrates.

To our knowledge, it is the **first time such a bifunctional ligase able to perform two distinct activities is being described**. Indeed, in *E. coli*, WaaL is exclusively involved in the O-chain ligation on the already synthesized core (Pérez *et al*., 2008), the last Glc subunit of the core being added by the glucosyltransferase WaaV (Whitfield *et al*., 1999). In *Helicobacter pylori*, the O-chain was as well described as monofunctional, ligating the O-chain on the last core sugar heptose (Hep), while it proposed that this Hep is added by a specific Hep transferase (Li *et al*., 2017). O-chain ligases in other Gram-negative species, identified as WaaL homologs, were also described as monofunctional proteins (Pérez-Burgos *et al.,* 2019; Schild *et al.,* 2005; Islam *et al*., 2010; Abeyrathne *et al.,*2005; Raetz & Whitfield, 2002).

It can be proposed that this *Brucella* specificity might be correlated to its distinct O-chain and outer core composition. Indeed, in this genus, the O-chain ligase has to perform the ligation to a Quin subunit. Interestingly, another genus in the alphaproteobacterial class, *Bradyrhizobium*, also presents a Quin in its O-chain composition (Carrion *et al.,* 1990) and holds a distinct O-chain ligase (*rfaL*), showing an 14% amino acid identity with *waaL* in *E. coli* (Noh *et al*., 2015) and a 12% identity with *wadA* in *B. abortus* (data not shown), which indicates a distant similarity, if any. This observation might suggest that the presence of a Quin in the LPS could have led to the evolution of specific O-chain ligases in these species. The *Bradyrhizobium* RfaL has yet again not been described as a bifunctional protein (Noh *et al*., 2015), its coding sequence presenting no conservation with the GT domain sequence of *Brucella,* indicating the two-activities protein to be specific to WadA.

CONCLUSION

Throughout this work, we were able to present data leading to the identification of the O-chain ligase in *Brucella* spp. Our results suggest that WaaL is not the main O-chain ligase in *Brucella*, contrary to the Gram-negative model *E. coli*; whereas WadA appears as the interesting candidate. While the construction of Δ*wadA* deletion mutant in *B. abortus* was not obtained, we were able to construct Δ*wadA* and the deletion of the O-chain ligase domain of *wadA* (Δ*OAg*) in *B. melitensis*. Both mutants were characterized as rough mutants suggesting WadA is the main O-chain ligase in this genus. Interestingly, WadA appears as a bifunctional enzyme bearing an O-chain ligase and a glycosyltransferase domain, able to add the last core sugar necessary for the O-chain ligation. To our knowledge, this is the first time such a bifunctional enzyme has been described for the S-LPS synthesis. The existence of an O-chain ligase potentially specific to this genus is intriguing, but could be explained by the distinct nature of the *Brucella* LPS sugars in the O-chain, compared to other Gram-negative species. Furthermore, it was suggested that WadA is essential in *B. abortus* due to toxic effects arising from BctPP saturation, impeding PG synthesis. We advocate for a common BctP pool shared by the O-chain and the PG syntheses pathways. It is further proposed that the recycling of the components involved in the PG and O-chain syntheses differs between the two closely related species *B. abortus* and *B. melitensis*. Moreover, we identified that the deletion of the GT domain only, and thus the absence of the last core sugar, leads to reduced growth and sensitivity to membrane stresses. As it was described that R-LPS co-localizes to Omps, we propose a potential interaction between these two compounds necessary to enable membrane stability, porin activity and intake of nutrients. We suggest investigating if this interaction could be dependent on the presence of a complete LPS, which would explain loss of membrane integrity in the absence of the last core sugar. Structural analysis of the LPS core of the various mutants would enable to further prove the presence of two WadA activities in both *Brucella* species.

MATERIAL AND METHODS

BLASTp

B. abortus sequences were compared to sequences of other *Brucella* species, as well as species from another genus, using Protein BLAST (Basic Local Alignment Search Tool - NCBI) (Madden T., 2003). Sequence alignments were performed using Clustal Omega (Madeira *et al.,* 2019).

Bacterial strains and media

Brucella abortus 544 was the wild type (WT) strain used in this study. This strain has been modified to be resistant to nalidixic acid (Nal^R). All the *B. abortus* strains were grown in liquid or solid tryptic soy broth (TSB) medium at 37°C. *B. melitensis* 16M was also used in this study and grown on 2YT (Yeast Extract and Tryptone; 1% yeast extract, 1.6% peptone, 0.5% NaCl). *E. coli* strains were cultured in Lennox lysogeny broth (LB) medium at 37°C on shaking.

When required, the appropriate antibiotic was added to the medium with the following concentrations: kanamycin sulfate (Kan) at 50µg/ml for plasmidic born cassette or 10µg/ml for genomic encoded resistance cassette; chloramphenicol (Cm) at 20 µg/mL; ampicillin (Amp) at 100 µg/mL, nalidixic acid sodium salt (Nal) at 25 µg/mL.

Polymerization chain reaction (PCR)

Preparative PCR

Q5 High Fidelity DNA Polymerase (2000 U/µm, BioLabs®) was used for the subsequent constructions due to its proof-reading activity. For each sample, the PCR mix contained forward primer (0.4 µM), reverse primer (0.4 µM), gDNA 544 template (200 to 300 ng), dNTP (5µM of each), High GC Enhancer Buffer (1:5, BioLabs®), Reaction Buffer (1:5, BioLabs®) and the Q5 High Fidelity DNA polymerase. Finally, water was added to the tubes to reach a final volume of 50 µL. The PCR program was composed of an initial DNA denaturation step at 98°C for 30 s, followed by 30 amplification cycles made of denaturation for 10 s at 98°C, primer annealing for 30 s, elongation at 72°C, with the elongation time adapted to the product length taking into consideration the polymerase amplification speed of 2000 pb/min. These 30 cycles were followed by a final elongation for 2 min at 72°C.

Joining PCR

This kind of PCR is used to combine two PCR products through sequence complementarity. PCR tubes were filled with 1 µL of each PCR product to be joined, dNTP (5µM of each), High GC Enhancer Buffer (1:5, BioLabs®), Reaction Buffer (1:5, BioLabs®), Q5 High Fidelity DNA polymerase (Biolabs) and water, for a final volume of 50 µL. The same protocol steps described for the preparation PCR were used, except that the cycles were first repeated five times to enable the annealing of the upstream and downstream PCR products. Finally, forward primer (0.4 µM) and reverse primer (0.4 µM) were added to the tubes and underwent 30 repeats following the previous settings.

Diagnostic PCR

This kind of PCR is used to check the presence and the size of a given DNA fragment. For each sample, we added 1 µL of bacterial sample, forward primer (0.4 µM), reverse primer (0.4 µM), DMSO 5%, dNTP (5µM of each), GoTaq Buffer (1:5, Promega®), GoTaq DNA polymerase (Promega®) and completed it with water to reach a final volume of 30 µL.

The PCR program was made of an initial denaturation step for 10 min at 98°C, followed by 30 cycles of denaturation for 1 min at 98°C, primer annealing for 30 s at 50°C, elongation at 72°C, with the elongation time adapted to the product length taking into consideration the polymerase amplification speed of 1000 pb/min. These 30 cycles were followed by a final elongation for 5 min at 72°C.

Strain construction (*Supplementary table 1*)

PCR

The first step of the strain construction was the amplification of the desired DNA fragments using specific primers (*Supplementary table 2*). Preparative PCR products were used for complementation mutants. Concerning deletion mutants, two preparative PCR products were amplified. These PCR products correspond to a fragment located upstream and a fragment located downstream the sequence to be deleted. By Joining PCR, these two PCR products were concatenated. The idea is to create a deletion mutant through homologous recombination.

Restriction

The resulting amplicons were first purified using NucleoSpin® Gel and PCR Clean-up (Macherey-Nagel) according to the manufacturer protocol, and then restricted, if necessary, as well as the plasmids, with the appropriate restriction enzymes. Deletion was done using pNPTS138 (integrative plasmid in *B. abortus*) restricted with EcoRV; complementation was done using pBBR1MCS (replicative plasmid in *B. abortus*) restricted with the appropriate restriction enzyme. Restriction was executed using 1 µL of each necessary restriction enzyme, template (amplicon or plasmid), CutSmart Buffer (1:10) and water was added to reach a final volume of 50 µL. The digestion was performed at 37°C for 15 min and the enzyme was afterwards inactivated following the manufacturer's instructions.

Ligation

Ligation of the amplicon to the plasmid was achieved by mixing the appropriate volume of plasmid and amplicon proportionate to the length of the sequences, ligase buffer (1:5), 1 µL of Ligase and water was added up to a final volume of 10 µL. The samples were incubated ON at 18°C.

Transformation

Transformation was initiated adding 5 µL of ligation product to 50 µL *of E. coli* DH10B or 2µL of ligation product to 20 µL *of E. coli* S17-1. The mixture was kept for 20 min on ice, before fluidifying the membranes by heatshock at 42°C for 2 min and then put back on ice again. 500 µL of LB medium were added and the samples were incubated at 37°C for 45 min with shaking. 100 µL of the sample were plated on LB medium containing the appropriate selection antibiotic, isopropyl ß-D-1-thiogalactopyranoside (IPTG, 1mM) and 5-bromo-4-chloro-3-indolyl-β-D-galactopyranoside (X-Gal, 20 µL/mL). For DH10B transformation, remainder was centrifuged (5000 rpm, 3min) and supernatant was discarded leaving approximatively 100 µL left. The pellet was resuspended in this volume before being plated on LB medium with selection antibiotic, IPTG and X-Gal. Plates were incubated ON at 37°C.

DH10B clones were screened by diagnostic PCR. Selected clones underwent plasmid extraction using NucleoSpin® Plasmid EasyPure (Macherey-Nagel) and plasmids were verified by sequencing. *E. coli* S17-1 strains were transformed with the selected plasmids.

Conjugation

Transformed *E. coli* S17-1 were grown in liquid LB medium and *B. abortus* strains into liquid TSB medium ON at 37°C. To allow conjugation, 50 µL of *E. coli* S17-1 overnight culture and 1 mL of *B. abortus* culture were mixed, centrifuged (7000 rpm, 2.5 min) and washed with TSB medium (7000 rpm, 2.5 min). Pellet was resuspended in 100 µL TSB medium and a droplet was placed TSB medium plate. The plate was incubated 4h at 37°C in case of a complementation and ON at room temperature (RT) for 24h in case of an integrative plasmid. After incubation, about ¼ of the dry droplet was resuspended in 500 µL of TSB and resuspended. 100 µL of this suspension were plated on TSB medium supplemented with Nal and the appropriate selection antibiotic. Plates were incubated at 37°C for four days. Colonies were streaked on TSB medium supplemented with the proper antibiotic, but no Nal, to allow the strain to grow better and incubated two days at 37°C. This was the last step for the construction of complementation strains. On the other hand, clones regarding deletion strains were grown in liquid TSB culture (ON, 37°C) without any antibiotic to allow the second recombination and the plasmid excision. 100 µL of the liquid cultures were plated on TSB medium containing 5% Sucrose. After incubation at 37°C for four days, clones were streaked in parallel on TSB-5% Sucrose and TSB-Antibiotic (plasmid selection) plates and incubated for two days at 37°C. Clones growing on the TSB-5% Sucrose plate, but not on the antibiotic plate were selected and screened by diagnostic PCR.

Microscopy

For microscope slide preparation, 2 µL of the sample preparation was placed on PBS-agarose 1% pads, covered with a thin cover slip and sealed with a VALAP mixture (1/3 Vaseline - 1/3 Lanoline - 1/3 Paraffine). Pictures were taken with an inverted microscope Nikon Eclipse Ti2 equipped with a phase-contrast objective Plan Apo λ DM100XK 1.45/0.13 PH3 and a Hamamatsu C13440-20CU ORCA-FLASH 4.0. Images were analyzed using FIJI v.2.0.0 (Schindelin *et al.,* 2012), a distribution of ImageJ. Bacteria were detected and analyzed using the ImageJ plugin MicrobeJ (Ducret *et al.,* 2016) and the look-up table (LUT) were adjusted to reach the best signal–noise ratio.

Immunofluorescence

Fluorescence microscopy was used to visualize the S-LPS and R-LPS. The labeling was performed starting with liquid cultures at exponential phase (OD 0.3 to 0.6). These were washed (7000 rpm, 2.5 min) twice with phosphate-buffered saline (PBS), before being resuspended in a hybridoma culture containing the appropriate primary antibody at a volume 1/5 of the starting culture volume. Labeling of the S-LPS was performed using A76/12G12 mouse IgG1 or B66/04F09 mouse IgG2a targeting *Brucella* S-LPS, while R-LPS labeling was done using A68/03F03/D05 mouse IgG2b targeting *Brucella* R-LPS. The samples were incubated at RT for 40 min on a rotating wheel. Afterwards, they were washed twice with PBS and resuspended in a PBS preparation containing the appropriate second antibody at a 1:500 dilution and incubated at RT for 60 min on a rotating wheel. The following secondary antibodies were used: goat anti-mouse IgG H+L AlexaFluor 514, goat anti-mouse IgG2a AlexaFluor 647, goat anti-mouse IgG2b AlexaFluor 488. Finally, bacteria were washed twice with PBS and resuspended in PBS.

Western Blot

Starting from a *Brucella* culture in exponential phase (OD between 0.3 and 0.6), samples were prepared to be at an OD of 10. Samples were centrifuged (7000 rpm, 2.5 min), the supernatant was discarded, and a PBS wash was executed. The samples were resuspended in ¾ of the final volume in PBS and bacteria were inactivated for 1h at 80°C. ¼ of the final volume of loading buffer (1M Tris-HCl pH 6.8, 10% SDS, Glycerol, β mercapto-ethanol, 1% Bromophonol blue, dH2O) was added, and the samples were boiled for 15 min at 95°C. 10 µL of sample were loaded in a SDS PAGE gel, made out of the stacking and the running gel. The migration was performed at 200V (constant) for 45 min. Proteins were transferred on nitrocellulose membrane using a Transblot turbo Bio-Rad machine (25V, 30 min) and blocked afterwards in a PBS solution with 0.05% Tween-20 and 5% milk (Nestl, Foam topping) at 4°C ON under agitation. The membrane was washed 3 times for 10 min with PBS-Tween 0.05% before adding the primary antibody A68/24D08/G09 anti-*Brucella*-R-LPS (1:100) contained in 5 mL PBS-0.05%Tween-0.5%milk and incubating at RT for 1h. After three PBS washes, the membrane was incubated at RT for 1h in 5 mL of PBS-0.05%Tween-0.5%milk with the goat secondary antibody anti-mouse (1:5000). The membrane was washed 3 times for 10 min. A mix of the peroxide and luminol solution (1/1) was added to the membrane to allow protein detection and the revelation was performed using Clarity Western ECL Substrate (Biorad) and Amersham Imager 600 (GE Healthcare Life Sciences).

Growth curve

B. abortus and *B. melitensis* (WT and mutants) were grown in pre-culture ON. In the morning, cultures were diluted 1:10 in order to reach an exponential phase in the afternoon (OD between 0.3 and 0.6). The samples were prepared by diluting the cultures in TSB or 2YT fresh medium to an OD of 0.1. 200 µL of each condition were put in technical triplicate in a 96 well plate. Biological triplicates for each sample was as well performed. Fresh TSB or 2YT medium was used as blank solution and sterile PBS was added between the wells to avoid evaporation issues during the read. The plate was introduced in the Bioscreen reader (Epoch 2 Microplate Spectrophotometer (BioTek)); and the OD measures were taken every 30 min for 72h at 37°C. Data was analyzed using Microsoft Excel (Microsoft Corporation, 2018) or GraphPad Prism.

LPS extraction and structure analysis

Overnight cultures were grown at 37°C in 50 mL of TSB or 2YT medium, for *B. abortus* or *B. melitensis* strains respectively. After incubation, bacteria were inactivated with 0.5 % phenol for 48h at 37°C with shaking. It was made sure that the phenol mixes evenly in the culture medium. Inactivated cultures were centrifuged for 10 min at 4°C and 8000 x g to collect bacteria. Pellets were sent to the research group of Raquel Conde Alvarez, which executed the LPS extraction and analysis by nuclear magnetic resonance spectroscopy (NMR spectroscopy).

Induction of S-LPS with IPTG

An inducible replicative plasmid, the pBBRi, was used for *gmd* complementation. This plasmid contained a copy of the *gmd* gene under the control of the p_{lac} promotor. This promotor is repressed by the constitutive expression of *lacI* when no lactose analog is present in the culture medium. However, when adding isopropyl β-d-1-thiogalactopyranoside (IPTG), the LacI repressor is inhibited, allowing the transcription of *gmd*.

Complementation constructions containing the pBBRi gmd plasmid were grown into TSB liquid culture, supplemented with Cm (20µg/ml), ON at 37°C. In the morning, the cultures were treated with 1mM of IPTG to induce Gmd expression. Induction was tested after 4 hours and 24 hours by immunofluorescence microscopy and CFU counting after 10-fold serial dilution. Additionally, growth curves were performed on these cultures. As a control group, the experiments were executed on the non-induced cultures as well.

Membrane stresses

Plates were prepared with TSB medium or 2YT medium and, in the desired cases, supplemented with 0.015% of sodium deoxycholate (DOC) or 0.001% of sodium dodecyl sulfate (SDS). The concentrations were chosen through results find by our colleague Adélie Lannoy, who tested the effect of various concentrations of these stresses on *B. abortus* in order to find sublethal concentrations for outer membrane mutants. 200 µL of the bacterial sample were placed into a 96-well plate and 10 fold-dilutions in PBS were executed. For the desired dilutions, 15 µL of the preparation was placed as a droplet on the desired plate. Plates were incubated at 37°C for 2 days.

Macrophage infection

Macrophage culture

J774 A1 macrophages were cultivated in Dulbecco's Modified Eagle Medium (DMEM) supplemented with 10% fetal bovine serum (FBS, Gibco) at 37°C and with 5% CO2 atmosphere. The medium was always heated at 37°C before working with the cells. Cell stocks (10^6 cells/mL) in liquid nitrogen were thawed for a few seconds at 37°C, before carefully adding 10 mL of medium. This cell suspension was centrifuged for 5 min at 100 x g in order to eliminate the remaining DMSO contained in the stock. The supernatant was discarded, and the cells were delicately resuspended with a micropipette in 1 mL of DMEM-FBS medium. Another 25 mL of medium were added before carefully placing the preparation in a culture flask. The culture was incubated at 37°C for 2 to 3 days.

After incubation, in case of the cell culture being at an 80% confluence, the culture medium is discarded, and 10 mL of fresh medium are added. Cells are gently detached from the flask using a rake. The cell suspension is placed in a flask and centrifuged for 5 min at 1000 rpm. The supernatant is discarded, and 10 mL of fresh medium are added. After resuspension, 1 mL of the cell suspension is placed into a flask containing 25 mL of fresh medium. The flask is put for incubation at 37°C.

Preparation of the macrophages for infection

After 2 to 3 days incubation of the cell culture, the flask containing the cells was emptied from its medium and 10 mL of new culture medium was added. Using a rake, the cells were gently detached form the flask. This step was done carefully in order to reduce stressing the cells. The preparation was placed in a falcon and centrifuged 5 min at 1000 rpm. The supernatant was discarded, and cells were resuspended in 10 mL of medium. 10 µL of this preparation were mixed with 10 µL of Trypan blue. This dye allows to distinguish live cells from dead cells. 10 µL of this mixture was placed on a Neuman cell counting chamber and living cells were counted in four large squares. The number of cells in 1 mL was determined, allowing to prepare a cell preparation of $1x10^5$ cells/mL. 500 µL of the preparation were added in each well of a 24-well plate. The plate was incubated ON at 37°C for the cells to adhere.

Infection of macrophages with *Brucella*

The next morning, the cells should have replicate by 1.5x. Therefore, we consider that each well contains 1.5 x 10^5 cells/mL. Before starting the infection, the cells were checked to determined that they are not overstressed. Bacteria were put into culture in order to be in exponential phase (OD between 0.3 and 0.6) the morning of infection. Bacteria were centrifuged (7000 rpm, 2.5 min) and washed in PBS (7000 rpm, 2.5 min). The pellet was resuspended in DMEM medium. Using the measured OD, the volume of culture was determined in order to obtain a MOI of 50 ($50*1.5*10^5=7.5x10^6$ bacteria for OD1 $\cong 3x10^9$ bacteria/mL). The calculated amount was added to the final volume to prepare the bacterial suspension.

The medium present in the wells containing the macrophages was discarded and 500 µL of the bacterial suspension was added to each well. The multiwell plate was centrifuged for 10 min at 1200 rpm & at 4°C in order to solidify the membrane and enable to synchronize the entry of bacteria. The plate was then incubated at 37°C, this moment being considered as T0H. Cells were incubated for 1H, before discarding the medium from the wells and replacing it with 500 µL of RAW DMEM medium supplemented with 50 µg/mL of gentamicin. The plate was replaced in the incubator for another hour, before replacing the medium with 500 µL RAW DMEM medium supplemented with 10 µg/mL of gentamicin.

The cells were collected at time 2H, 4H, 24H and 48H post infection. The medium was discarded from the wells and two washed were done with 500 µL of PBS. 100 µL of PBS - Triton1% were added to each well and the volume was flushed 10 times to detach the cells. Of this suspension, 200 µL were put into a 96-well plate to perform 10-fold serial dilutions. On a TSB medium plate, three 20 µL drops of the desired dilutions were placed and the plate was incubated 3 to 4 days at 37°C. After incubation, Colony-forming units (CFU) were counted.

SUPPLEMENTARY MATERIAL

Supplementary table 1: Strains constructed during this master thesis

Strain	Name	Resistance/Sensitivity
***E. coli* DH10B**	pBBR MCSI *wadAc*	CmR
	pMR10 *wadAc*	CmR
	pBBR *wadA GTc*	CmR
	pNPTS Δ*GT*	KanR/SucS
	pNPTS Δ*OAg*	KanR/SucS
	pNPTS *wadA* mTq	KanR/SucS
	pBBR MCSI *wadA* R614A	CmR
	pGEM AM-*OAgc*	AmpR
	pGEM *OAgc*	AmpR
	pBBR MCSI *Oagc*	CmR
***E. coli* BW25**	pJMPt2 *wadA* CRISPRi	AmpR
***E. coli* MFD Pir**	pJMPt2 *wadA* CRISPRi	AmpR/DAP
***E. coli* S17**	pBBRi *gmd*	CmR
	pJQK Δ*wadA*	KanR/SucS
	pNPTS Δ*wadA*	KanR/SucS
	pBBR MCSI *waaLc*	CmR
	pBBR MCSI *wadAc*	CmR
	pMR10 *wadAc*	CmR
	pBBR *wadA GTc*	CmR
	pNPTS Δ*GT*	KanR/SucS
	pNPTS Δ*OAg*	KanR/SucS
	pNPTS Δ*gmd*	KanR/SucS
	pNPTS *wadA* mTq	KanR/SucS
	pBBR MCSI *wadA* R614A	CmR
	pBBR MCSI *Oagc*	CmR
***B. abortus* 544**	Δ*waaL*	-
	pBBR *wadA*c	CmR
	Δ*wadA* in Δ*gmd*	-
	Δ*OAg* in Δ*gmd*	-
	Δ*wadC* in Δ*gmd*	-
	Δ*wadC*	-
	pBBRi *gmd* in Δ*gmd*	CmR
	pBBRi *gmd* in Δ*wadA*Δ*gmd*	CmR
	pBBRi *gmd* in Δ*OAg*Δ*gmd*	CmR
	Δ*wadA* in Δ*wzm*	-
	Δ*wadA* in Δ*wadC*Δ*gmd*	-

	Δ*gmd* in *Omp2b*-3F-VDGK	-
	Δ*wadA* in WT **(30°C)**	-
	Δ*wadA* in Δ*wzm*	-
	Δ*GT* in Δ*gmd*	-
	pJMPt2 sg *wadA*	KanR
	pBBR *wadA* in Δ*wadA*Δ*gmd*	CmR
	pBBR *GTc* in Δ*GT*Δ*gmd*	CmR
	pBBR *wadA* R614A	CmR
	pBBR *wadA* R614A in Δ*GT*Δ*gmd*	CmR
	pBBR *Oagc* in Δ*wadA*Δ*gmd*	CmR
	pBBR *Oagc* in Δ*OAg*Δ*gmd*	CmR
	pBBR *Oagc* in Δ*GT*Δ*gmd*	CmR
***B. melitensis* 16M**	Δ*wadA*	-
	Δ*OAg*	-
	Δ*gmd* in Δ*wadA*	-
	Δ*gmd* in Δ*OAg*	-
	Δ*gmd*	-
	pBBR *wadA* in Δ*wadA*	CmR
	pBBR *wadA* in Δ*OAg*	CmR
	pBBR *GTc* in Δ*wadA*	CmR
	pBBR *wadA* R614A #1	CmR
	pBBR *wadA* R614A #2	CmR
	pBBR *Oagc* in Δ*wadA*	CmR
	pBBR *Oagc* in Δ*OAg*Δ*gmd*	CmR

Supplementary table 2: Primer table representing all the primers during this master thesis

Primer name	5' — 3' sequence
del_wadA-AMF	gatcaagcaggtgctcatc
del_wadA-AMR	**tgtaaaagtggaaccgctc**taattcgcttgcctcagc
del_wadA-AVF	gagcggttccacttttaca
del_wadA-AVR	gcaaatatcagcgcaacg
del_waaL-AMF	aattgcaatgcctataatgc
del_waaL-AMR	**ttcatgaagtcactccga**tcagatatccaaaatgtgcc
del_waaL-AVF	tcggagtgacttcatgaa
del_waaL-AVR	cgccatatgcagatgttcg
check-d-wadA-R	aacgcatatcgaagcttt
check-d-wadA-F	gaaacggtgcggataatc
Xho-GT-compl-F	aaaCTCGAGatttctcgctcgatcgc
del_GT-wadA-AMF	ttcaccaaaacccataccgg

del_GT-wadA-AMR	ctgtgtcgctgtatgccca
del-GT-wadA-AVF	cacaaagcccggctgttc
wadA-GT-c-R	aaaGGTACCcagcttataggctccggact
del-GT-wadA-AVR	gaaggcgaccgcaatgag
seq-wadAc-R-ok	ctgaggcaagcgaattaatg
delGT-AVF-ok	**tgggcatacagcgacacag**cacaaagcccggctgttc
AM-check-sacB-F	gcctttgatgttcagcag
AM-check-sacB-R	acagatgaaattgaacgc
AM-wadA-inside-F	tgaaacagatgcaggtga
AM-wadA-inside-R	tgtatggtgaacacgcac
del-O-Ag-p-AMF	cgaggttcgcatatatctatc
del-O-Ag-p-AMR	taacaattcccaggatgtatt
del-O-Ag-p-AVF	**aatacatcctgggaattgtta**attcgctatggatttctgg
del-O-Ag-p-AVR	gaagtgctggcaaacttt
pBBRi-wadAc-F	tttCTGCAGatttctcgctcgatcgc
pBBRi-wadAc-R	tttCTCGAGattacaggcttgtcaggg
pBBRi-GT-wadA-R	tttCTCGAGcagcttataggctccgga
check-d-wadA-R	aacgcatatcgaagcttt
check-d-wadA-F	gaaacggtgcggataatc
wadA-mTq/NG-AM-F	tgcactggtgtgcattct
wadA-mTq/NG-AM-R	**ggatccggttgccgaacg**gaagtaggtgcgcgggta
wadA-mTq-F	cgttcggcaaccggatcc**gtctcgaagggcgaagaa**
wadA-mTq-R	tcacttatacagttcgtccatgc
wadA-mTq-AV-F	**gcatggacgaactgtataagtga**gagcggttccacttttacac
wadA-mTq/NG-AV-R	ggaacatatggcgctgacc
check d-gmd for	agctaacttgctggcataag
check d-gmd rev	caggtcgagtcgatcatg
Plac-UppS-AMF	tttaagcttgcgcaacgcaattaatgtg
Plac-UppS-AMR	ttttCATATGagctgtttcctgtgtgaaatt
Plac-UppS-AVF	aaaCATATGtccgatccgcgccacat
PlaCUppS-AVR	tttCTGCAGctagactgccgctcccttg
wadA-Oag-AMR	aaaaCATATGcattaattcgcttgcctcag
wadA-Oag-AVF	aaaCATATGtccgatcagaattcaggtt
wA-H605A-AMR-ok	cattgcgagcagggtgaagt
wA-H605A-AVF-ok	**acttcaccctgctcgcaaatgg**atatctggaaattgccattcg
wA-R614-AMR-ok	cataggcaatggcaatttccag
wA-R614-AVF-ok	**ctggaaattgccattgcctatgg**atttctgggcttgctgt
wadA-Oag-AMF-ok	ttttGAGCTCatttctcgctcgatcgc
wadA-Oag-AVR-ok	aaaaCTGCAGattacaggcttgtcaggg

Restriction sites are marked in UPPERCASE
Nucleotides not hybridizing are shown in **bold**.
Point mutations are shown in grey.

Supplementary table 3: Plasmids used during this master thesis

Name	Description in *Brucella*	Resistance
pBBR MCSI	Replicative	Cm
pMR10	Replicative	Cm
pNPTS	Integrative	Kan
pGEM	Replicative	Amp
pJMPt21339	Replicative	Amp
pJMPt21039	Replicative	Amp

Supplementary table 4: List of antibodies used during this stufy

- Primary antibodies

Name	Recognized structure	Host / Isotype	Application	References
A68/03F03/D05	*Brucella* R-LPS	Mouse IgG2b	IF	(Cloeckaert et al, 1990)
A68/24D08/G09	*Brucella* R-LPS	Mouse (unknown)	Western Blot	(Bowden et al., 1995)
A76/12G12	*Brucella* S-LPS	Mouse IgG1	IF, Western Blot	(Cloeckaert et al, 1993)
B66/4F09	*Brucella* S-LPS	Mouse IgG2a	IF	(Cloeckaert et al, 1992)

- Secondary antibodies

Target	Conjugate	Host	Application	References
Mouse IgG H+ L	AlexaFluor 514	Goat	IF	Life technologies
Mouse IgG2b	AlexaFluor 488	Goat	IF	Life technologies
Mouse Immunoglobulins	HPR	Rabbit	Western Blot	Dako

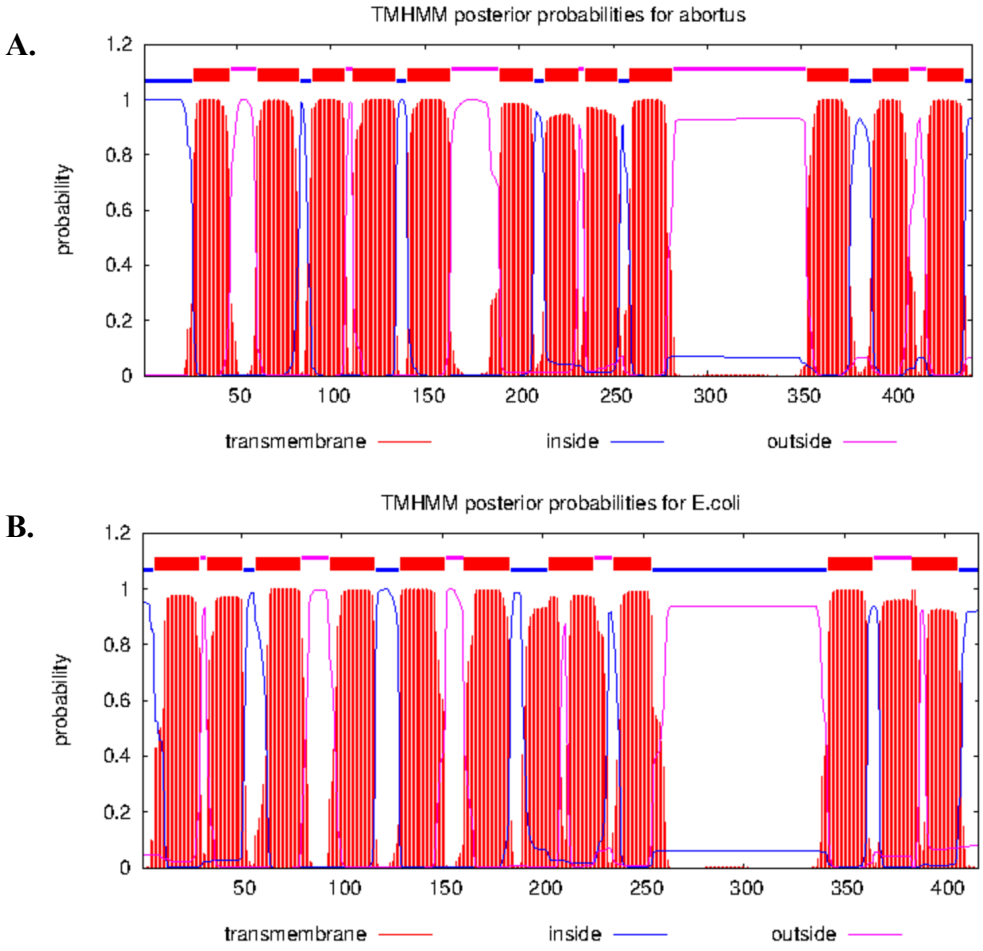

Figure S1: Prediction of transmembrane segments for A. BAB2_0106 in *B. abortus* and B. *waaL* in *E. coli*. Prediction were done using the TMHMM tool (Krogh *et al.,* 2001). Putative transmembrane domains are represented red, cytosolic domains in blue and periplasmic domains in pink.

```
Escherichia coli       ------------------------------------------MSFCW--------NEINSGI     12
Brucella abortus       MSNIVTRTRTDARMPDATGPQARIRRIALVIASVIFGVLLISFRPFTPAGGAETETGGDI     60
                                                                 :**          .* ...*

Escherichia coli       KSLILILCIFS--LMTLSLWDDVATKFLHAAGIISA-----LYFLATPKKTITNNPTLLI     65
Brucella abortus       INQLGFSCVGAVALASMAMFAN----LRKLAGIIRPGWLVMLVFLFASIFASSDPATAVR     116
                        . : : *: :  * ::::: :    : : ****       * ** :   : ::  * :

Escherichia coli       FISLCLLGIVNIIWYSHYKVSGSVYTNAYRGPMETGKIALCSAFIFLVLFAKNEMRTKIK     125
Brucella abortus       GVLLTTVGIVAIIAVLVLPQDGDGYSALLVS--------------------VASVVIVIS     156
                        : *  :*** **       .*. *:    .                        .:   *.

Escherichia coli       FGKLILFASLATQL----LFFAHAMWQHFYLNVDRVALSASHATTAGYIILFPSLLASIL     181
Brucella abortus       YAGVVLLPSLGTHGADAIEPQNSFLWRGVFSHKN----------IAGPVMAVF-AFAGLY     205
                       :. ::*: **.*:           :*: .: : :           ** :: .   :*.:

Escherichia coli       ILKSDFRHKTTLYTINFMLSLCA---VIVTETRAAILVFPFFALILIVMDSYINKR-INY     237
Brucella abortus       LWRRGWKTSG------LLIGLSALGFVSQTGSKTTMALVPFA-MLLVVLPGLMGLRKLTA     258
                       : : .:: .       :::.*.*   *  * ::::: :.**  ::*:*: . :. * :.

Escherichia coli       KLYCFITIALLAGVFSFKDTLLMRMNDLNNDLVNYSHDNTRTSVGARLAMYEVGLKTYSP     297
Brucella abortus       GLIFAI--QLAFATFIFGVVLFEPIRRLVE---NMDV---DATFTGRVSIWKFALEALSK     310
                        *   *   *  ..* * .*:  :. * :   * .     ::. .*::::::.*:: *

Escherichia coli       I---GQSLEKRAEKIHELEEKEPRLSGALPYVDSHLHNDLIDTLSTRGIPGVVLTILAFS     354
Brucella abortus       RPWTGYGYESFWSSAYARHAARPYYLDWDVRGIVHGHNSYLDVAMTMGIPALLCAIAVII     370
                           * . *.  .. :  .  .*   .       * **. :*.  * ***.:: :* .:

Escherichia coli       A--ILIYA-LRTAKEPYI------LILLFSLLVVGLSDVILFSKPVPTAVFITIIILLCAY     405
Brucella abortus       VMPLVHYARCRPVRENMLLADFFLMIVLFGTLNA-MMESFYFRRMDP--VWLTLILAIFG     427
                       .  :: **  * .:*  :      :*:**. * . : : : * :  *  *::*:**

Escherichia coli       FKAQSDQCLLEK---  417
Brucella abortus       -LGMTAKVVIPKRSV  441
                         . : : :: *
```

Figure S2: Sequence alignment between the WaaL sequence in *E. coli* (Q9ZIT0-1, identified by UniProt (2021)) and the homolog WaaL (BAB2_0106) found in *B. abortus*.

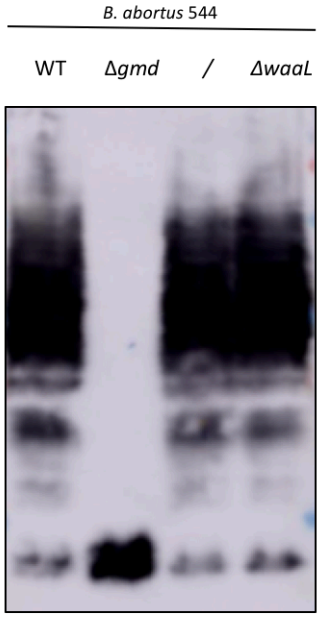

Figure S3 : Western Blot of different *B. abortus* strains (WT, Δ*gmd*, failed conjugation, Δ*waaL*) labeled with A68/24D08/G09, an anti-R-LPS antibody. This antibody binds to the LPS core, thereby enabling to visualize signal given from R-LPS or signal given from S-LPS. WT strain is a S-LPS phenotype control, while Δgmd is a R-LPS phenotype control.

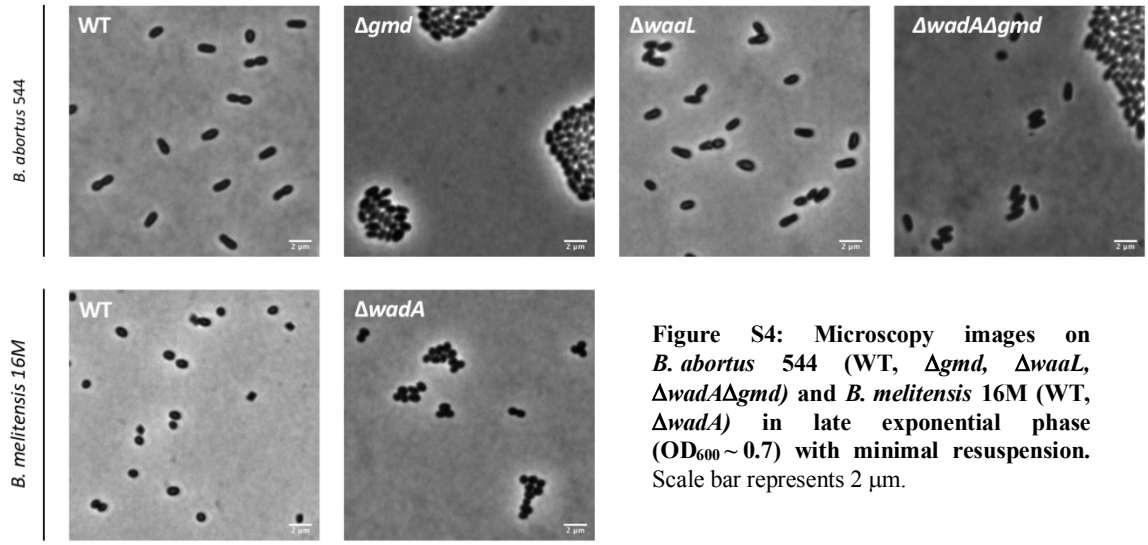

Figure S4: Microscopy images on *B. abortus* 544 (WT, Δ*gmd,* Δ*waaL,* Δ*wadA*Δ*gmd)* and *B. melitensis* 16M (WT, Δ*wadA)* in late exponential phase (OD_{600} ~ 0.7) with minimal resuspension. Scale bar represents 2 µm.

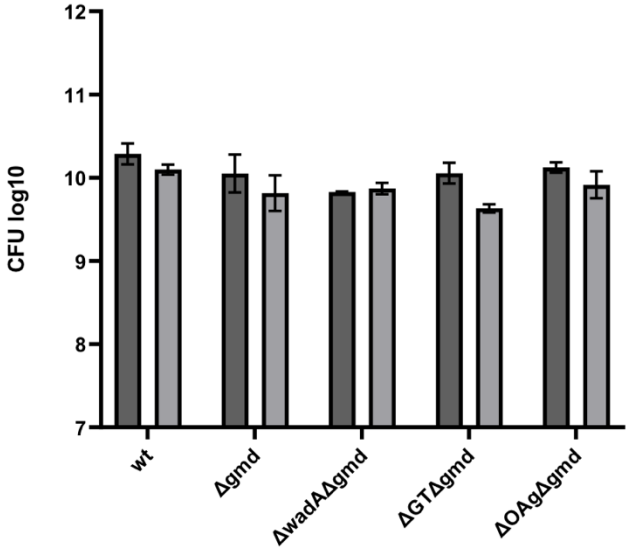

Figure S5 : CFU count for different B. abortus strains in exponential phase (OD_{600} ~ 0.4) (dark grey) and the same cultures after 18h incubation at 37°C (light grey). CFU count was normalized to an OD_{600}=1 for 1mL and expressed under log_{10}. (N=3)

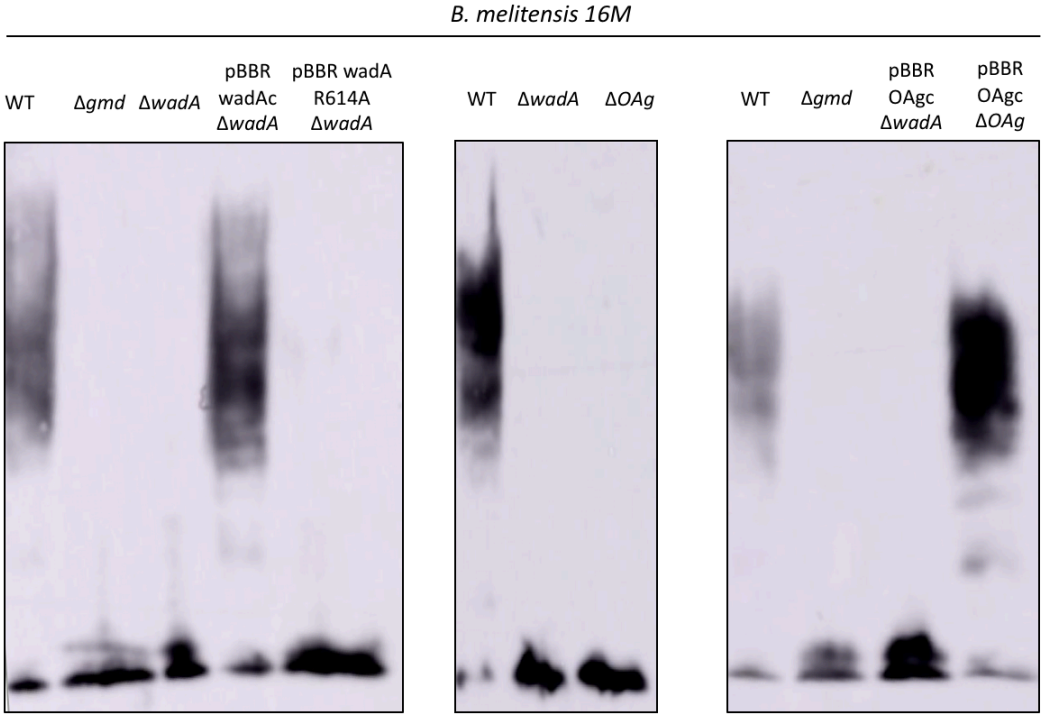

Figure S6 : Three Western Blots of different *B. melitensis* strains labeled with A68/24D08/G09, an anti-R-LPS antibody. These WB were used to form *Figure 38 + 41.*

```
CLUSTAL O(1.2.4) multiple sequence alignment

Mesorhizobium-sophorae          ---------------------------------------------MNLPIFAINLDRET   14
Mesorhizobium-loti              ---------------------------------------------MDLPIFAINLDTEV   14
Mesorhizobium-sp.-Pch-S         ---------------------------------------------MDLPIFAINLDTEV   14
B.vulpis                        ---------------------------------------------MILPVFVINMASQP   14
B.inopinata                     ---------------------------------------------MILPVFVINMASQP   14
B.canis                         ---------------------------------------------MILPVFVINMASQP   14
B.ovis                          ---------------------------------------------MILPVFVINMASQP   14
B.abortus                       ---------------------------------------------MILPVFVINMASQP   14
B.melitensis                    MTPAKKGGISDRNPLMVYERTIKVSSDKLKGGHHAKNRKCAEASELMILPVFVINMASQP   60
B.suis                          ---------------------------------------------MILPVFVINMASQP   14
Aminobacter-sp.-J44             -------------------------------------------MSGRVQLRAYVINLAKNP   18
Aquamicrobium-sp-cd1            --------------MTLERSSASASSNMLGSDQSVTR-DTRIGKGDALRAYVINLAKNP   44
                                                                          *  :.**:  :

Mesorhizobium-sophorae          GRWSELLASAEA--AGLTLQRIAAIDGRALAKADWTEIDLPTARKLSGRDILPGEYACYR   72
Mesorhizobium-loti              DRWEELAGNASA--AGLSLRRVSAINGRTLPVENWNGVDLTIAKTQNGRDILPTEYACYQ   72
Mesorhizobium-sp.-Pch-S         DRWEELAGNASS--AGLSLRRVSAIDGRGLPVENWNGVDLATARARSGREILPTEYACYQ   72
B.vulpis                        AAYKTVAASIEAYGQGFQLHRIDAVNGHTATQ--RIGIDDARFDAINGREMLPGEYGCYR   72
B.inopinata                     AAYKTVAASIEAYGQGFQLHRIDAVNGHTATQ--RIGIDDARFDAINGREMLPGEYGCYR   72
B.canis                         AAYKTVAASIEAYGQGFQLHRIDAVNGHTATQ--RIGIDDARFDAINGREMLPGEYGCYR   72
B.ovis                          AAYKTVAASIEAYGQGFQLHRIDAVNGHTATQ--RIGIDDARFDAINGREMLPGEYGCYR   72
B.abortus                       AAYKTVAASIEAYGQGFQLHRIDAVNGHTATQ--RIGIDDARFDAINGREMLPGEYGCYR   72
B.melitensis                    AAYKTVAASIEAYGQGFQLHRIDAVNGHTATQ--RIGIDDARFDAINGREMLPGEYGCYR   118
B.suis                          AAYKTVAASIEAYGQGFQLHRIDAVNGHTATQ--RIGIDDARFDAINGREMLPGEYGCYR   72
Aminobacter-sp.-J44             KRWEEVARSAAAFEPGIALTRIDAVDGRDAAHAAREQADVATFERINGRDMLPGEYGCYL   78
Aquamicrobium-sp-cd1            QRWEAIARSAADFAPGIELVRIDAVNGRAPEHAGREAADVPTFERLNGRDMLPGEYGCYL   104
                                  :. :  .      *: * *: *::*:          *       .**::** **.**

Mesorhizobium-sophorae          SHIQALETFLAGGSAYGLIVEDDVLFSENTMRRIQAIIAAVPDFDVIKLNNHRMSFFMRA   132
Mesorhizobium-loti              SHLTALRTFLDEGKPYGLIIEDDVAFDDSTLPRIEAIITAVPDFDAIKLTTHRTGLFMRA   132
Mesorhizobium-sp.-Pch-S         SHLTALRTFLDEGKPYGLIIEDDVAFNEDTLSRIEAIVAAVPNFDAIKLTTHRTGLFIRA   132
B.vulpis                        SHLKALESFLSDGSPYGLILEDDVVFTETTSARIHDIIKSLPDFDVVKLVNHRSPLFMSL   132
B.inopinata                     SHLKALESFLSDGSPYGLILEDDVVFTETTSARIHDIIKSLPDFDVVKLVNHRSPLFMSL   132
B.canis                         SHLKALESFLSDGSPYGLILEDDVVFTETTSARIHDIIKSLPDFDVVKLVNHRSPLFMSL   132
B.ovis                          SHLKALESFLSDGAPYGLILEDDVVFTETTSARIHDIIKSLPDFDVVKLVNHRSPLFMSL   132
B.abortus                       SHLKALESFLSDGSPYGLILEDDVVFTETTSARIHDIIKSLPDFDVVKLVNHRSPLFMSL   132
B.melitensis                    SHLKALESFLSDGSPYGLILEDDVVFTETTSARIHDIIKSLPDFDVVKLVNHRSPLFMSL   178
B.suis                          SHLKALESFLSDGSPYGLILEDDVVFTETTSARIHDIIKSLPDFDVVKLVNHRSPLFMSL   132
Aminobacter-sp.-J44             SHLKALRTFLDDGVPYGMILEDDVAFTEDSEARIRAIIDELPQFGVVKLVNHRAKLLIEL   138
Aquamicrobium-sp-cd1            SHLEALRQFLDDGSQYGLILEDDVAFEEGSEARIRAIINELPAFGAVKLVNHRAKFLVEL   164
                                **: **. **  *  **:*:**** * : :  **. *:  :* *..:** .**  :::

Mesorhizobium-sophorae          VETTEGDEIGRALHGPQGSAAAYLVTREGAQGLLSALAVMKMPWDVALERFWDTGLKVYS   192
Mesorhizobium-loti              VTTSRGDEIGRALHGPQGSAAAYLVTRRGAQKLISQLATMTLPWDIALERFWDSGLEVYS   192
Mesorhizobium-sp.-Pch-S         VTTSQGDEIGRALHGPQGSAAAYLVTRQGAQKLISKLATMTLPWDIALERFWDSGLEVYS   192
B.vulpis                        LETDAGDRIGCAIHGPQGSAAAYLVSREGARKLLSALSTMELPWDVAMERFWHHKARLFS   192
B.inopinata                     LETDAGDRIGRAIHGPQGSAAAYLVSREGARKLLSALSTMELPWDVAMERFWHHKARLFS   192
B.canis                         LETDAGDTIGRAIHGPQGSAAAYLVSREGARKLLSALSTMELPWDVAMERFWHHKARLFS   192
B.ovis                          LETDAGDRIGRVIHGPQGSAAAYLVSREGARKLLSALSTMELPWDVAMERFWYHKARLFS   192
B.abortus                       LETDAGDRIGRAIHGPQGSAAAYLVSREGARKLLSALSTMELPWDVAMERFWHHKARLFS   192
B.melitensis                    LETDAGDRIGRAIHGPQGSAAAYLVSREGARKLLSALSTMELPWDVAMERFWHHKARLFS   238
B.suis                          LETDAGDRIGRAIHGPQGSAAAYLVSREGARKLLSALSTMELPWDVAMERFWHHKARLFS   192
Aminobacter-sp.-J44             CSTKKGDKVGRTIHGPQGSAAAYLVTREGAQKLLDRLSKMVLPWDVALERFWHHGAEVYS   198
Aquamicrobium-sp-cd1            LSTSEHDRIGRTVHGPQGSAAAYLVTREAAQRLLDALSTMTLPWDVALEGAWHHGTEIFS   224
                                  *   * :* .:************:*..*: *:. *: * :***:*:*  *    .::*

Mesorhizobium-sophorae          VRKNVLGFAASSKISGIAGPSGSYKFARLAWPSRLDAGAFRAKDELSRLHHVLLRPPLPR   252
Mesorhizobium-loti              ARQNVLSFTPRSAVSSIAGPSGSYKGARFSWWKRLGTASFRAKDQFRRLHHVFLQPPIAS   252
Mesorhizobium-sp.-Pch-S         TRKNVLSFTSRSAVSSIAGPSGSYKGARFSWWKRLGTASFRAQDQFRRLHHVFLRPPLDS   252
B.vulpis                        SDENILAFSSHSEISNISDQNSGYDEAKYPWHKRLRTSLFRTFDYYVRVHHTLLQPQNPD   252
B.inopinata                     SDENILAFSSHSEISNISDQNSGYDEAKYPWYKRLRTSLFRTFDYYVRVHHTLLQPQNPD   252
B.canis                         SDENILAFSSHSEISNISDQNSGYDEAKHPWYMRLRTSLFRTFDYYVRVHHTLLQPQNPD   252
B.ovis                          SDENILAFSSHSEISNISDQNSGYDEAKHPWYMRLRTSLFRTFDYYVRVHHTLLQPQNPD   252
B.abortus                       SDENILAFSSHSEISNISDQNSGYDEAKHPWYMRLRTSLFRTFDYYVRVHHTLLQPQNPD   252
B.melitensis                    SDENILAFSSHSEISNISDQNSGYDEAKHPWYMRLRTSLFRTFDYYVRVHHTLLQPQNPD   298
B.suis                          SDENILAFSSHSEISNISDQNSGYDEAKHPWYMRLRTSLFRTFDYYVRVHHTLLQPQNPD   252
Aminobacter-sp.-J44             VRSNVLAFTEERKKSDIS--GGGYAKAKYPWYRRLGAARARTSDYVRRLSHVIQRPQRAL   256
Aquamicrobium-sp-cd1            VEKNVLAFTEEREKSDIS--GGGYAKAKYPWYQRFGAASARSRDYRRRIGYAFTRPDHAG   282
                                  .*:*.*:     *.*:  ...*  *:  *  *: :.  *: *   *: :.: :*
```

```
Mesorhizobium-sophorae      EIP---DYARADAPRYTVF-LVLAVFAILAMASAVWREADTYRFAGMALAAVAAIRWFRR  308
Mesorhizobium-loti          ETP---DYATPKQHL--LW-QILATLLVLAFVSPVWREADTYRYAGILLFIAGIIRWLGK  306
Mesorhizobium-sp.-Pch-S     ERA---DFAASTQPL--LW-QMLATLLVLAFISPVWREADTYRYAGVLLFLAGIFRWLGK  306
B.vulpis                    DSSMKSQSGAYRLPGISLTGELIAAISLLVFMSTVWVETDAYRYIALGFVVAALIRYART  312
B.inopinata                 GSSIKSQSGAYRLPGISLTGELIAAISLLVFMSTVWIETDAYRYIALGFVVAALIRYART  312
B.canis                     GSSMKSQSGAYKLPGISLTGELIAAISLLVFMSTVWVETDAYRYIALGFVVAALIRYART  312
B.ovis                      GSSMKSQSGAYKLPGISLTGELIAAISLLVFMSTVWVETDAYRYIALGFVVAALIRYART  312
B.abortus                   GSSMKSQSGAYKLPGISLTGELIAAISLLVFMSTVWVETDAYRYIALGFVVAALIRYART  312
B.melitensis                GSSMKSQSGAYKLPGISLTGELIAAISLLVFMSTVWVETDAYRYIALGFVVAALIRYART  358
B.suis                      GSSMKSQSGAYKLPGISLTGELIAAISLLVFMSTVWVETDAYRYIALGFVVAALIRYART  312
Aminobacter-sp.-J44         VDAEDPV----------SWKQILAGFLVLVLVSAVWAESDAYRFAGAALILAALWRYYCT  306
Aquamicrobium-sp-cd1        VAQAEPL----------PWQQMAAGILFLAFISAVWLESDAYRISGGLLILAALWRYYSK  332
                                             : * : .*.: * ** *:*:**  .  :  ..  *:

Mesorhizobium-sophorae      DLWTYSK-PLIGWVGGLCLGWSLYVFIRLAIVYFGT--HQLGAAEGIYLFPLFYATTGFA  365
Mesorhizobium-loti          DLWTYGK-PLIGGVGYFCFGWTFYVFARLAIVYFSS--GQLGTAEGIYLFPALYATTGFT  363
Mesorhizobium-sp.-Pch-S     DLWTYGK-PLIGGVGYLCFGWTFYVFARLAVVYFTS--GQLGASEGIYLFPALYATTGFT  363
B.vulpis                    DFWKYEK-PMVGWAGLLCVAWTFYVLARFAYIYLFYPEMGTGSAEGIYLFPLFYPTLGFA  371
B.inopinata                 DFWKYEK-PMVGWAGLLCVAWTFYVLARFAYIYLFYPEMGTGSAEGIYLFPLFYPTLGFA  371
B.canis                     DFWKYEK-PMVGWAGLLCVAWTFYVLARFAYIYLFYPEMGTGSAEGIYLFPLFYPTLGFA  371
B.ovis                      DFWKYEK-PMVGWAGLLCVAWTFYVLARFAYIYLFYPEMGTGSAEGIYLFPLFYPTLGFA  371
B.abortus                   DFWKYEK-PMVGWAGLLCVAWTFYVLARFAYIYLFYPEMGTGSAEGIYLFPLFYPTLGFA  371
B.melitensis                DFWKYEK-PMVGWAGLLCVAWTFYVLARFAYIYLFYPEMGTGSAEGIYLFPLFYPTLGFA  417
B.suis                      DFWKYEK-PMVGWAGLLCVAWTFYVLARFAYIYLFYPEMGTGSAEGIYLFPLFYPTLGFA  371
Aminobacter-sp.-J44         DIWNYRRFPEIGWMGHVCLLWGIYVLARFGVSLAVEPERGIGSAEGIYLLPALYPTLGYA  366
Aquamicrobium-sp-cd1        DIWDYRRLPEIGWMGRFCLLWGAYVLIRFGISLSTEPDKGIGSSEGIYLLPALYPTLGYA  392
                            *:* * : * :*  * .*. *  **: *:.           *::*****:* :* * *::

Mesorhizobium-sophorae      LLLFVRRPGQLVLWFMILSLVFLAADTGYSDILHGTRPEPWLFNNPIHASVAAGFIFLCT  425
Mesorhizobium-loti          LLAYIRRPAIVAVSFMTVSFAFLAVGTEYTAILQGLRPGPGLFNNTIHAAVAAGFVFLCA  423
Mesorhizobium-sp.-Pch-S     LLAYVRRPSIAAASFMALSLAFLAATTGYAAILQGLKPEPVLFNNPIHAAIGAGFIFLCA  423
B.vulpis                    LLLFIRRPFLIAVAFMAISLVILIFGFHYDPS-WNERAVTLLQHNPIHAAVSSGFIALCA  430
B.inopinata                 LLLFIRRPFLIAVAFMAISLVILIFGFHYDLS-WNERAVTLLQHNPIHAAVSSGFIALCA  430
B.canis                     LLLFIRRPFLIAVAFMTISLVILIFGFHYDLL-WNERAVTLLQHNPIHAAVSSGFIALCA  430
B.ovis                      LLLFIRRPFLIAVAFMAISLVILIFGFHYDLS-WNERAVTLLQHNPIHAAVSSGFIALCA  430
B.abortus                   LLLFIRRPFLIAVAFMAISLVILIFGFHYDLS-WNERAVTLLQHNPIHAAVSSGFIALCA  430
B.melitensis                LLLFIRRPFLIAVAFMAISLVILIFGFHYDLS-WNERAVTLLQHNPIHAAVSSGFIALCA  476
B.suis                      LLLFIRRPFLIAVAFMAISLVILIFGFHYDLS-WNERAVTLLQHNPIHAAVSSGFIALCA  430
Aminobacter-sp.-J44         MSLFVRRPFILATAFMVISLLALSLGIDHTG--ADVRADALLQHNPIHASVAAGLICLCV  424
Aquamicrobium-sp-cd1        MYLFVRRPFLIASIFMVVSLAALGFGIDYLG--PEIRARARLQNNPIHASVAVGLICLCA  450
                            :  ::***   .  ** :*:  *     :       :    * :* ***::. *:: **.

Mesorhizobium-sophorae      LQFMAYTAQRTDLNKVSRSLHWALSTAVLLFAFANIIALRSKGVWLALALVLLLLAIM-T  484
Mesorhizobium-loti          LQFAIYTGQRADLRAAKRIVYGLLAVAVMFLTIVNIVALRSKGVWLALAASIFLLGIF-T  482
Mesorhizobium-sp.-Pch-S     LQFAIYTMQRSDLGAGGKVLFWLLSAAVLAFAVVNIVALRSKGVWFALAAALLLLVVL-T  482
B.vulpis                    MAFGIHTLNRNTLNTKARVVLCLLALATFIAALIAIYSLYSKGVWLAMAIAFPTFVVLVA  490
B.inopinata                 MAFGIHTLNRNTLDTRARVVLCLLALATFIAALIAIYSLYSKGVWLAMAIAFPTFVVLVA  490
B.canis                     MAFGIHTLNRNTLDTRARVVLCLLALATFIAALIAIYSLYSKGVWLAMAIAFPTFVVLVA  490
B.ovis                      MAFGIHTLNRNTLDTRARVVLCLLALATFIAALIAIYSLYSKGVWLAMAIAFPTFVVLVA  490
B.abortus                   MAFGIHTLNRNTLDTRARVVLCLLALATFIAALIAIYSLYSKGVWLAMAIAFPTFVVLVA  490
B.melitensis                MAFGIHTLNRNTLDTRARVVLCLLALATFIAALIAIYSLYSKGVWLAMAIAFPTFVVLVA  536
B.suis                      MAFGIHTLNRNTLDTRARVVLCLLALATFIAALIAIYSLYSKGVWLAMAIAFPTFVVLVA  490
Aminobacter-sp.-J44         VPYALHVLRRRDLARPLKFGLVVFSAIVFVFSGLAIYGLWSKGVWLAMIVAXPVLLLTLM  484
Aquamicrobium-sp-cd1        VPYAVHALRRRDLGMALRGTLAALSLLVFILSGIAIYNLWSKGVWLAMIVALPVLLMTMI  510
                            : :  :. .*  *    :     ::  .:  :   *  * *****:*:      : :

Mesorhizobium-sophorae      LARGHRRELMIGGGVLAIVAASVVAMHNIFWSTAGDTMIFVKNLVSDALS-HGVLPAFDR  543
Mesorhizobium-loti          LVRGDRRQRLIGAGVLVAVLTGVFFSYGILSSTAGDTVAFVRTLTSDVAS-NGIWNALDH  541
Mesorhizobium-sp.-Pch-S     VLRGSRRHVLVAMGALALILVGLFFSYGILSSTAGDTVAFVGRSIADAAT-NGVGNALEH  541
B.vulpis                    LTDKSQTSRMAALVCILIGLLSVFAGEHILQRVGGNTANTSWELLSDLKTGDNIMQDFDK  550
B.inopinata                 LTDKSQTSRMAALVCILIGLLSVFAGEHILQRVGGNTANTSWELLSDLKTGDNIMQDFDK  550
B.canis                     LTDKSQTSRMAALVCILIGLLSVFAGEHILQRVGGNTANTSWELLSDLKTGDNIMQDFDK  550
B.ovis                      LTDKSQTSRMAALVCILIGLLSVFAGEHILQRVGGNTANTSWELLSDLKTGDNIMQDFDK  550
B.abortus                   LTDKSQTSRMAALVCILIGLLSVFAGEHILQRVGGNTANTSWELLSDLKTGDNIMQDFDK  550
B.melitensis                LTDKSQTSRMAALVCILIGLLSVFAGEHILQRVGGNTANTSWELLSDLKTGDNIMQDFDK  596
B.suis                      LTDKSQTSRMAALVCILIGLLSVFAGEHILQRVGGNTANTSWELLSDLKTGDNIMQDFDK  550
Aminobacter-sp.-J44         AA-GGHHGKSLAMATAIVAVVGVILNYDTVARVAGGTIETTSLLISELLHGRPGLQALDV  543
Aquamicrobium-sp-cd1        AA-GSRTGKQIAVAAALIALAGVVLNYQTLVQVAGGTVGTTALLLAELQQGNSATDTLRV  569
                                 :     .          .:.     .  ..*.*        ::          :
```

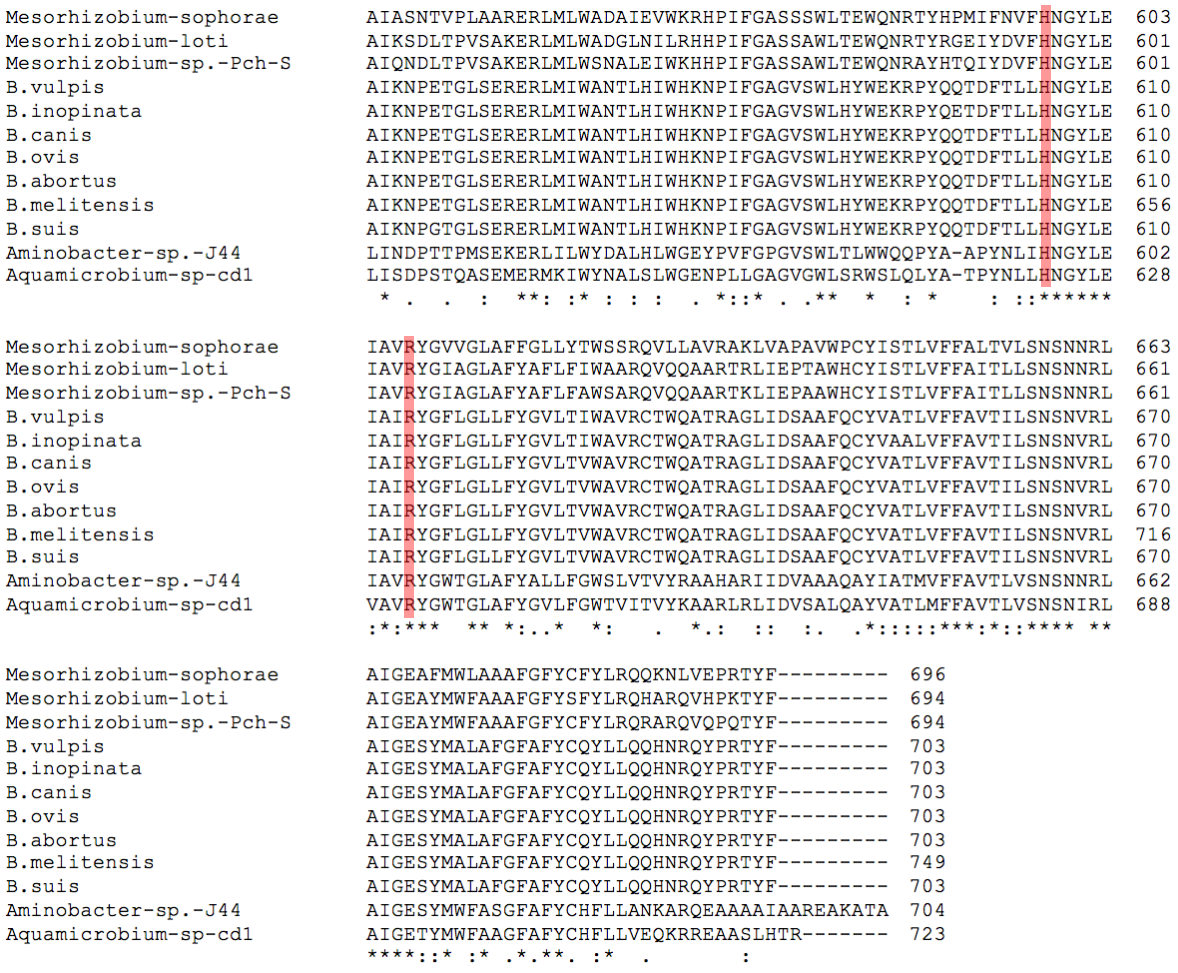

Figure S7: Enlarged sequence alignments of BAB1_0639 of *B. abortus* and other α-proteobacteria with highlighting of two conserved amino acids (red) believed to represent catalytic sites of the OAg domain. The sequences were found by BLAST. Identification of the two putative catalytic sites were carried out by taking the data found by Jorgenson & Young (2016) and locate similar amino acids in the large periplasmic loop of OAg. We predicted R614 and H605 to represent the potential catalytic sites in *B. abortus*.

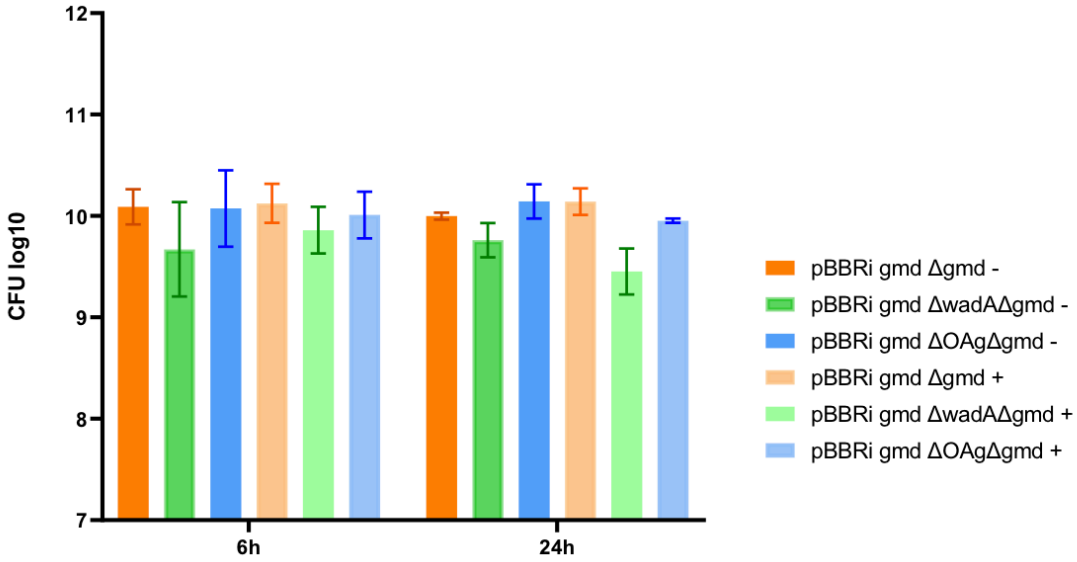

Figure S8: CFU count of *B. abortus* strains Δ*gmd,* pBBRi gmd Δ*gmd,* pBBRi gmd Δ*wadA*Δ*gmd* and pBBRi gmd Δ*OAg*Δ*gmd* without (-) and with (+) induction of gmd expression. CFU count was normalized to an OD_{600}=1 for 1mL and expressed under log_{10}. IPTG was added at time 0h. (N=3)

REFERENCES

Abeyrathne, P. D., Daniels, C., Poon, K. K., Matewish, M. J., & Lam, J. S. (2005). Functional characterization of WaaL, a ligase associated with linking O-antigen polysaccharide to the core of Pseudomonas aeruginosa lipopolysaccharide. *Journal of bacteriology*, *187*(9), 3002-3012.

Al Dahouk, S., Hofer, E., Tomaso, H., Vergnaud, G., Le Flèche, P., Cloeckaert, A., Koylass, M.S., Whatmore, A.M., Nöckler, K., and Scholz, H.C. (2012). Intraspecies Biodiversity of the Genetically Homologous Species Brucella microti. Appl Environ Microbiol *78*, 1534–1543.s

Arunmanee, W., Pathania, M., Solovyova, A. S., Le Brun, A. P., Ridley, H., Baslé, A., Van der Berg, B., Lakey, J. H. (2016). Gram-negative trimeric porins have specific LPS binding sites that are essential for porin biogenesis. *Proceedings of the National Academy of Sciences*, *113*(34), E5034-E5043.

Atluri, V.L., Xavier, M.N., de Jong, M.F., den Hartigh, A.B., and Tsolis, R.M. (2011). Interactions of the Human Pathogenic *Brucella* Species with Their Hosts. Annu. Rev. Microbiol. *65*, 523–541.

Bagheri, M., Keller, S., and Dathe, M. (2011). Interaction of W-Substituted Analogs of Cyclo-RRRWFW with Bacterial Lipopolysaccharides: the Role of the Aromatic Cluster in Antimicrobial Activity. Antimicrob Agents Chemother *55*, 788–797.

Bang, B. (1897). The etiology of epizootic abortion. *J. Comp. Path. Therap.*, 10: 125-149.

Batut, J., Andersson, S.G.E., and O'Callaghan, D. (2004). The evolution of chronic infection strategies in the α-proteobacteria. Nat Rev Microbiol *2*, 933–945.

Bello, G., Eriksson, J., Terry, A., Edwards, K., Lawrence, M.J., Barlow, D., and Harvey, R.D. (2015). Characterization of the Aggregates Formed by Various Bacterial Lipopolysaccharides in Solution and upon Interaction with Antimicrobial Peptides. Langmuir *31*, 741–751.

Berger S. (2016) Brucellosis: Global Status. Los Angeles, CA: GIDEON Informatics, Inc.

Bialer, M.G., Ruiz-Ranwez, V., Sycz, G., Estein, S.M., Russo, D.M., Altabe, S., Sieira, R., and Zorreguieta, A. (2019). MapB, the Brucella suis TamB homologue, is involved in cell envelope biogenesis, cell division and virulence. Sci Rep *9*, 2158.

Bowden, RA., Cloeckaert, A., Zygmunt, MS., Bernard, S., Dubray, G. (1995). Surface exposure of outer membrane protein and lipopolysaccharide epitopes in Brucella species studied by enzymelinked immunosorbent assay and flow cytometry. Infect Immun 63: 3945-52

Braun, W. (1946). Dissociation in *Brucella abortus*: a demonstration of the role of inherent and environmental factors in bacterial variation. *J. Bacteriol.* 51, 327–349.

Bruce D. (1887) Note on the recovery of a microorganism in Malta fever. Practitioner. 1887;39:161.

Bruce, D. (1889). Observations on Malta Fever. BMJ *1*, 1101–1105.

Bundle, D.R., Cherwonogrodzky, J.W., Gidney, M.A., Meikle, P.J., Perry, M.B., and Peters, T. (1989). Definition of Brucella A and M epitopes by monoclonal typing reagents and synthetic oligosaccharides. Infect Immun *57*, 2829–2836.

Cardoso, P.G., Macedo, G.C., Azevedo, V., and Oliveira, S.C. (2006). Brucella spp noncanonical LPS: structure, biosynthesis, and interaction with host immune system. Microb Cell Fact *5*, 13.

Carrion, M. I. G. U. E. L., Bhat, U. R., Reuhs, B. R. A. D., & Carlson, R. W. (1990). Isolation and characterization of the lipopolysaccharides from Bradyrhizobium japonicum. *Journal of bacteriology*, *172*(4), 1725-1731.

Celli, J. (2006). Surviving inside a macrophage: The many ways of Brucella. Research in Microbiology *157*, 93–98.

Celli, J. (2019). The Intracellular Life Cycle of *Brucella* spp. Microbiol Spectr *7*.

Chng, S.-S., Ruiz, N., Chimalakonda, G., Silhavy, T.J., and Kahne, D. (2010). Characterization of the two-protein complex in Escherichia coli responsible for lipopolysaccharide assembly at the outer membrane. Proceedings of the National Academy of Sciences *107*, 5363–5368.

Cloeckaert A, de Wergifosse P, Dubray G, Limet JN (1990) Identification of seven surface-exposed Brucella outer membrane proteins by use of monoclonal antibodies: immunogold labeling for electron microscopy and enzyme-linked immunosorbent assay. Infect Immun 58: 3980-7

Cloeckaert A, Jacques I, Bowden RA, Dubray G, Limet JN (1993) Monoclonal antibodies to Brucella rough lipopolysaccharide: characterization and evaluation of their protective effect against B. abortus. Res Microbiol 144: 475-84

Cloeckaert A, Zygmunt MS, de Wergifosse P, Dubray G & Limet JN (1992) Demonstration of peptidoglycan-associated Brucella outer-membrane proteins by use of monoclonal antibodies. J Gen Microbiol 138: 1543-1550.

Conde-Álvarez, R., Arce-Gorvel, V., Iriarte, M., Manček-Keber, M., Barquero-Calvo, E., Palacios-Chaves, L., Chacón-Díaz, C., Chaves-Olarte, E., Martirosyan, A., von Bargen, K., et al. (2012). The Lipopolysaccharide Core of Brucella abortus Acts as a Shield Against Innate Immunity Recognition. PLoS Pathog *8*, e1002675.

Conde-Álvarez, R., Palacios-Chaves, L., Gil-Ramírez, Y., Salvador-Bescós, M., Bárcena-Varela, M., Aragón-Aranda, B., Martínez-Gómez, E., Zúñiga-Ripa, A., de Miguel, M.J., Bartholomew, T.L., et al. (2018). Identification of lptA, lpxE, and lpxO, Three Genes Involved in the Remodeling of Brucella Cell Envelope. Front. Microbiol. *8*, 2657.

Corbel, M. J, Food and Agriculture Organization of the United Nations, World Health Organization & World Organisation for Animal Health. (2006). Brucellosis in humans and animals. World Health Organization

D Ferguson, A., Welte, W., Hofmann, E., Lindner, B., Holst, O., Coulton, J.W., and Diederichs, K. (2000). A conserved structural motif for lipopolysaccharide recognition by procaryotic and eucaryotic proteins. Structure *8*, 585–592.

D'Anastasio, R., Zipfel, B., Moggi-Cecchi, J., Stanyon, R., and Capasso, L. (2009). Possible Brucellosis in an Early Hominin Skeleton from Sterkfontein, South Africa. PLoS ONE *4*, e6439.

Dean, A.S., Crump, L., Greter, H., Schelling, E., and Zinsstag, J. (2012). Global Burden of Human Brucellosis: A Systematic Review of Disease Frequency. PLoS Negl Trop Dis *6*, e1865.

Ducret, A., Quardokus, E.M., and Brun, Y.V. (2016). MicrobeJ, a tool for high throughput bacterial cell detection and quantitative analysis. Nat Microbiol *1*, 16077.

Egan, A.J.F., Errington, J., and Vollmer, W. (2020). Regulation of peptidoglycan synthesis and remodelling. Nat Rev Microbiol *18*, 446–460.

El Ghachi, M., Bouhss, A., Blanot, D., Mengin-Lecreulx, D. (2004). The bacA Gene of E. coli Encodes an Undecaprenyl pyrophasphatse phosphatase activity. J Biol Chem. 279(29), 30106-13

Elzer, P. H., Phillips, R. W., Kovach, M. E., Peterson, K. M., & Roop 2nd, R. M. (1994). Characterization and genetic complementation of a Brucella abortus high-temperature-requirement A (htrA) deletion mutant. *Infection and immunity*, *62*(10), 4135-4139.

Fernandez-Prada, C.M., Nikolich, M., Vemulapalli, R., Sriranganathan, N., Boyle, S.M., Schurig, G.G., Hadfield, T.L., and Hoover, D.L. (2001). Deletion of *wboA* Enhances Activation of the Lectin Pathway of Complement in *Brucella abortus* and *Brucella melitensis*. Infect Immun *69*, 4407–4416.

Fontana, C., Conde-Álvarez, R., Ståhle, J., Holst, O., Iriarte, M., Zhao, Y., Arce-Gorvel, V., Hanniffy, S., Gorvel, J.-P., Moriyón, I., et al. (2016). Structural Studies of Lipopolysaccharide-defective Mutants from Brucella melitensis Identify a Core Oligosaccharide Critical in Virulence. Journal of Biological Chemistry *291*, 7727–7741.

Freer, E., Moreno, E., Moriyón, I., Pizarro-Cerdá, J., Weintraub, A., and Gorvel, J.P. (1996). Brucella-Salmonella lipopolysaccharide chimeras are less permeable to hydrophobic probes and more sensitive to cationic peptides and EDTA than are their native Brucella sp. counterparts. Journal of Bacteriology *178*, 5867–5876.

Frirdich, E., Lindner, B., Holst, O., and Whitfield, C. (2003). Overexpression of the waaZ Gene Leads to Modification of the Structure of the Inner Core Region of Escherichia coli Lipopolysaccharide, Truncation of the Outer Core, and Reduction of the Amount of O Polysaccharide on the Cell Surface. JB *185*, 1659–1671.

Godessart, P., Lannoy, A., Dieu, M., Van der Verren, S.E., Soumillion, P., Collet, J.-F., Remaut, H., Renard, P., and De Bolle, X. (2021). β-Barrels covalently link peptidoglycan and the outer membrane in the α-proteobacterium Brucella abortus. Nat Microbiol *6*, 27–33.

Godfroid, F., Cloeckaert, A., Taminiau, B., Danese, I., Tibor, A., De Bolle, X., ... & Letesson, J. J. (2000). Genetic organisation of the lipopolysaccharide O-antigen biosynthesis region of Brucella melitensis 16M (wbk). *Research in microbiology*, *151*(8), 655-668.

Godfroid, J., Nielsen, K., and Saegerman, C. (2010). Diagnosis of Brucellosis in Livestock and Wildlife. Croat Med J *51*, 296–305.

González, D., Grilló, M.-J., De Miguel, M.-J., Ali, T., Arce-Gorvel, V., Delrue, R.-M., Conde-Álvarez, R., Muñoz, P., López-Goñi, I., Iriarte, M., et al. (2008). Brucellosis Vaccines: Assessment of Brucella melitensis Lipopolysaccharide Rough Mutants Defective in Core and O-Polysaccharide Synthesis and Export. PLoS ONE *3*, e2760.

Haag, A.F., Myka, K.K., Arnold, M.F.F., Caro-Hernández, P., and Ferguson, G.P. (2010). Importance of Lipopolysaccharide and Cyclic *β* -1,2-Glucans in *Brucella* -Mammalian Infections. International Journal of Microbiology *2010*, 1–12.

Halling, S. M., Peterson-Burch, B. D., Bricker, B. J., Zuerner, R. L., Qing, Z., Li, L. L., Kapur, V., Alt, D. P., Olsen, S. C. (2005). Completion of the genome sequence of Brucella abortus and comparison to the highly similar genomes of Brucella melitensis and Brucella suis. *Journal of Bacteriology*, *187*(8), 2715-2726.

Han, W., Wu, B., Li, L., Zhao, G., Woodward, R., Pettit, N., Cai, L., Thon, V., and Wang, P.G. (2012). Defining Function of Lipopolysaccharide O-antigen Ligase WaaL Using Chemoenzymatically Synthesized Substrates. Journal of Biological Chemistry *287*, 5357–5365.

Hull, N.C., and Schumaker, B.A. (2018). Comparisons of brucellosis between human and veterinary medicine. Infection Ecology & Epidemiology *8*, 1500846.

Islam, S.T., Taylor, V.L., Qi, M., and Lam, J.S. (2010). Membrane Topology Mapping of the O-Antigen Flippase (Wzx), Polymerase (Wzy), and Ligase (WaaL) from Pseudomonas aeruginosa PAO1 Reveals Novel Domain Architectures. MBio *1*, e00189-10.

Jorgenson, M.A., and Young, K.D. (2016). Interrupting Biosynthesis of O Antigen or the Lipopolysaccharide Core Produces Morphological Defects in Escherichia coli by Sequestering Undecaprenyl Phosphate. J Bacteriol *198*, 3070–3079.

Kay, G.L., Sergeant, M.J., Giuffra, V., Bandiera, P., Milanese, M., Bramanti, B., Bianucci, R., and Pallen, M.J. (2014). Recovery of a Medieval Brucella melitensis Genome Using Shotgun Metagenomics. MBio *5*.

Koplow, J., & Goldfine, H. (1974). Alterations in the outer membrane of the cell envelope of heptose-deficient mutants of Escherichia coli. *Journal of bacteriology*, *117*(2), 527–543.

Krogh, A., Larsson, B., von Heijne, G., and Sonnhammer, E.L.L. (2001). Predicting transmembrane protein topology with a hidden markov model: application to complete genomes11Edited by F. Cohen. Journal of Molecular Biology *305*, 567–580.

Lapaque, N., Forquet, F., de Chastellier, C., Mishal, Z., Jolly, G., Moreno, E., Moriyon, I., Heuser, J.E., He, H.-T., and Gorvel, J.-P. (2006). Characterization of Brucella abortus lipopolysaccharide macrodomains as mega rafts. Cell Microbiol *8*, 197–206.

Laurent, T.C., Mertens, P., Dierick, J.-F., Letesson, J.-J., Lambert, C., and De Bolle, X. (2004). Functional, molecular and structural characterisation of five anti-Brucella LPS mAb. Molecular Immunology *40*, 1237–1247.

Lerouge, I., and Vanderleyden, J. (2002). O-antigen structural variation: mechanisms and possible roles in animal/plant–microbe interactions. FEMS Microbiol Rev *26*, 17–47.

Li, H., Yang, T., Liao, T., Debowski, A. W., Nilsson, H. O., Fulurija, A., ... & Benghezal, M. (2017). The redefinition of Helicobacter pylori lipopolysaccharide O-antigen and core-oligosaccharide domains. *PLoS pathogens*, *13*(3), e1006280.

Liu, Y., and Breukink, E. (2016). The Membrane Steps of Bacterial Cell Wall Synthesis as Antibiotic Targets. Antibiotics *5*, 28.

Liu, D., Hunt, M., and Tsai, I.J. (2018). Inferring synteny between genome assemblies: a systematic evaluation. BMC Bioinformatics *19*, 26.

Madden, T. (2003). The BLAST sequence analysis tool. *The NCBI handbook*.

Madeira, F., Park, Y. mi, Lee, J., Buso, N., Gur, T., Madhusoodanan, N., Basutkar, P., Tivey, A.R.N., Potter, S.C., Finn, R.D., et al. (2019). The EMBL-EBI search and sequence analysis tools APIs in 2019. Nucleic Acids Research *47*, W636–W641.

Manat, G., Roure, S., Auger, R., Bouhss, A., Barreteau, H., Mengin-Lecreulx, D., & Touzé, T. (2014). Deciphering the metabolism of undecaprenyl-phosphate: the bacterial cell-wall unit carrier at the membrane frontier. *Microbial Drug Resistance*, *20*(3), 199-214.

Mancilla, M. (2016). Smooth to Rough Dissociation in Brucella: The Missing Link to Virulence. Front. Cell. Infect. Microbiol. *5*.

Mancilla, M., López-Goñi, I., Moriyón, I., and Zárraga, A.M. (2010). Genomic Island 2 Is an Unstable Genetic Element Contributing to *Brucella* Lipopolysaccharide Spontaneous Smooth-to-Rough Dissociation. J Bacteriol *192*, 6346–6351.

Mancilla, M., Marín, C.M., Blasco, J.M., Zárraga, A.M., López-Goñi, I., and Moriyón, I. (2012). Spontaneous Excision of the O-Polysaccharide *wbkA* Glycosyltranferase Gene Is a Cause of Dissociation of Smooth to Rough Brucella Colonies. J Bacteriol *194*, 1860–1867.Meltzer, E., Sidi, Y., Smolen, G., Banai, M., Bardenstein, S., and Schwartz, E. (2010). Sexually Transmitted Brucellosis in Humans. CLIN INFECT DIS *51*, e12–e15.

Meltzer, E., Sidi, Y., Smolen, G., Banai, M., Bardenstein, S., and Schwartz, E. (2010). Sexually Transmitted Brucellosis in Humans. CLIN INFECT DIS *51*, e12–e15.

Meyer K, Shaw EA. (1920). Comparison of the morphologic, Cultural and Biochemical Characteristics of B. Nov Gen I J Infect Dis. 1920;27(3):173–184.

Microsoft Corporation, 2018. *Microsoft Excel*, Available at: https://office.microsoft.com/excel

Moreno, E. (2014). Retrospective and prospective perspectives on zoonotic brucellosis. Front Microbiol *5*, 213.

Moreno, E. (2021). The one hundred year journey of the genus *Brucella* (Meyer and Shaw 1920). FEMS Microbiology Reviews *45*, fuaa045.

Moreno, E., and Moriyón, I. (2006). The Genus Brucella. In The Prokaryotes, M. Dworkin, S. Falkow, E. Rosenberg, K.-H. Schleifer, and E. Stackebrandt, eds. (New York, NY: Springer New York), pp. 315–456.

Moreno, E., Cloeckaert, A., and Moriyón, I. (2002). Brucella evolution and taxonomy. Veterinary Microbiology *90*, 209–227.

Moriyón, I., and López-Goñi, I. (1998). Structure and properties of the outer membranes of Brucella abortus and Brucella melitensis. Int Microbiol *1*, 19–26.

Moriyón, I., Grill, M.J., Monreal, D., Gonzlez, D., Marn, C., Lpez-Goi, I., Mainar-Jaime, R.C., Moreno, E., and Blasco, J.M. (2004). Rough vaccines in animal brucellosis: Structural and genetic basis and present status. Vet. Res. *35*, 1–38.

Noh, J. G., Jeon, H. E., So, J. S., & Chang, W. S. (2015). Effects of the Bradyrhizobium japonicum waaL (rfaL) gene on hydrophobicity, motility, stress tolerance, and symbiotic relationship with soybeans. *International journal of molecular sciences*, *16*(8), 16778-16791.

Pappas, G., Papadimitriou, P., Akritidis, N., Christou, L., and Tsianos, E.V. (2006). The new global map of human brucellosis. The Lancet Infectious Diseases *6*, 91–99.

Pérez, J.M., McGarry, M.A., Marolda, C.L., and Valvano, M.A. (2008). Functional analysis of the large periplasmic loop of the *Escherichia coli* K-12 WaaL O-antigen ligase. Molecular Microbiology *70*, 1424–1440.

Pérez-Burgos, M., García-Romero, I., Jung, J., Valvano, M.A., and Søgaard-Andersen, L. (2019). Identification of the lipopolysaccharide O-antigen biosynthesis priming enzyme and the O-antigen ligase in *Myxococcus xanthus*: critical role of LPS O-antigen in motility and development. Mol Microbiol *112*, 1178–1198.

Peters, J.M., Koo, B.-M., Patino, R., Heussler, G.E., Hearne, C.C., Qu, J., Inclan, Y.F., Hawkins, J.S., Lu, C.H.S., Silvis, M.R., et al. (2019). Enabling genetic analysis of diverse bacteria with Mobile-CRISPRi. Nat Microbiol *4*, 244–250.

PFAM Database. (2006) In Encyclopedic Reference of Genomics and Proteomics in Molecular Medicine, (Berlin, Heidelberg: Springer Berlin Heidelberg), pp. 1392–1392.

Porte, F., Naroeni, A., Ouahrani-Bettache, S., & Liautard, J. P. (2003). Role of the Brucella suis lipopolysaccharide O antigen in phagosomal genesis and in inhibition of phagosome-lysosome fusion in murine macrophages. *Infection and immunity*, *71*(3), 1481-1490.

Raetz, C.R.H., and Whitfield, C. (2002). Lipopolysaccharide Endotoxins. Annu. Rev. Biochem. *71*, 635–700.

Randich, A.M., and Brun, Y.V. (2015). Molecular mechanisms for the evolution of bacterial morphologies and growth modes. Front. Microbiol. *6*.

Reeves, P. (1995). Role of O-antigen variation in the immune response. Trends in Microbiology *3*, 381–386.

Ruan, X., and Valvano, M.A. (2013). In Vitro O-Antigen Ligase Assay. In Glycosyltransferases, I. Brockhausen, ed. (Totowa, NJ: Humana Press), pp. 185–197.

Ruan, X., Loyola, D.E., Marolda, C.L., Perez-Donoso, J.M., and Valvano, M.A. (2012). The WaaL O-antigen lipopolysaccharide ligase has features in common with metal ion-independent inverting glycosyltransferases*. Glycobiology *22*, 288–299.

Rubbi, C. P. 1991. Antígenos Proteicos de Brucella abortus: Aislamiento y Estudio de su Asociación al LPS y de Factores que Afectan a la Producción de Anticuerpos Monoclonales Contra los Mismos (PhD thesis). Facultad de Ciencias Exactas, Universidad Nacional de la Plata. La Plata , Argentina. 1–137.

Salcedo, S.P., Chevrier, N., Lacerda, T.L.S., Ben Amara, A., Gerart, S., Gorvel, V.A., de Chastellier, C., Blasco, J.M., Mege, J.-L., and Gorvel, J.-P. (2013). Pathogenic Brucellae Replicate in Human Trophoblasts. The Journal of Infectious Diseases *207*, 1075–1083.

Salvador-Bescós, M., Gil-Ramírez, Y., Zúñiga-Ripa, A., Martínez-Gómez, E., de Miguel, M.J., Muñoz, P.M., Cloeckaert, A., Zygmunt, M.S., Moriyón, I., Iriarte, M., et al. (2018). WadD, a New Brucella Lipopolysaccharide Core Glycosyltransferase Identified by Genomic Search and Phenotypic Characterization. Front. Microbiol. *9*, 2293.

Schild, S., Lamprecht, A.-K., and Reidl, J. (2005). Molecular and Functional Characterization of O Antigen Transfer inVibriocholerae. Journal of Biological Chemistry *280*, 25936–25947.

Schindelin, J., Arganda-Carreras, I., Frise, E., Kaynig, V., Longair, M., Pietzsch, T., Preibisch, S., Rueden, C., Saalfeld, S., Schmid, B., et al. (2012). Fiji: an open-source platform for biological-image analysis. Nat Methods *9*, 676–682.

Schindler, H., & Rosenbusch, J. P. (1978). Matrix protein from Escherichia coli outer membranes forms voltage-controlled channels in lipid bilayers. *Proceedings of the National Academy of Sciences*, *75*(8), 3751-3755.

Shearer, J., Jefferies, D., & Khalid, S. (2019). Outer membrane proteins OmpA, FhuA, OmpF, EstA, BtuB, and OmpX have unique lipopolysaccharide fingerprints. *Journal of chemical theory and computation*, *15*(4), 2608-2619.

Singh, K. (2009). Laboratory-Acquired Infections. CLIN INFECT DIS *49*, 142–147.

Slade, J.A., Brockett, M., Singh, R., Liechti, G.W., and Maurelli, A.T. (2019). Fosmidomycin, an inhibitor of isoprenoid synthesis, induces persistence in Chlamydia by inhibiting peptidoglycan assembly. PLoS Pathog *15*, e1008078.

Soler-Lloréns, P., Gil-Ramírez, Y., Zabalza-Baranguá, A., Iriarte, M., Conde-Álvarez, R., Zúñiga-Ripa, A., San Román, B., Zygmunt, M.S., Vizcaíno, N., Cloeckaert, A., et al. (2014). Mutants in the lipopolysaccharide of Brucella ovis are attenuated and protect against B. ovis infection in mice. Vet Res *45*, 72.

Sperandeo, P., Martorana, A.M., and Polissi, A. (2017). The lipopolysaccharide transport (Lpt) machinery: A nonconventional transporter for lipopolysaccharide assembly at the outer membrane of Gram-negative bacteria. Journal of Biological Chemistry *292*, 17981–17990.

Starr, T., Ng, T.W., Wehrly, T.D., Knodler, L.A., and Celli, J. (2008). Brucella Intracellular Replication Requires Trafficking Through the Late Endosomal/Lysosomal Compartment. Traffic *9*, 678–694.

Sternon, J.-F., Godessart, P., Gonçalves de Freitas, R., Van der Henst, M., Poncin, K., Francis, N., Willemart, K., Christen, M., Christen, B., Letesson, J.-J., et al. (2018). Transposon Sequencing of Brucella abortus Uncovers Essential Genes for Growth *In Vitro* and Inside Macrophages. Infect Immun *86*.

Stranahan, L. W., & Arenas-Gamboa, A. M. (2021). When the Going Gets Rough: The Significance of Brucella Lipopolysaccharide Phenotype in Host–Pathogen Interactions. *Frontiers in Microbiology*, *12*.

Tsolis, R.M., Seshadri, R., Santos, R.L., Sangari, F.J., Lobo, J.M.G., de Jong, M.F., Ren, Q., Myers, G., Brinkac, L.M., Nelson, W.C., et al. (2009). Genome Degradation in Brucella ovis Corresponds with Narrowing of Its Host Range and Tissue Tropism. PLoS ONE *4*, e5519.

Ugalde, J.E., Czibener, C., Feldman, M.F., and Ugalde, R.A. (2000). Identification and Characterization of the *Brucella abortus* Phosphoglucomutase Gene: Role of Lipopolysaccharide in Virulence and Intracellular Multiplication. Infect Immun *68*, 5716–5723.

UniProt: the universal protein knowledgebase in 2021. *Nucleic Acids Research*, 2021, vol. 49, no D1, p. D480-D489.

Vallenet, D. (2006). MaGe: a microbial genome annotation system supported by synteny results. Nucleic Acids Research *34*, 53–65.

Vallenet, D., Calteau, A., Dubois, M., Amours, P., Bazin, A., Beuvin, M., Burlot, L., Bussell, X., Fouteau, S., Gautreau, G., et al. (2019). MicroScope: an integrated platform for the annotation and exploration of microbial gene functions through genomic, pangenomic and metabolic comparative analysis. Nucleic Acids Research gkz926.

Van der Henst, C., de Barsy, M., Zorreguieta, A., Letesson, J.-J., and De Bolle, X. (2013). The Brucella pathogens are polarized bacteria. Microbes and Infection *15*, 998–1004.

Vassen V. (2018). Polarity of envelope growth and heterogeneity of the outer membrane of *Brucella abortus* (PhD thesis). Faculty of science. University of Namur. Belgium.

Vassen, V., Valotteau, C., Feuillie, C., Formosa-Dague, C., Dufrêne, Y.F., and De Bolle, X. (2019). Localized incorporation of outer membrane components in the pathogen *Brucella abortus*. EMBO J *38*.

Verdiguel-Fernández, L., Oropeza-Navarro, R., Basurto-Alcántara, F.J., Castañeda-Ramírez, A., and Verdugo-Rodríguez, A. (2017). Omp31 plays an important role on outer membrane properties and intracellular survival of Brucella melitensis in murine macrophages and HeLa cells. Arch Microbiol *199*, 971–978.

Wang, G. (2008). NMR of Membrane-Associated Peptides and Proteins. CPPS *9*, 50–69.

Watarai, M., Makino, S., Fujii, Y., Okamoto, K., and Shirahata, T. (2002). Modulation of Brucella-induced macropinocytosis by lipid rafts mediates intracellular replication. Cell Microbiol *4*, 341–355.

Weinstein, R. A., & Singh, K. (2009). Laboratory-acquired infections. *Clinical Infectious Diseases*, *49*(1), 142-147.

Whatmore, A.M., and Foster, J.T. (2021). Emerging diversity and ongoing expansion of the genus Brucella. Infection, Genetics and Evolution *92*, 104865.

Whitfield, C., Heinrichs, D. E., Yethon, J. A., Amor, K. L., Monteiro, M. A., & Perry, M. B. (1999). Assembly of the R1-type core oligosaccharide of Escherichia coli lipopolysaccharide. *Journal of Endotoxin Research*, *5*(3), 151-156.

Whitfield, C., and Trent, M.S. (2014). Biosynthesis and Export of Bacterial Lipopolysaccharides. Annu. Rev. Biochem. *83*, 99–128.

World Health Organisation (WHO). (2020, July 29). Brucellosis. Retrieved from https://www.who.int/news-room/fact-sheets/detail/brucellosis

Wyatt, H.V. (2010). Surgeon Captain Sheldon F Dudley and the person to person spread of brucellosis by inhalation. J R Nav Med Serv *96*, 185–187.

Zammit T. (1905) A preliminary note on the susceptibility of goats to Malta Fever. Proc R Soc 1905;76B: 377-8. [Also *J R Army Med Corps* 1905;**5**:341-2, and shortened version in *Reports of the MFC* Part III; 1905:83]